Postprint of Science 378 (6622): 915-920 (2022)

Title: Grazing and ecosystem service delivery in global drylands

Authors: Fernando T. Maestre[1,2,*], Yoann Le Bagousse-Pinguet[3], Manuel Delgado-Baquerizo[4,5], David J. Eldridge[6], Hugo Saiz[7,8], Miguel Berdugo[9,10], Beatriz Gozalo[1], Victoria Ochoa[1,11], Emilio Guirado[1], Miguel García-Gómez[12], Enrique Valencia[13], Juan J. Gaitán[14,15,16], Sergio Asensio[1], Betty J. Mendoza[13], César Plaza[11], Paloma Díaz-Martínez[11], Ana Rey[17], Hang-Wei Hu[18,19], Ji-Zheng He[18,19], Jun-Tao Wang[20,21,22], Anika Lehmann[23,24], Matthias C. Rillig[23,24], Simone Cesarz[25,26], Nico Eisenhauer[25,26], Jaime Martínez-Valderrama[1], Eduardo Moreno-Jiménez[27], Osvaldo Sala[28,29,30], Mehdi Abedi[31], Negar Ahmadian[31], Concepción L. Alados[32], Valeria Aramayo[33], Fateh Amghar[34], Tulio Arredondo[35], Rodrigo J. Ahumada[36], Khadijeh Bahalkeh[34], Farah Ben Salem[37], Niels Blaum[38], Bazartseren Boldgiv[39], Matthew A. Bowker[40,41], Donaldo Bran[33], Chongfeng Bu[42,43], Rafaella Canessa[44,45], Andrea P. Castillo-Monroy[46], Helena Castro[47], Ignacio Castro[48], Patricio Castro-Quezada[49], Roukaya Chibani[37], Abel A. Conceição[50], Courtney M. Currier[28,30], Anthony Darrouzet-Nardi[51], Balázs Deák[52], David A. Donoso[46,53], Andrew J. Dougill[54], Jorge Durán[47,55], Batdelger Erdenetsetseg[39], Carlos I. Espinosa[56], Alex Fajardo[57,58], Mohammad Farzam[59], Daniela Ferrante[60,61], Anke S.K. Frank[62,65,75], Lauchlan H. Fraser[63], Laureano A. Gherardi[64], Aaron C. Greenville[65], Carlos A. Guerra[25,66], Elizabeth Gusmán-Montalvan[56], Rosa M. Hernández-Hernández[48], Norbert Hölzel[67], Elisabeth Huber-Sannwald[35], Frederic M. Hughes[50,68], Oswaldo Jadán-Maza[49], Florian Jeltsch,[24,38], Anke Jentsch[69], Kudzai F. Kaseke[70], Melanie Köbel[71], Jessica E. Koopman[72], Cintia V. Leder[16,73], Anja Linstädter[74,75], Peter C. le Roux[76], Xinkai Li[42,43], Pierre Liancourt[45,77,78], Jushan Liu[79], Michelle A. Louw[76], Gillian Maggs-Kölling[80], Thulani P. Makhalanyane[72], Oumarou Malam Issa[81], Antonio J. Manzaneda[82,83], Eugene Marais[80], Juan P. Mora[57], Gerardo Moreno[84], Seth M. Munson[85], Alice Nunes[71], Gabriel Oliva[60,61], Gastón R. Oñatibia[86], Guadalupe Peter[16,73], Marco O.D. Pivari[87], Yolanda Pueyo[32], R. Emiliano Quiroga[36,88], Soroor Rahmanian[59,89], Sasha C. Reed[90], Pedro J. Rey[82,83], Benoit Richard[91], Alexandra Rodríguez[46], Víctor Rolo[84], Juan G. Rubalcaba[92], Jan C. Ruppert[44], Ayman Salah[93], Max A. Schuchardt[69], Sedona Spann[40], Ilan Stavi[94], Colton R. A.Stephens[63], Anthony M. Swemmer[95], Alberto L. Teixido[96,] Andrew D. Thomas[97], Heather L. Throop[98], Katja Tielbörger[45], Samantha Travers[99], James Val[100], Orsolya Valkó[52], Liesbeth van den Brink[45], Sergio Velasco Ayuso[86], Frederike Velbert[67], Wanyoike Wamiti[101], Deli Wang[79], Lixin Wang[102], Glenda M. Wardle[65], Laura Yahdjian[86], Eli Zaady[103], Yuanming Zhang[104], Xiaobing Zhou[104], Brajesh K. Singh[20,21], Nicolas Gross[105].

Affiliations:

[1]Instituto Multidisciplinar para el Estudio del Medio "Ramón Margalef", Universidad de Alicante; Alicante, Spain.

[2]Departamento de Ecología, Universidad de Alicante; Alicante, Spain.

[3]Aix Marseille Univ, CNRS, Avignon Université, IRD, IMBE; Aix-en-Provence, France.

[4]Laboratorio de Biodiversidad y Funcionamiento Ecosistémico. Instituto de Recursos Naturales y Agrobiología de Sevilla (IRNAS), CSIC; Sevilla, Spain.

[5]Unidad Asociada CSIC-UPO (BioFun). Universidad Pablo de Olavide; Sevilla, Spain.

[6]Department of Planning and Environment, c/o Centre for Ecosystem Science, School of Biological, Earth and Environmental Sciences, University of New South Wales; Sydney, Australia.

[7]Departamento de Ciencias Agrarias y Medio Natural, Escuela Politécnica Superior, Instituto Universitario de Investigación en Ciencias Ambientales de Aragón (IUCA), Universidad de Zaragoza; Huesca, Spain.

[8]Institute of Plant Sciences, University of Bern; Bern, Switzerland.

[9]Institut de Biología Evolutiva (UPF-CSIC); Barcelona, Spain.

[10] Department of Environmental Systems Science, ETH Zurich; Zurich, Switzerland.

[11]Instituto de Ciencias Agrarias, Consejo Superior de Investigaciones Científicas; Madrid, Spain.

[12]Departamento de Ingeniería y Morfología del Terreno, Escuela Técnica Superior de Ingenieros de Caminos, Canales y Puertos, Universidad Politécnica de Madrid; Madrid, Spain.

[13]Departamento de Biología y Geología, Física y Química Inorgánica, Universidad Rey Juan Carlos; Móstoles, Spain.

[14]Instituto Nacional de Tecnología Agropecuaria (INTA), Instituto de Suelos-CNIA; Buenos Aires, Argentina.

[15]Universidad Nacional de Luján, Departamento de Tecnología; Luján, Argentina.

[16]Consejo Nacional de Investigaciones Científicas y Técnicas de Argentina (CONICET); Buenos Aires, Argentina.

[17]Museo Nacional de Ciencias Naturales, Consejo Superior de Investigaciones Científicas; Madrid, Spain.

[18]Key Laboratory for Humid Subtropical Eco-geographical Processes of the Ministry of Education, School of Geographical Science, Fujian Normal University; Fuzhou, China.

[19]Faculty of Veterinary and Agricultural Sciences, The University of Melbourne; Victoria, Australia.

[20]Global Centre for Land-Based Innovation, Western Sydney University; New South Wales, Australia.

[21]Hawkesbury Institute for the Environment, Western Sydney University; New South Wales, Australia.

[22]State Key Laboratory of Urban and Regional Ecology, Research Center for Eco-Environmental Sciences, Chinese Academy of Sciences; Beijing, China.

[23]Freie Universität Berlin, Institute of Biology; Berlin, Germany.

[24]Berlin-Brandenburg Institute of Advanced Biodiversity Research (BBIB); Berlin, Germany.

[25]German Centre for Integrative Biodiversity Research (iDiv) Halle-Jena-Leipzig; Leipzig, Germany.

[26]Leipzig University, Institute of Biology; Leipzig, Germany.

[27]Department of Agricultural and Food Chemistry, Faculty of Sciences, Universidad Autónoma de Madrid; Madrid, Spain.

[28]School of Life Sciences, Arizona State University; Tempe, Arizona, USA.

[29]School of Sustainability, Arizona State University; Tempe, Arizona, USA.

[30]Global Drylands Center, Arizona State University; Tempe, Arizona, USA.

[31]Department of Range Management, Faculty of Natural Resources and Marine Sciences, Tarbiat Modares University; Noor, Mazandaran Province, I. R. Iran.

[32]Instituto Pirenaico de Ecología (IPE, CSIC); Zaragoza, Spain.

[33]Instituto Nacional de Tecnología Agropecuaria (INTA), Estación Experimental Agropecuaria Bariloche; Bariloche, Río Negro, Argentina.

[34]Laboratoire de Recherche: Biodiversité, Biotechnologie, Environnement et Développement Durable (BioDev), Faculté des Sciences, Université M'hamed Bougara de Boumerdès; Boumerdès, Algérie.

[35]Instituto Potosino de Investigación Científica y Tecnológica, A.C.; San Luis Potosí, México.

[36]Instituto Nacional de Tecnología Agropecuaria, Estación Experimental Agropecuaria Catamarca; Catamarca, Argentina.

[37]Laboratory of Range Ecology; Institut des Régions Arides (IRA); Médenine, Tunisia.

[38]University of Potsdam, Plant Ecology and Conservation Biology; Potsdam, Germany.

[39]Laboratory of Ecological and Evolutionary Synthesis, Department of Biology, School of Arts and Sciences, National University of Mongolia; Ulaanbaatar, Mongolia.

[40]School of Forestry, Northern Arizona University; Flagstaff, AZ, USA.

[41]Center for Ecosystem Science and Society, Northern Arizona University; Flagstaff, AZ, USA.

[42]Institute of Soil and Water Conservation, Northwest A & F University; Yangling, Shaanxi, China.

[43]Institute of Soil and Water Conservation, Chinese Academy of Sciences and Ministry of Water Resources; Yangling, Shaanxi, China.

[44]Ecological Plant Geography, Faculty of Geography, University of Marburg; Marburg, Germany.

[45]Plant Ecology Group, University of Tübingen; Tübingen, Germany.

[46]Departamento de Biología, Escuela Politécnica Nacional; Quito, Ecuador.

[47]University of Coimbra, Centre for Functional Ecology, Department of Life Sciences; Coimbra, Portugal.

[48]Universidad Nacional Experimental Simón Rodríguez (UNESR), Instituto de Estudios Científicos y Tecnológicos (IDECYT); Centro de Estudios de Agroecología Tropical (CEDAT); Miranda, Venezuela.

[49]Universidad de Cuenca, Facultad de Ciencias Agropecuarias, Carrera de Ingeniería Agronómica, Grupo de Agroforestería, Manejo y Conservación del paisaje; Cuenca, Ecuador.

[50]Universidade Estadual de Feira de Santana (UEFS), Departamento de Ciências Biológicas; Bahia, Brasil.

[51]Department of Biological Sciences, University of Texas at El Paso; El Paso, TX, USA.

[52]Lendület Seed Ecology Research Group, Institute of Ecology and Botany, Centre for Ecological Research; Vácrátót, Hungary.

[53]Centro de Investigación de la Biodiversidad y Cambio Climático, Universidad Tecnológica Indoamérica; Quito, Ecuador.

[54]School of Earth and Environment, University of Leeds; Leeds, U.K.

[55]Misión Biolóxica de Galicia, CSIC; Pontevedra, Spain

[56]Departamento de Ciencias Biológicas, Universidad Técnica Particular de Loja; Loja, Ecuador.

[57]Universidad de Talca; Talca, Chile.

[58]Instituto de Investigación Interdisciplinario (I^3); Talca, Chile.

[59]Department of Range and Watershed Management, Ferdowsi University of Mashhad; Mashhad, Iran.

[60]Instituto Nacional de Tecnología Agropecuaria EEA Santa Cruz; Río Gallegos, Santa Cruz, Argentina.

[61]Universidad Nacional de la Patagonia Austral; Río Gallegos, Santa Cruz, Argentina.

[62]School of Agriculture, Environmental and Veterinary Sciences, Charles Sturt University; Port Macquarie, Australia.

[63]Department of Natural Resource Science, Thompson Rivers University; British Columbia, Canada.

[64]Department of Environmental Science, Policy and Management, University of California; Berkeley, USA.

[65]Desert Ecology Research Group, School of Life and Environmental Sciences, The University of Sydney; Sydney, Australia.

[66]Institute of Biology, Martin-Luther University Halle Wittenberg; Halle (Saale), Germany.

[67]Institute of Landscape Ecology, University of Münster; Münster, Germany.

[68]Instituto Nacional da Mata Atlântica (INMA); Espírito Santo, Brazil.

[69]Department of Disturbance Ecology, Bayreuth Center of Ecology and Environmental Research BayCEER, University of Bayreuth; Bayreuth, Germany.

[70]Earth Research Institute, University of California Santa Barbara; California, USA.

[71]Centre for Ecology, Evolution and Environmental Changes, Faculdade de Ciências, Universidade de Lisboa; Lisboa, Portugal.

[72]Microbiome@UP, Department of Biochemistry, Genetics and Microbiology, University of Pretoria; Pretoria, South Africa.

[73]Universidad Nacional de Río Negro, Sede Atlántica, CEANPa; Río Negro, Argentina.

[74]Biodiversity Research/ Systematic Botany Group, Institute of Biochemistry and Biology, University of Potsdam; Potsdam, Germany.

[75]Institute of Crop Science and Resource Conservation, University of Bonn; Bonn, Germany.

[76]Department of Plant and Soil Sciences, University of Pretoria; Pretoria, South Africa.

[77]Institute of Botany, Czech Academy of Sciences; Pruhonice, Czech Republic.

[78]Institute Botany Department. State Museum of Natural History Stuttgart; Stuttgart, Germany.

[79]Key Laboratory of Vegetation Ecology of the Ministry of Education, Jilin Songnen Grassland Ecosystem National Observation and Research Station, Institute of Grassland Science, Northeast Normal University; Changchun, China.

[80]Gobabeb-Namib Research Institute; Walvis Bay, Namibia.

[81]Institut d’Écologie et des Sciences de l'Environnement de Paris (iEES-Paris), Sorbonne Université, IRD, CNRS, INRAE, Université Paris Est Creteil, Université de Paris, Centre IRD de France Nord; Bondy, France.

[82]Instituto Interuniversitario de Investigación del Sistema Tierra en Andalucía, Universidad de Jaén; Jaén, Spain.

[83]Departamento de Biología Animal, Biología Vegetal y Ecología. Universidad de Jaén; Jaén, Spain.

[84]Forestry School, INDEHESA, Universidad de Extremadura; Plasencia, Spain.

[85]U.S. Geological Survey, Southwest Biological Science Center; Flagstaff, AZ, USA.

[86]Cátedra de Ecología, Facultad de Agronomía, Universidad de Buenos Aires. Instituto de Investigaciones Fisiológicas y Ecológicas Vinculadas a la Agricultura (IFEVA-CONICET); Ciudad Autónoma de Buenos Aires, Argentina.

[87]Departamento de Botânica, Universidade Federal de Minas Gerais; Minas Gerais, Brazil.

[88]Cátedra de Manejo de Pastizales Naturales, Facultad de Ciencias Agrarias, Universidad Nacional de Catamarca; Catamarca, Argentina.

[89]Department of Forest Engineering, Forest Management Planning and Terrestrial Measurements, Faculty of Silviculture and Forest Engineering, Transilvania University of Brasov; Brasov, Romania

[90]US Geological Survey, Southwest Biological Science Center; Moab, UT, USA.

[91]Normandie Univ, UNIROUEN, INRAE, ECODIV; Rouen, France.

[92]Deparment of Biology, McGill University; Montreal, Quebec, Canada.

[93]Al Quds University; Palestine.

[94]Dead Sea and Arava Science Center; Yotvata, Israel.

[95]South African Environmental Observation Network (SAEON); Phalaborwa, Kruger National Park, South Africa.

[96]Departamento de Botânica e Ecologia, Instituto de Biociências, Universidade Federal de Mato Grosso; Mato Grosso, Brazil.

[97]Department of Geography and Earth Sciences. Aberystwyth University; Wales, U.K.

[98]School of Earth & Space Exploration and School of Life Sciences, Arizona State University; Tempe, AZ, USA.

[99]Centre for Ecosystem Science, School of Biological, Earth and Environmental Sciences, University of New South Wales; Sydney, New South Wales, Australia.

[100]Science Division, Department of Planning, Industry and Environment, New South Wales Government; Buronga, New South Wales, Australia.

[101]Zoology Department, National Museums of Kenya, P.O. Box 40658-00100; Nairobi, Kenya

[102]Department of Earth Sciences, Indiana University-Purdue University Indianapolis (IUPUI); Indianapolis, Indiana, USA.

[103]Department of Natural Resources, Agricultural Research Organization, Institute of Plant Sciences, Gilat Research Center; Mobile Post Negev, Israel.

[104]State Key Laboratory of Desert and Oasis Ecology, Xinjiang Institute of Ecology and Geography, Chinese Academy of Sciences; Urumqi, China.

[105]Université Clermont Auvergne, INRAE, VetAgro Sup, Unité Mixte de Recherche Ecosystème Prairial; Clermont-Ferrand, France.

*Corresponding author. Email: ft.maestre@ua.es

Abstract: Grazing is the most extensive land use worldwide. Yet its impacts on ecosystem services remain uncertain because pervasive interactions among grazing pressure, climate, soil properties, and biodiversity may occur but have never been addressed simultaneously. Using a standardized survey at 98 sites across six continents, we showed that interactions among grazing pressure, climate, soil, and biodiversity are critical to explain the delivery of fundamental ecosystem services across drylands worldwide. Increasing grazing pressure reduced ecosystem service delivery in warmer and species-poor drylands, while positive effects of grazing were observed in colder and species-rich areas. Considering interactions among grazing and local abiotic and biotic factors is key for understanding the fate of dryland ecosystems under climate change and increasing human pressure.

One-Sentence Summary: Interactions among grazing, climate, and biodiversity explain the delivery of ecosystem services across drylands globally.

Main Text:

Grazing accounts for 77% of global agricultural land (*1*), sustains billions of people worldwide, and is closely linked to 10 of 17 UN Sustainable Development Goals (*2*). Despite its importance, there is no consensus on how grazing affects ecosystem services (*3*–*6*), which may depend on the co-evolutionary history between vegetation and herbivores (*3*), grazing pressure (*4*), and local climatic, edaphic, and biodiversity conditions (*7*, *8*). Most field assessments have focused on local to regional scales (*3*, *4*, *6*, *8*), have studied a limited number of taxa −mostly plants− and single ecosystem services (*3*, *4*, *9*), and have not considered domestic and wild herbivores simultaneously. Another major source of uncertainty relates to interactions between grazing pressure and abiotic and biotic features, resulting in strong context-dependent ecological impacts of grazing (*3*, *4*, *10*, *11*). Large-scale, standardized field surveys exploring how such impacts depend on above- and belowground biodiversity, soils, and climate to drive multiple ecosystem services across contrasting regions and environmental contexts are currently lacking, but sorely needed to evaluate whether general patterns emerge beyond these context-dependencies (*12*).

Investigating the effects of grazing pressure across global abiotic and biotic gradients is particularly important in drylands (areas with an aridity index [precipitation/potential evapotranspiration] < 0.65, *13*) because they constitute 78% of rangelands worldwide (*14*) and support around one billion people that rely on grazing by livestock as a critical source of protein and income (*15*). While grazing may have beneficial effects by reducing fuel loads, enhancing primary production and plant diversity under certain conditions (*3*, *16*), increasing grazing pressure is also considered a major driver of rangeland degradation and desertification across drylands worldwide (*17*). These contrasting effects of grazing likely depend on local climate, soil conditions, and both plant and soil diversity, which largely influence dryland functioning (*18*, *19*). However, the interactions of these factors with grazing pressure have never been assessed. Identifying under which environmental conditions and biodiversity levels increasing grazing pressure will favor or detract ecosystem service delivery is a crucial step towards achieving multiple Sustainable Development Goals (*2*) and other international initiatives related to dryland desertification and restoration (*20*).

Here, we used a standardized field survey (*13*) carried out at 98 sites from 25 countries and six continents (Fig. 1 and Movie S1) to assess how the effects of grazing pressure on nine essential ecosystem services depend on biodiversity, climate, and soil conditions across global drylands. Each site included a collection of three to four 45 m × 45 m plots representing local gradients of grazing pressure (from ungrazed or low grazing pressure to high grazing pressure; *13*), resulting in a total of 326 plots. These gradients were mostly driven by livestock (fig. S1), although wild herbivores were also present in each site and taken into account. In each plot, we assessed vascular plant, mammalian herbivore (accounting for domestic and wild herbivores) and belowground (soil bacteria, fungi, protists, and invertebrates) diversity, and multiple regulating (water regulation, soil carbon storage, organic matter decomposition, and erosion control), supporting (soil fertility and aboveground plant biomass and its temporal stability), and provisioning (wood quantity, forage quantity, and quality) ecosystem services (table S1). Our survey captured most climatic conditions harboring livestock grazing in drylands, as well as a wide range of ecosystem types, soil properties, plant, soil, and mammalian diversities, and grazing pressure levels (figs. S2 to S9 and table S2). These unique features of our global study rendered grazing pressure largely independent of climate, soil, and biodiversity attributes (*13*, table S3), and allowed us to: (i) evaluate the main and interactive effects of grazing pressure, climate, soil properties, and biodiversity on ecosystem service delivery across global drylands;

(ii) identify the environmental and biodiversity conditions under which the effects of grazing pressure on ecosystem services are positive or negative; and (iii) simultaneously assess relationships among plant, soil, and mammalian herbivore diversity and multiple ecosystem services.

We fitted linear mixed models to data from all sites and grazing pressure levels, and applied a multimodel inference procedure based on Akaike Information Criterion (AIC) to select the set of best-fitting models (i.e., those within a ΔAIC <2, *13*). We also considered potential indirect effects of grazing through the modification of local biodiversity and soil parameters using confirmatory path analyses (*13*). We found that increasing grazing pressure affects ecosystem services through direct (no significant indirect effects through changes in soil properties or biodiversity were found; figs. S10 and S11 and tables S4 to S12) and interactive (grazing × climate, grazing × soil properties, or grazing × biodiversity interactions were selected in 86% of the best-fitting models, Fig. 2 and tables S13 to S28) effects.

Grazing × climate interactions were selected in 48% of the best-fitting models (fig. S12), with grazing primarily interacting with mean annual temperature (40% of the best-fitting models) and rainfall seasonality (20% of the best-fitting models), and to a lesser extent with mean annual precipitation (9% of the best-fitting models). A negative relationship between mean annual temperature and soil carbon storage, organic matter decomposition, and erosion control was found under high, but not under low, grazing pressure (Fig. 3A, 3B, and 3C). Our results provide an empirical validation of the importance of interactions among climate change drivers, grazing, and soil carbon storage predicted by global modeling studies (*21*). They also indicate that considering grazing pressure can improve our capacity to assess soil carbon-temperature feedbacks, a key process involved in climate warming (*22*).

Soil texture also regulated grazing pressure effects on multiple ecosystem services (grazing × sand content interactions were selected in 37% of the best-fitting models; fig. S12). These ecosystem services include soil fertility, which declined more steeply under high grazing pressure (Fig. 3E), wood quantity, which increased under high but declined under low grazing pressure (Fig. 3G), and forage quality, which declined under high but increased under low grazing pressure (Fig. 3I), as sand content increased. These findings illustrate how increases in grazing pressure interact with soil properties to either increment or reduce the delivery of multiple ecosystem services.

Biodiversity impacts on ecosystem functioning and services are typically examined in isolation from other drivers in experimental and observational studies (*23*). However, we found grazing × biodiversity interactions in 44% of the best-fitting models (Fig. 2 and fig. S12). For instance, increasing grazing pressure shifted the relationships between plant species richness and water regulation from positive to negative (Fig. 3D), and between plant species richness and both wood quantity and aboveground plant biomass and its temporal stability from negative to positive (Fig. 3F and 3G). We also found positive relationships among plant species richness and soil carbon storage, organic matter decomposition, erosion control, and both forage quality and quantity (Fig. 3A, 3B, 3C, 3H, and 3I), and between belowground diversity and organic matter decomposition (fig. S13), irrespective of grazing pressure. These results broaden and validate previous findings on the relationship between biodiversity and ecosystem functioning (*18*, *19*), and support arguments for conserving and restoring diverse plant communities to prevent land degradation, increase forage production, and mitigate climate change in grazed drylands (*20*).

Mammalian herbivore richness – selected in 33% of the best-fitting models (fig. S12) – was positively related to multiple ecosystem services. Greater herbivore richness positively correlated with soil carbon storage regardless of grazing pressure (fig. S13), with aboveground plant biomass and its temporal stability under high grazing pressure (fig. S14), and with forage quality under low grazing pressure (fig. S15). Both domestic and wild herbivore species can exhibit strong feeding niche differences (*24*, *25*), thus increasing their diversity can enhance ecosystem functioning (*25*). Despite a renewed interest in mixed-species grazing, studies have been conducted only at a handful of sites or with a limited suite of herbivores (*25*-*27*). Our findings provide empirical evidence of the potential benefits of increasing herbivore richness to enhance the delivery of key ecosystem services across contrasting environmental and biodiversity conditions. They also suggest that efforts to promote diverse grazing systems may enhance soil carbon storage and reduce negative impacts of increased grazing pressure. To date, such results have only been modeled or observed locally (*26*, *27*).

The multiple interactions observed highlight that the effect of grazing pressure on ecosystem services can be positive or negative depending on local climate, soil, and biodiversity conditions (Fig. 4). On average, increasing grazing pressure had positive effects on ecosystem services in colder sites with high plant species richness, but negative effects in warmer sites with high rainfall seasonality and low plant species richness (Fig. 4E and 4I). When sets of ecosystem services were considered separately, responses to grazing pressure ranged from mostly neutral to positive (regulating and supporting services, Fig. 4B and 4C), and from negative to neutral (provisioning services, Fig. 4D). These results allow us to identify ecological conditions under which ecosystem services are positively or negatively associated with changes in grazing pressure (Fig. 4 and figs. S16 to S18), and to frame novel hypotheses that explore the local context-dependencies of grazing impacts. For instance, we observed negative effects of increasing grazing pressure on ecosystem services in plant species-poor drylands, as reported in recent local-scale studies (e.g., *11*), while positive effects of grazing were mostly observed in species-rich drylands. Thus, protecting biodiversity in species-rich areas or restoring it in species-poor areas could minimize some of the negative effects of increasing grazing pressure on ecosystem service delivery (fig. S19).

The effects of increasing grazing pressure on ecosystem services were mostly negative in warmer drylands (Fig. 4 and fig. S17), where a large proportion of the human population relies heavily on livestock for subsistence (*15*). Limiting grazing pressure through livestock removal is neither socially nor economically feasible in these areas (2), yet they are expected to experience high warming rates and water shortages under most climate change scenarios (*17*). Our results thus suggest that grazing pressure may interact with climate change to reduce ecosystem service delivery in warmer drylands, with potentially devastating implications for the fate of these ecosystems (e.g., increased land degradation and desertification; *17*) and their inhabitants (e.g., greater poverty, migration, and/or social unrest; *28*). Although dryland pastoralists have historically adopted strategies to cope with environmental uncertainty (e.g., nomadism, transhumance), benefits of these strategies will wane if livestock concentrates in particular areas due to resource scarcity or droughts (*29*).

In summary, our findings urge us to account for interactions among grazing and local abiotic and biotic factors when assessing ecosystem service delivery in drylands. They also illustrate those climate change and biodiversity loss drivers that are the most likely to interact with increases in grazing pressure. Understanding these drivers is critical to predict the fate of dryland ecosystems under increasing temperature, biodiversity loss, and demand for animal products. Our study also allowed us to overcome uncertainties in grazing assessments arising from the use of unstandardized data (*30*), and provides abundant ground data to validate remote sensing products used when mapping and modeling grazing impacts at the global scale (*5*). Finally, we deliver empirical evidence of the positive links between mammalian herbivore richness and the provision of multiple ecosystem services across contrasting environmental conditions, plant/soil diversities, and grazing pressure levels. Together, our work addresses a key knowledge gap that can lead to better management of drylands, the largest rangeland area on Earth.

References and Notes

1. H. Ritchie, M. Roser, *Land Use. Published online at OurWorldInData.org.* Retrieved from https://ourworldindata.org/land-use (2013).
2. Z. Mehrabi, M. Gill, M. van Wijk, M. Herrero, N. Ramankutty, Livestock policy for sustainable development. *Nat. Food* **1**, 160–165 (2020).
3. D. G. Milchunas, W. K. Lauenroth, Quantitative effects of grazing on vegetation and soils over a global range of environments. *Ecol. Monogr.* **63**, 328–366 (1993).
4. D. J. Eldridge, A. G. B. Poore, M. Ruiz-Colmenero, M. Letnic, S. Soliveres, Ecosystem structure, function, and composition in rangelands are negatively affected by livestock grazing. *Ecol. Appl.* **26**, 1273–1283 (2016).
5. K. Petz, R. Alkemade, M. Bakkenes, C. J. E. Schulp, M. van der Velde, R. Leemans, Mapping and modelling trade-offs and synergies between grazing intensity and ecosystem services in rangelands using global-scale datasets and models. *Glob. Environ. Change*. **29**, 223–234 (2014).
6. D. J. Eldridge, M. Delgado-Baquerizo, Continental-scale impacts of livestock grazing on ecosystem supporting and regulating services. *Land Degrad. Dev.* **28**, 1473–1481

(2017).

7. J. A. Mavromihalis, J. Dorrough, S. G. Clark, V. Turner, C. Moxham, Manipulating livestock grazing to enhance native plant diversity and cover in native grasslands. *Rangel. J.* **35**, 95–108 (2013).

8. J. J. Gaitán, D. E. Bran, G. E. Oliva, M. R. Aguiar, G. G. Buono, D. Ferrante, V. Nakamatsu, G. Ciari, J. M. Salomone, V. Massara, G. G. Martínez, F. T. Maestre, Aridity and overgrazing have convergent effects on ecosystem structure and functioning in Patagonian rangelands. *Land Degrad. Dev.* **29**, 210–218 (2018).

9. P. D'Ottavio, M. Francioni, L. Trozzo, E. Sedić, K. Budimir, P. Avanzolini, M. F. Trombetta, C. Porqueddu, R. Santilocchi, M. Toderi, Trends and approaches in the analysis of ecosystem services provided by grazing systems: A review. *Grass Forage Sci.* **73**, 15–25 (2018).

10. A. Linstädter, J. Schellberg, K. Brüser, C. A. Moreno García, R. J. Oomen, C. C. du Preez, J. C. Ruppert, F. Ewert, Are there consistent grazing indicators in drylands? Testing plant functional types of various complexity in South Africa's grassland and savanna biomes. *PLoS One*. **9**, e104672 (2014).

11. M. Liang, C. Liang, Y. Hautier, K. R. Wilcox, S. Wang, Grazing-induced biodiversity loss impairs grassland ecosystem stability at multiple scales. *Ecol. Lett*. **24**, 2054–2064 (2021).

12. P. Manzano, D. Burgas, L. Cadahía, J. T. Eronen, Á. Fernández-Llamazares, S. Bencherif, Ø. Holand, O. Seitsonen, B. Byambaa, M. Fortelius, M. E. Fernández-Giménez, K. A. Galvin, M. Cabeza, N. Chr. Stenseth, Toward a holistic understanding of pastoralism. *One Earth* **4**, 651–665 (2021).

13. See Materials and Methods.

14. ILRI, IUCN, FAO, WWF, UNEP, ILC, *Rangelands Atlas* (ILRI, Nairobi, 2021).

15. UN-EMG, *Global Drylands: A UN System-Wide Response*. (United Nations Environment World Conservation Monitoring Centre, Cambridge, 2011).

16. S. E. Koerner, M. D. Smith, D. E. Burkepile, N. P. Hanan, M. L. Avolio, S. L. Collins, A. K. Knapp, N. P. Lemoine, E. J. Forrestel, S. Eby, D. I. Thompson, G. A. Aguado-Santacruz, J. P. Anderson, T. M. Anderson, A. Angassa, S. Bagchi, E. S. Bakker, G. Bastin, L. E. Baur, K. H. Beard, E. A. Beever, P. J. Bohlen, E. H. Boughton, D. Canestro, A. Cesa, E. Chaneton, J. Cheng, C. M. D'Antonio, C. Deleglise, F. Dembélé, J. Dorrough, D. J. Eldridge, B. Fernandez-Going, S. Fernández-Lugo, L. H. Fraser, B. Freedman, G. García-Salgado, J. R. Goheen, L. Guo, S. Husheer, M. Karembé, J. M. H. Knops, T. Kraaij, A. Kulmatiski, M.-M. Kytöviita, F. Lezama, G. Loucougaray, A. Loydi, D. G. Milchunas, S. J. Milton, J. W. Morgan, C. Moxham, K. C. Nehring, H. Olff, T. M. Palmer, S. Rebollo, C. Riginos, A. C. Risch, M. Rueda, M. Sankaran, T. Sasaki, K. A. Schoenecker, N. L. Schultz, M. Schütz, A. Schwabe, F. Siebert, C. Smit, K. A. Stahlheber, C. Storm, D. J. Strong, J. Su, Y. V. Tiruvaimozhi, C. Tyler, J. Val, M. L. Vandegehuchte, K. E. Veblen, L. T. Vermeire, D. Ward, J. Wu, T. P. Young, Q. Yu, T. J. Zelikova, Change in dominance determines herbivore effects on plant biodiversity. *Nat. Ecol. Evol.* **2**, 1925–1932 (2018).

17. A. Mirzabaev, J. Wu, J. Evans, F. García-Oliva, I. A. Hussein, M. H. Iqbal, J. Kimutai, T. Knowles, F. Meza, D. Nedjroaoui, "Desertification" in *Climate Change and Land: an IPCC special report on climate change, desertification, land degradation, sustainable land management, food security, and greenhouse gas fluxes in terrestrial*

ecosystems, P.R. Shukla, J. Skea, E. Calvo Buendia, V. Masson-Delmotte, H.-O. Pörtner, D.C. Roberts, P. Zhai, R. Slade, S. Connors, R. van Diemen, M. Ferrat, E. Haughey, S. Luz, S. Neogi, M. Pathak, J. Petzold, J. Portugal Pereira, P. Vyas, E. Huntley, K. Kissick, M. Belkacemi, J. Malley, Eds (In press, 2019), pp. 249-344.

18. F. T. Maestre, J. L. Quero, N. J. Gotelli, A. Escudero, V. Ochoa, M. Delgado-Baquerizo, M. García-Gómez, M. A. Bowker, S. Soliveres, C. Escolar, P. García-Palacios, M. Berdugo, E. Valencia, B. Gozalo, A. Gallardo, L. Aguilera, T. Arredondo, J. Blones, B. Boeken, D. Bran, A. A. Conceição, O. Cabrera, M. Chaieb, M. Derak, D. J. Eldridge, C. I. Espinosa, A. Florentino, J. Gaitán, M. G. Gatica, W. Ghiloufi, S. Gómez-González, J. R. Gutiérrez, R. M. Hernández, X. Huang, E. Huber-Sannwald, M. Jankju, M. Miriti, J. Monerris, R. L. Mau, E. Morici, K. Naseri, A. Ospina, V. Polo, A. Prina, E. Pucheta, D. A. Ramírez-Collantes, R. Romão, M. Tighe, C. Torres-Díaz, J. Val, J. P. Veiga, D. Wang, E. Zaady, Plant species richness and ecosystem multifunctionality in global drylands. *Science*. **335**, 214–218 (2012).

19. M. Delgado-Baquerizo, F. T. Maestre, P. B. Reich, T. C. Jeffries, J. J. Gaitan, D. Encinar, M. Berdugo, C. D. Campbell, B. K. Singh, Microbial diversity drives multifunctionality in terrestrial ecosystems. *Nat. Commun.* **7**, 1–8 (2016).

20. N. M. Gadzama, Attenuation of the effects of desertification through sustainable development of Great Green Wall in the Sahel of Africa. *World J. Sci. Technol. Sustain. Dev.* **14**, 279–289 (2017).

21. J. Chang, P. Ciais, T. Gasser, P. Smith, M. Herrero, P. Havlík, M. Obersteiner, B. Guenet, D. S. Goll, W. Li, V. Naipal, S. Peng, C. Qiu, H. Tian, N. Viovy, C. Yue, D. Zhu, Climate warming from managed grasslands cancels the cooling effect of carbon

sinks in sparsely grazed and natural grasslands. *Nat. Commun.* **12**, 118 (2021).

22. P. García-Palacios, T. W. Crowther, M. Dacal, I. P. Hartley, S. Reinsch, R. Rinnan, J. Rousk, J. van den Hoogen, J.-S. Ye, M. A. Bradford, Evidence for large microbial-mediated losses of soil carbon under anthropogenic warming. *Nat. Rev. Earth Environ.* **2**, 507–517 (2021).
23. J. E. Duffy, C. M. Godwin, B. J. Cardinale, Biodiversity effects in the wild are common and as strong as key drivers of productivity. *Nature*. **549**, 261–264 (2017).
24. E. S. Forbes, J. H. Cushman, D. E. Burkepile, T. P. Young, M. Klope, H. S. Young, Synthesizing the effects of large, wild herbivore exclusion on ecosystem function. *Funct. Ecol.* **33**, 1597–1610 (2019).
25. L. Wang, M. Delgado-Baquerizo, D. Wang, F. Isbell, J. Liu, C. Feng, J. Liu, Z. Zhong, H. Zhu, X. Yuan, Q. Chang, C. Liu, Diversifying livestock promotes multidiversity and multifunctionality in managed grasslands. *Proc. Natl. Acad. Sci. U. S. A.* **116**, 6187–6192 (2019).
26. J. P. G. M. Cromsigt, M. te Beest, G. I. H. Kerley, M. Landman, E. le Roux, F. A. Smith, Trophic rewilding as a climate change mitigation strategy? *Philos. Trans. R. Soc. B Biol. Sci.* **373**, 20170440 (2018).
27. N. Pettorelli, S. M. Durant, J. T. du Toit, Eds., *Rewilding* (Cambridge University Press, Cambridge, 2019).
28. C. Almer, J. Laurent-Lucchetti, M. Oechslin, Water scarcity and rioting: Disaggregated evidence from Sub-Saharan Africa. *J. Environ. Econ. Manag.* **86**, 193–209 (2017).
29. S. A. Mousavi, M. Sarshad Ghahfarokhi, S. Soltani Koupaei, Negative impacts of

nomadic livestock grazing on common rangelands' function in soil and water conservation. *Ecol. Indic.* **110**, 105946 (2020).

30. T. Fetzel, P. Havlik, M. Herrero, J. O. Kaplan, T. Kastner, C. Kroisleitner, S. Rolinski, T. Searchinger, P. M. V. Bodegom, S. Wirsenius, K.-H. Erb, Quantification of uncertainties in global grazing systems assessment. *Glob. Biogeochem. Cycles*. **31**, 1089–1102 (2017).

31. D. J. Pratt, M. D. Gwynne, *Rangeland management and ecology in East Africa* (Hodder & Stoughton, London, 1977).

32. N. Middleton, D.S.G. Thomas, Eds, *UNEP World Atlas of Desertification* (Edward Arnold, London, 1992).

33. M. Gilbert, G. Nicolas, G. Cinardi, T. P. Van Boeckel, S. O. Vanwambeke, G. R. Wint, T. P. Robinson, Global distribution data for cattle, buffaloes, horses, sheep, goats, pigs, chickens and ducks in 2010. *Sci. Data*. **5**, 180227 (2018).

34. L. Sörensen, *A Spatial Analysis Approach to the Global Delineation of Dryland Areas of Relevance to the CBD Programme of Work on Dry and Sub-Humid Lands*. (UNEP-WCMC, Cambridge, UK, 2007).

35. S. E. Fick, R. J. Hijmans, WorldClim 2: new 1-km spatial resolution climate surfaces for global land areas. *Int. J. Climatol.* **37**, 4302–4315 (2017).

36. A. Trabucco, R. J. Zomer, Global aridity index and potential evapotranspiration (ET0) climate database v2. figshare. Dataset. https://doi.org/10.6084/m9.figshare.7504448.v3 (2019).

37. IUSS Working Group WRB, *World Reference Base for Soil Resources* 2006 (FAO, Rome, 2006).

38. C. Plaza, C. Zaccone, K. Sawicka, A. M. Méndez, A. Tarquis, G. Gascó, G. Heuvelink, E. A. Schuur, F. T. Maestre, Soil resources and element stocks in drylands to face global issues. *Sci. Rep.* **8**, 13788 (2018).

39. J. Bellot, F. T. Maestre, N. Hernández, Spatio-temporal dynamics of chlorophyll fluorescence in a semi-arid Mediterranean shrubland. *J. Arid Environ.* **58**, 295–308 (2004).

40. A. Gómez-Plaza, M. Martınez-Mena, J. Albaladejo, V. M. Castillo, Factors regulating spatial distribution of soil water content in small semiarid catchments. *J. Hydrol.* **253**, 211–226 (2001).

41. P. Kutiel, H. Lavee, Effect of slope aspect on soil and vegetation properties along an aridity transect. *Isr. J. Plant Sci.* **47**, 169–178 (1999).

42. P. B. Adler, S. A. Hall, The development of forage production and utilization gradients around livestock watering points. *Landsc. Ecol.* **20**, 319–333 (2005).

43. R. J. Fensham, R. J. Fairfax, Water-remoteness for grazing relief in Australian arid-lands. *Biol. Conserv.* **141**, 1447–1460 (2008).

44. S. W. Todd, Gradients in vegetation cover, structure and species richness of Nama-Karoo shrublands in relation to distance from livestock watering points. *J. Appl. Ecol.* **43**, 293–304 (2006).

45. R. J. Fensham, R. J. Fairfax, J. M. Dwyer, Vegetation responses to the first 20 years of cattle grazing in an Australian desert. *Ecology*. **91**, 681–692 (2010).

46. H. J. R. Pringle, J. Landsberg, Predicting the distribution of livestock grazing pressure in rangelands. *Austral Ecol.* **29**, 31–39 (2004).

47. S. O. Jawuoro, O. K. Koech, G. N. Karuku, J. S. Mbau, Plant species composition and

diversity depending on piospheres and seasonality in the southern rangelands of Kenya. *Ecol. Process.* **6**, 16 (2017).

48. V. Chillo, R. A. Ojeda, M. Anand, J. F. Reynolds, A novel approach to assess livestock management effects on biodiversity of drylands. *Ecol. Indic.* **50**, 69–78 (2015).

49. E. Shahriary, H. Azarnivand, M. Jafary, M. M. Saravi, M. R. Javadi, Response of Landscape Function to Grazing Pressure Around Mojen Piosphere. *Res. J. Environ. Sci.* **12**, 83–89 (2018).

50. M. Nsinamwa, N. Moleele, R. Sebego, Vegetation patterns and nutrients in relation to grazing pressure and soils in the sandveld and hardveld communal grazing areas of Botswana. *Afr. J. Range Forage Sci.* **22**, 17–28 (2005).

51. R. Teague, F. Provenza, U. Kreuter, T. Steffens, M. Barnes, Multi-paddock grazing on rangelands: Why the perceptual dichotomy between research results and rancher experience? *J. Environ. Manage.* **128**, 699–717 (2013).

52. G. R. Oñatibia, M. R. Aguiar, Paddock size mediates the heterogeneity of grazing impacts on vegetation. *Rangel. Ecol. Manag.* **71**, 470–480 (2018).

53. D. R. Kemp, K. Behrendt, W. B. Badgery, G. D. Han, P. Li, Y. Zhang, J. Wu, F. J. Hou, Chinese degraded grasslands–pathways for sustainability. *Rangel. J.* **42**, 339–346 (2020).

54. E. T. Borer, W. S. Harpole, P. B. Adler, E. M. Lind, J. L. Orrock, E. W. Seabloom, M. D. Smith, Finding generality in ecology: a model for globally distributed experiments. *Methods Ecol. Evol.* **5**, 65–73 (2014).

55. L. Yahdjian, O. E. Sala, J. M. Piñeiro-Guerra, A. K. Knapp, S. L. Collins, R. P.

Phillips, M. D. Smith, Why Coordinated Distributed Experiments Should Go Global. *BioScience*. **71**, 918–927 (2021).

56. M. Pärtel, C. P. Carmona, M. Zobel, M. Moora, K. Riibak, R. Tamme, DarkDivNet – A global research collaboration to explore the dark diversity of plant communities. *J. Veg. Sci.* **30**, 1039–1043 (2019).

57. L. Estes, P. R. Elsen, T. Treuer, L. Ahmed, K. Caylor, J. Chang, J. J. Choi, E. C. Ellis, The spatial and temporal domains of modern ecology. *Nat. Ecol. Evol.* **2**, 819–826 (2018).

58. D. D. Briske, J. D. Derner, J. R. Brown, S. D. Fuhlendorf, W. R. Teague, K. M. Havstad, R. L. Gillen, A. J. Ash, W. D. Willms, Rotational Grazing on Rangelands: Reconciliation of Perception and Experimental Evidence. *Rangel. Ecol. Manag.* **61**, 3–17 (2008).

59. G. D. Schwenke, M. B. Peoples, G. L. Turner, D. F. Herridge, Does nitrogen fixation of commercial, dryland chickpea and faba bean crops in north-west New South Wales maintain or enhance soil nitrogen? *Aust. J. Exp. Agric.* **38**, 61–70 (1998).

60. J. J. Gaitán, D. Bran, G. Oliva, G. Ciari, V. Nakamatsu, J. Salomone, D. Ferrante, G. Buono, V. Massara, G. Humano, D. Celdrán, W. Opazo, F. T. Maestre, Evaluating the performance of multiple remote sensing indices to predict the spatial variability of ecosystem structure and functioning in Patagonian steppes. *Ecol. Indic.* **34**, 181–191 (2013).

61. A. Dara, M. Baumann, M. Freitag, N. Hölzel, P. Hostert, J. Kamp, D. Müller, A. V. Prishchepov, T. Kuemmerle, Annual Landsat time series reveal post-Soviet changes in grazing pressure. *Remote Sens. Environ.* **239**, 111667 (2020).

62. W. Hanke, J. Böhner, N. Dreber, N. Jürgens, U. Schmiedel, D. Wesuls, J. Dengler, The impact of livestock grazing on plant diversity: an analysis across dryland ecosystems and scales in southern Africa. *Ecol. Appl.* **24**, 1188–1203 (2014).

63. J. D. Derner, D. J. Augustine, D. A. Frank, Does Grazing Matter for Soil Organic Carbon Sequestration in the Western North American Great Plains? *Ecosystems* **22**, 1088–1094 (2019).

64. A. J. Bisigato, M. B. Bertiller, Grazing effects on patchy dryland vegetation in northern Patagonia. *J. Arid Environ.* **36**, 639–653 (1997).

65. R. P. Piana, S. J. Marsden, Impacts of cattle grazing on forest structure and raptor distribution within a neotropical protected area. *Biodivers. Conserv.* **23**, 559–572 (2014).

66. A. J. Plumptre, S. Harris, Estimating the biomass of large mammalian herbivores in a tropical montane forest: a method of faecal counting that avoids assuming a "steady state" system. *J. Appl. Ecol.* **32**, 111–120 (1995).

67. J. Val, D. J. Eldridge, S. K. Travers, I. Oliver, Livestock grazing reinforces the competitive exclusion of small-bodied birds by large aggressive birds. *J. Appl. Ecol.* **55**, 1919–1929 (2018).

68. F. F. C. Marques, S. T. Buckland, D. Goffin, C. E. Dixon, D. L. Borchers, B. A. Mayle, A. J. Peace, Estimating deer abundance from line transect surveys of dung: sika deer in southern Scotland. *J. Appl. Ecol.* **38**, 349–363 (2001).

69. T. Miyashita, M. Suzuki, D. Ando, G. Fujita, K. Ochiai, M. Asada, Forest edge creates small-scale variation in reproductive rate of sika deer. *Popul. Ecol.* **50**, 111–120 (2008).

70. C. N. Johnson, P. J. Jarman, Macropod studies at Wallaby Creek. 6. A validation of the use of dung-pellet counts for measuring absolute densities of populations of macropodids. *Wildl. Res.* **14**, 139–145 (1987).

71. S. D. Albon, M. J. Brewer, S. O'brien, A. J. Nolan, D. Cope, Quantifying the grazing impacts associated with different herbivores on rangelands. *J. Appl. Ecol.* **44**, 1176–1187 (2007).

72. B. Howland, D. Stojanovic, I. J. Gordon, A. D. Manning, D. Fletcher, D. B. Lindenmayer, Eaten out of house and home: impacts of grazing on ground-dwelling reptiles in Australian grasslands and grassy woodlands. *PloS One*. **9**, e105966 (2014).

73. P. R. Hesse, The identification of the spoor and dung of East African mammals. Part 1. The Antelopes. *J. East Africa Nat. Hist. Soc.* **22**, 107–110 (1954).

74. B. Triggs, *Tracks, scats, and other traces: a field guide to Australian mammals.* (Oxford University Press, USA, 2004).

75. J. Landsberg, J. Stol, W. Muller, Telling the sheep (dung) from the goats'. *Rangel. J.* **16**, 122–134 (1994).

76. C. McLaren, *Dry sheep equivalents for comparing different classes of livestock. Notes Series AG0590.* (Department of Natural Resources and Environment: Melbourne, 1997).

77. R. T. Lange, M. C. Willcocks, The relation between sheep-time spent and egesta accumulated within an arid zone paddock. *Aust. J. Exp. Agric.* **18**, 764–767 (1978).

78. N. Lunt, A. E. Bowkett, A. B. Plowman, Implications of assumption violation in density estimates of antelope from dung-heap counts: a case study on grey duiker (Sylvicapra grimmia) in Zimbabwe. *Afr. J. Ecol.* **45**, 382–389 (2007).

79. D. M. Kimuyu, K. E. Veblen, C. Riginos, R. M. Chira, J. M. Githaiga, T. P. Young, Influence of cattle on browsing and grazing wildlife varies with rainfall and presence of megaherbivores. *Ecol. Appl.* **27**, 786–798 (2017).

80. H. B. Rasmussen, O. Kahindi, F. Vollrath, I. Douglas-Hamilton, Estimating elephant densities from wells and droppings in dried out riverbeds. *Afr. J. Ecol.* **43**, 312–319 (2005).

81. M. Stumpp, K. Wesche, V. Retzer, G. Miehe, Impact of Grazing Livestock and Distance from Water Source on Soil Fertility in Southern Mongolia. *Mt. Res. Dev.* **25**, 244–251 (2005).

82. C. Goutte, P. Toft, E. Rostrup, F. Å. Nielsen, L. K. Hansen, On Clustering fMRI Time Series. *NeuroImage*. **9**, 298–310 (1999).

83. R. T. Lange, The piosphere: Sheep track and dung patterns. *J Range Manag*. **22**, 396 (1969).

84. I. Stavi, E. D. Ungar, H. Lavee, P. Sarah, Livestock Modify Ground Surface Microtopography and Penetration Resistance in a Semi-Arid Shrubland. *Arid Land Res. Manag.* **23**, 237–247 (2009).

85. Maestre, F. T., D. E. Eldridge, N. Gross, Y. Le Bagousse-Pinguet, H. Saiz, B. Gozalo, V. Ochoa, J. J. Gaitán, The BIODESERT survey: Assessing the impacts of grazing on the structure and functioning of global drylands. *Web Ecol.* (in press).

86. E. B. Levy, E. A. Madden, The point method for pasture analysis. *N. Z. J. Agri*. **46**, 267–279 (1933).

87. W. G. Whitford, *Ecology of Desert Systems* (Academic Press, San Diego, 2002).

88. C. E. Pake, D. L. Venable, Seed banks in desert annuals: Implications for persistence

and coexistence in variable environments. *Ecology* **77**, 1427–1435 (1996).

89. N. Pérez-Harguindeguy, S. Díaz, E. Garnier, S. Lavorel, H. Poorter, P. Jaureguiberry, M. S. Bret-Harte, W. K. Cornwell, J. M. Craine, D. E. Gurvich, C. Urcelay, E. J. Veneklaas, P. B. Reich, L. Poorter, I. J. Wright, P. Ray, L. Enrico, J. G. Pausas, A. C. de Vos, N. Buchmann, G. Funes, F. Quétier, J. G. Hodgson, K. Thompson, H. D. Morgan, H. ter Steege, M. G. A. van der Heijden, L. Sack, B. Blonder, P. Poschlod, M. V. Vaieretti, G. Conti, A. C. Staver, S. Aquino, J. H. C. Cornelissen, New handbook for standardised measurement of plant functional traits worldwide. *Aust. J. Bot.* **61**, 167–234 (2013).

90. C. A. Schneider, W. S. Rasband, K. W. Eliceiri, NIH Image to ImageJ: 25 years of image analysis. *Nat. Methods*. **9**, 671–675 (2012).

91. T. A. Kettler, J. W. Doran, T. L. Gilbert, Simplified method for soil particle-size determination to accompany soil-quality analyses. *Soil Sci. Soc. Am. J.* **65**, 849–852 (2001).

92. J. S. Lefcheck, J. E. K. Byrnes, F. Isbell, L. Gamfeldt, J. N. Griffin, N. Eisenhauer, M. J. S. Hensel, A. Hector, B. J. Cardinale, J. E. Duffy, Biodiversity enhances ecosystem multifunctionality across trophic levels and habitats. *Nat. Commun.* **6**, 1–7 (2015).

93. B. J. Cardinale, K. L. Matulich, D. U. Hooper, J. E. Byrnes, E. Duffy, L. Gamfeldt, P. Balvanera, M. I. O'Connor, A. Gonzalez, The functional role of producer diversity in ecosystems. *Am. J. Bot.* **98**, 572–592 (2011).

94. F. van der Plas, Biodiversity and ecosystem functioning in naturally assembled communities. *Biol. Rev.* **94**, 1220–1245 (2019).

95. D. P. Herlemann, M. Labrenz, K. Jürgens, S. Bertilsson, J. J. Waniek, A. F.

Andersson, Transitions in bacterial communities along the 2000 km salinity gradient of the Baltic Sea. *ISME J.* **5**, 1571–1579 (2011).

96. L. A. Amaral-Zettler, E. A. McCliment, H. W. Ducklow, S. M. Huse, A method for studying protistan diversity using massively parallel sequencing of V9 hypervariable regions of small-subunit ribosomal RNA genes. *PloS One* **4**, e6372 (2009).

97. T. Stoeck, D. Bass, M. Nebel, R. Christen, M. D. Jones, H.-W. BREINER, T. A. Richards, Multiple marker parallel tag environmental DNA sequencing reveals a highly complex eukaryotic community in marine anoxic water. *Mol. Ecol.* **19**, 21–31 (2010).

98. R. C. Edgar, Search and clustering orders of magnitude faster than BLAST. *Bioinformatics*. **26**, 2460–2461 (2010).

99. R. C. Edgar, https://www.biorxiv.org/content/10.1101/081257v1 (2016).

100. R. C. Edgar, H. Flyvbjerg, Error filtering, pair assembly and error correction for next-generation sequencing reads. *Bioinformatics*. **31**, 3476–3482 (2015).

101. C. Quast, E. Pruesse, P. Yilmaz, J. Gerken, T. Schweer, P. Yarza, J. Peplies, F. O. Glöckner, The SILVA ribosomal RNA gene database project: improved data processing and web-based tools. *Nucleic Acids Res.* **41**, D590–D596 (2012).

102. L. Guillou, D. Bachar, S. Audic, D. Bass, C. Berney, L. Bittner, C. Boutte, G. Burgaud, C. de Vargas, J. Decelle, The Protist Ribosomal Reference database (PR2): a catalog of unicellular eukaryote small sub-unit rRNA sequences with curated taxonomy. *Nucleic Acids Res.* **41**, D597–D604 (2012).

103. J. G. Caporaso, J. Kuczynski, J. Stombaugh, K. Bittinger, F. D. Bushman, E. K. Costello, N. Fierer, A. G. Peña, J. K. Goodrich, J. I. Gordon, QIIME allows analysis of

high-throughput community sequencing data. *Nat. Methods* **7**, 335–336 (2010).

104. E. Allan, O. Bossdorf, C. F. Dormann, D. Prati, M. M. Gossner, T. Tscharntke, N. Blüthgen, M. Bellach, K. Birkhofer, S. Boch, S. Böhm, C. Börschig, A. Chatzinotas, S. Christ, R. Daniel, T. Diekötter, C. Fischer, T. Friedl, K. Glaser, C. Hallmann, L. Hodac, N. Hölzel, K. Jung, A. M. Klein, V. H. Klaus, T. Kleinebecker, J. Krauss, M. Lange, E. K. Morris, J. Müller, H. Nacke, E. Pašalić, M. C. Rillig, C. Rothenwöhrer, P. Schall, C. Scherber, W. Schulze, S. A. Socher, J. Steckel, I. Steffan-Dewenter, M. Türke, C. N. Weiner, M. Werner, C. Westphal, V. Wolters, T. Wubet, S. Gockel, M. Gorke, A. Hemp, S. C. Renner, I. Schöning, S. Pfeiffer, B. König-Ries, F. Buscot, K. E. Linsenmair, E.-D. Schulze, W. W. Weisser, M. Fischer, Interannual variation in land-use intensity enhances grassland multidiversity. *Proc. Natl. Acad. Sci. U.S.A.* **111**, 308-313 (2013).

105. M. Delgado-Baquerizo, P. B. Reich, C. Trivedi, D. J. Eldridge, S. Abades, F. D. Alfaro, F. Bastida, A. A. Berhe, N. A. Cutler, A. Gallardo, L. García-Velázquez, S. C. Hart, P. E. Hayes, J.-Z. He, Z.-Y. Hseu, H.-W. Hu, M. Kirchmair, S. Neuhauser, C. A. Pérez, S. C. Reed, F. Santos, B. W. Sullivan, P. Trivedi, J.-T. Wang, L. Weber-Grullon, M. A. Williams, B. K. Singh, Multiple elements of soil biodiversity drive ecosystem functions across biomes. *Nat. Ecol. Evol.* **4**, 210–220 (2020).

106. M. Holmberg, T. Aalto, A. Akujärvi, A. N. Arslan, I. Bergström, K. Böttcher, I. Lahtinen, A. Mäkelä, T. Markkanen, F. Minunno, M. Peltoniemi, K. Rankinen, P. Vihervaara, M. Forsius, Ecosystem services related to carbon cycling – modeling present and future impacts in boreal forests. *Front. Plant Sci.* **10**, 343 (2019).

107. M. Potschin, R. Haines-Young, R. Fish, R. K. Turner, *Routledge Handbook of*

Ecosystem Services (Routledge, London, 2016).

108. M. R. Raupach, "Ecosystem Services and the Global Carbon Cycle" in *Ecosystem Services and Carbon Sequestration in the Biosphere*, R. Lal, K. Lorenz, R. F. Hüttl, B. U. Schneider, J. von Braun, Eds. (Springer, Dordrecht, 2013), pp. 155–181.

109. A. Affek, M. Degórski, J. Wolski, J. Solon, A. Kowalska, E. Roo-Zielinska, B. Grabinska, B. Kruczkowska, *Ecosystem service potentials and their indicators in postglacial landscapes: assessment and mapping* (Elsevier, Amsterdam, 2019).

110. P. Smith, M. R. Ashmore, H. I. J. Black, P. J. Burgess, C. D. Evans, T. A. Quine, A. M. Thomson, K. Hicks, H. G. Orr, The role of ecosystems and their management in regulating climate, and soil, water and air quality. *J. Appl. Ecol.* **50**, 812–829 (2013).

111. C. Neely, S. Bunning, A. Wilkes (eds.), *Review of Evidence on Drylands Pastoral Systems and Climate Change: Implications and Opportunities for Mitigation and Adaptation. Land and Water Discussion Paper 8* (FAO, Rome, 2009).

112. H. Suich, C. Howe, G. Mace, Ecosystem services and poverty alleviation: A review of the empirical links. *Ecosyst. Serv.* **12**, 137–147 (2015).

113. A. K. Knapp, M. D. Smith, Variation among biomes in temporal dynamics of aboveground primary production. *Science* **291**, 481–484 (2001).

114. A. Aldezabal, I. Odriozola, G. García-Baquero, Grazing abandonment delays the effect of temperature on aboveground net primary production in Atlantic grasslands. *Rangel. Ecol. Manag.* **72**, 822–831 (2019).

115. D. D. Briske, D. L. Coppock, A. W. Illius, S. D. Fuhlendorf, Strategies for global rangeland stewardship: Assessment through the lens of the equilibrium–non-equilibrium debate. *J. Appl. Ecol.* **57**, 1056–1067 (2020).

116. B. L. Markham, W. C. Boncyk, D. L. Helder, J. L. Barker, Landsat-7 Enhanced Thematic Mapper Plus Radiometric Calibration. *Can. J. Remote Sens.* **23**, 318–332 (1997).

117. A. M. Wilson, J. A. Silander, A. Gelfand, J. H. Glenn, Scaling up: Linking field data and remote sensing with a hierarchical model. *Int. J. Geogr. Inf. Sci.* **25**, 509-521 (2011).

118. N. Gholami Baghi, J. Oldeland, Do soil-adjusted or standard vegetation indices better predict above ground biomass of semi-arid, saline rangelands in North-East Iran?. *Int. J. Remote Sens.* **40**, 8223-8235 (2019).

119. F. Moradi, S. M. M. Sadeghi, H. B. Heidarlou, A. Deljouei, E. Boshkar, S. A. Borz, Above-ground biomass estimation in a Mediterranean sparse coppice oak forest using Sentinel-2 data. *Ann. For. Res.* **65**, 165-182 (2022).

120. G. L. Anderson, J. D. Hanson, R. H. Haas, Evaluating Landsat Thematic Mapper derived vegetation indices for estimating above-ground biomass on semiarid rangelands. *Remote Sens. Environ.* **45**, 165-175 (1993).

121. J. L. Olsen, S. Miehe, P. Ceccato, R. Fensholt, Does EO NDVI seasonal metrics capture variations in species composition and biomass due to grazing in semi-arid grassland savannas? *Biogeosciences* **12**, 4407–4419 (2015).

122. H. Mahyou, B. Tychon, M. Lang, R. Balaghi, Phytomass estimation using eMODIS NDVI and ground data in arid rangelands of Morocco. *Afr. J. Range Forage Sci.* **35**, 1-12 (2018).

123. J. J. Gaitán, F. T. Maestre, D. E. Bran, G. G. Buono, A. J. Dougill, G. García Martínez, D. Ferrante, R. T. Guuroh, A. Linstädter, V. Massara, A. D. Thomas, G. E. Oliva,

Biotic and abiotic drivers of topsoil organic carbon concentration in drylands have similar effects at regional and global scales. *Ecosystems* **22**, 1445–1456 (2019)

124. G. L. Schmidt, C. B. Jenkerson, J. Masek, E. Vermote, F. Gao, "Landsat ecosystem disturbance adaptive processing system (LEDAPS) algorithm description" (U.S. Geological Survey Open-File Report 2013–1057, 2013; https://doi.org/10.3133/ofr20131057).

125. Z. Zhu, S. Wang, C. E. Woodcock, Improvement and expansion of the Fmask algorithm: Cloud, cloud shadow, and snow detection for Landsats 4–7, 8, and Sentinel 2 images. *Remote Sens. Environ.* **159**, 269–277 (2015).

126. L. Milich, E. Weiss, GAC NDVI interannual coefficient of variation (CoV) images: ground truth sampling of the Sahel along north-south transects. *Int. J. Remote Sens.* **21**, 235–260 (2000).

127. C. M. Godde, R. B. Boone, A. J. Ash, K. Waha, L. L. Sloat, P. K. Thornton, M. Herrero. Global rangeland production systems and livelihoods at threat under climate change and variability. *Environ. Res. Lett.* **15**, 044021 (2020).

128. D. Tilman, The ecological consequences of changes in biodiversity: a search for general principles. *Ecology* **80**, 1455-1474 (1999).

129. F. de Bello, S. Lavorel, L. M. Hallett, E. Valencia, E. Garnier, C. Roscher, L. Conti, T. Galland, M. Goberna, M. Májeková, A. Montesinos-Navarro, J. G. Pausas, M. Verdú, A. E-Vojtkó, L. Götzenberger, J. Lepš, Functional trait effects on ecosystem stability: assembling the jigsaw puzzle. *Trends Ecol. Evol.* **36**, 822-836 (2021).

130. J. Lepš, M. Májeková, A. Vítová, J. Doležal, F. de Bello, Stabilizing effects in temporal fluctuations: management, traits, and species richness in high-diversity

communities. *Ecol.* **99**, 360-371 (2018).

131. H. Wayne Polley, B. J. Wilsey, J. D. Derner, Dominant species constrain effects of species diversity on temporal variability in biomass production of tallgrass prairie. *Oikos* **116**, 2044-2052 (2007).

132. P. García-Palacios, N. Gross, J. Gaitán, F. T. Maestre, Climate mediates the biodiversity–ecosystem stability relationship globally. *Proc. Natl. Acad. Sci. U.S.A.* **115**, 8400–8405 (2018).

133. N. Middleton. Rangeland management and climate hazards in drylands: dust storms, desertification and the overgrazing debate. *Nat. hazards* **92**, 57-70 (2018).

134. I. Abdelkader, A. Ferchichi, M. Chaieb, Aboveground biomass production of *Cenchrus ciliaris* in Tunisian arid zone. *J. Biol. Sci.* **7**, 985–988 (2007).

135. P. Flombaum, O. E. Sala, A non-destructive and rapid method to estimate biomass and aboveground net primary production in arid environments. *J. Arid Environ.* **69**, 352–358 (2007).

136. L. G. Houessou, A. Teka, M. Oumorou, B. Sinsin, Hemicryptophytes plant species as indicator of grassland state in semi-arid region: Case study of W Biosphere Reserve and its surroundings area in Benin (West Africa). *Int. J. Biol. Chem. Sci.* **6**, 1271–1280 (2012).

137. J. Ferner, S. Schmidtlein, R. T. Guuroh, J. Lopatin, A. Linstädter, Disentangling effects of climate and land-use change on West African drylands' forage supply. *Glob. Environ. Change*. **53**, 24–38 (2018).

138. S. Díaz, J. Kattge, J. H. C. Cornelissen, I. J. Wright, S. Lavorel, S. Dray, B. Reu, M. Kleyer, C. Wirth, I. C. Prentice, E. Garnier, G. Bönisch, M. Westoby, H. Poorter, P. B.

Reich, A. T. Moles, J. Dickie, A. N. Gillison, A. E. Zanne, J. Chave, S. J. Wright, S. N. Sheremet'ev, H. Jactel, C. Baraloto, B. Cerabolini, S. Pierce, B. Shipley, D. Kirkup, F. Casanoves, J. S. Joswig, A. Günther, V. Falczuk, N. Rüger, M. D. Mahecha, L. D. Gorné, The global spectrum of plant form and function. *Nature*. **529**, 167–171 (2016).

139. I. J. Wright, P. B. Reich, M. Westoby, D. D. Ackerly, Z. Baruch, F. Bongers, J. Cavender-Bares, T. Chapin, J. H. C. Cornelissen, M. Diemer, J. Flexas, E. Garnier, P. K. Groom, J. Gulias, K. Hikosaka, B. B. Lamont, T. Lee, W. Lee, C. Lusk, J. J. Midgley, M.-L. Navas, Ü. Niinemets, J. Oleksyn, N. Osada, H. Poorter, P. Poot, L. Prior, V. I. Pyankov, C. Roumet, S. C. Thomas, M. G. Tjoelker, E. J. Veneklaas, R. Villar, The worldwide leaf economics spectrum. *Nature*. **428**, 821–827 (2004).

140. H.-H. Yeoh, Y.-C. Wee, Leaf protein contents and nitrogen-to-protein conversion factors for 90 plant species. *Food Chem.* **49**, 245–250 (1994).

141. J. Mosse, Nitrogen-to-protein conversion factor for ten cereals and six legumes or oilseeds. A reappraisal of its definition and determination. Variation according to species and to seed protein content. *J. Agric. Food Chem.* **38**, 18–24 (1990).

142. I. E. Ezeagu, J. K. Petzke, C. C. Metges, A. O. Akinsoyinu, A. D. Ologhobo, Seed protein contents and nitrogen-to-protein conversion factors for some uncultivated tropical plant seeds. *Food Chem.* **78**, 105–109 (2002).

143. K. Milton, F. R. Dintzis, Nitrogen-to-protein conversion factors for tropical plant samples. *Biotropica*. **13**, 177–181 (1981).

144. M. A. Lee, A global comparison of the nutritive values of forage plants grown in contrasting environments. *J. Plant Res.* **131**, 641–654 (2018).

145. G. W. Garcia, T. U. Ferguson, F. A. Neckles, K. A. E. Archibald, The nutritive value

and forage productivity of *Leucaena leucocephala*. *Anim. Feed Sci. Technol.* **60**, 29–41 (1996).

146. G. Lemaire, G. Belanger, Allometries in plants as drivers of forage nutritive value: A review. *Agriculture* **10**, 5 (2020).

147. L. da S. Pontes, J.-F. Soussana, F. Louault, D. Andueza, P. Carrère, Leaf traits affect the above-ground productivity and quality of pasture grasses. *Funct. Ecol.* **21**, 844–853 (2007).

148. A. Elger, N. J. Willby, Leaf dry matter content as an integrative expression of plant palatability: the case of freshwater macrophytes. *Funct. Ecol.* **17**, 58–65 (2003).

149. F. P. Massey, A. R. Ennos, S. E. Hartley, Grasses and the resource availability hypothesis: the importance of silica-based defences. *J. Ecol.* **95**, 414–424 (2007).

150. S. McIntyre, The role of plant leaf attributes in linking land use to ecosystem function in temperate grassy vegetation. *Agric. Ecosyst. Environ.* **128**, 251–258 (2008).

151. K. Niu, J. He, S. Zhang, M. J. Lechowicz, Tradeoffs between forage quality and soil fertility: Lessons from Himalayan rangelands. *Agric. Ecosyst. Environ.* **234**, 31–39 (2016).

152. E. R. Beaty, J. L. Engel, Forage quality measurements and forage research: a review, critique and interpretation. *J. Range Manag.* **33**, 49–54 (1980).

153. J. Walter, K. Grant, C. Beierkuhnlein, J. Kreyling, M. Weber, A. Jentsch, Increased rainfall variability reduces biomass and forage quality of temperate grassland largely independent of mowing frequency. *Agric. Ecosyst. Environ.* **148**, 1–10 (2012).

154. P. Aguirre Castro, M. F. Garbulsky, Spectral normalized indices related with forage quality in temperate grasses: scaling up from leaves to canopies. *Int. J. Remote Sens.*

39, 3138–3163 (2018).

155. M. Hejcman, P. Hejcmanová, V. Pavlů, A. G. Thorhallsdottir, Forage quality of leaf fodder from the main woody species in Iceland and its potential use for livestock in the past and present. *Grass Forage Sci.* **71**, 649–658 (2016).

156. C. M. Pauler, J. Isselstein, M. Suter, J. Berard, T. Braunbeck, M. K. Schneider, Choosy grazers: Influence of plant traits on forage selection by three cattle breeds. *Funct. Ecol.* **34**, 980–992 (2020).

157. P. L. Woomer, A. Touré, M. Sall, Carbon stocks in Senegal's Sahel Transition Zone. *J. Arid Environ.* **59**, 499–510 (2004).

158. V. P. Tewari, B. Singh, Total and merchantable wood volume equations for *Eucalyptus* hybrid trees in Gujarat State, India. *Arid Land Res. Manag.* **20**, 147–159 (2006).

159. R. Foroughbakhch, A. Carrillo Parra, J. L. Hernández Piñero, M. A. Alvarado Vázquez, A. Rocha Estrada, M. L. Cardenas, Wood volume production and use of 10 woody species in semiarid Zones of Northeastern Mexico. *Int. J. For. Res.* **2012**, e529829 (2012).

160. M.-F. Dignac, D. Derrien, P. Barré, S. Barot, L. Cécillon, C. Chenu, T. Chevallier, G. T. Freschet, P. Garnier, B. Guenet, M. Hedde, K. Klumpp, G. Lashermes, P.-A. Maron, N. Nunan, C. Roumet, I. Basile-Doelsch, Increasing soil carbon storage: mechanisms, effects of agricultural practices and proxies. A review. *Agron. Sustain. Dev.* **37**, 14 (2017).

161. R. Kindler, A. Miltner, H.-H. Richnow, M. Kästner, Fate of gram-negative bacterial biomass in soil—mineralization and contribution to SOM. *Soil Biol. Biochem.* **38**,

2860–2870 (2006).

162. H. Y. Gan, I. Schöning, P. Schall, C. Ammer, M. Schrumpf, Soil organic matter mineralization as driven by nutrient stoichiometry in soils under differently managed forest stands. *Front. For. Glob. Change*. **3**, 99 (2020).

163. K. Witzgall, A. Vidal, D. I. Schubert, C. Höschen, S. A. Schweizer, F. Buegger, V. Pouteau, C. Chenu, C. W. Mueller, Particulate organic matter as a functional soil component for persistent soil organic carbon. *Nat. Commun.* **12**, 4115 (2021).

164. P. Nannipieri, L. Giagnoni, G. Renella, E. Puglisi, B. Ceccanti, G. Masciandaro, F. Fornasier, M. C. Moscatelli, S. Marinari, Soil enzymology: classical and molecular approaches. *Biol. Fertil. Soils*. **48**, 743–762 (2012).

165. J. Liu, J. Chen, G. Chen, J. Guo, Y. Li, Enzyme stoichiometry indicates the variation of microbial nutrient requirements at different soil depths in subtropical forests. *PloS One* **15**, e0220599 (2020).

166. P. Nannipieri, J. Ascher, M. Ceccherini, L. Landi, G. Pietramellara, G. Renella, Microbial diversity and soil functions. *Eur. J. Soil Sci.* **54**, 655–670 (2003).

167. M. A. Tabatabai, J. M. Bremner, Use of p-nitrophenyl phosphate for assay of soil phosphatase activity. *Soil Biol. Biochem.* **1**, 301–307 (1969).

168. M. A. Tabatabai, “Soil Enzymes” in *Methods of soil analysis Part 2, Chemical and Microbiological Properties*, A. L. Page, R. H. Miller, R. H. Keeney, Eds. (American Society of Agronomy, 1982), pp. 903–947.

169. R. P. Dick, L. K. Dick, S. Deng, X. Li, E. Kandeler, C. Poll, C. Freeman, T. G. Jones, M. N. Weintraub, K. A. Esseili, J. Saxena, Cross-laboratory comparison of fluorimetric microplate and colorimetric bench-scale soil enzyme assays. *Soil Biol.*

Biochem. **121**, 240–248 (2018).

170. A. Rey, C. Oyonarte, T. Morán-López, J. Raimundo, E. Pegoraro, Changes in soil moisture predict soil carbon losses upon rewetting in a perennial semiarid steppe in SE Spain. *Geoderma*. **287**, 135–146 (2017).
171. G. P. Robertson, D. C. Coleman, P. Sollins, C. S. Bledsoe, *Standard Soil Methods for Long-term Ecological Research* (Oxford University Press, New York, 1999).
172. S. E. Allen, H. M. Grimshaw, A. P. Rowland, “Chemical Analysis” in *Methods in Plant Ecology*, S. B. Chapman, P. D. Moore, Eds. (Blackwell Science, Oxford, 1986).
173. S. Scheu, Automated measurement of the respiratory response of soil microcompartments: active microbial biomass in earthworm faeces. *Soil Biol. Biochem.* **24**, 1113–1118 (1992).
174. J. P. Anderson, K. H. Domsch, A physiological method for the quantitative measurement of microbial biomass in soils. *Soil Biol. Biochem.* **10**, 215–221 (1978).
175. T. Beck, R. G. Joergensen, E. Kandeler, F. Makeschin, E. Nuss, H. R. Oberholzer, S. Scheu, An inter-laboratory comparison of ten different ways of measuring soil microbial biomass C. *Soil Biol. Biochem.* **29**, 1023–1032 (1997).
176. M. W. Schmidt, M. S. Torn, S. Abiven, T. Dittmar, G. Guggenberger, I. A. Janssens, M. Kleber, I. Kögel-Knabner, J. Lehmann, D. A. Manning, Persistence of soil organic matter as an ecosystem property. *Nature*. **478**, 49–56 (2011).
177. R. Amundson, A. A. Berhe, J. W. Hopmans, C. Olson, A. E. Sztein, D. L. Sparks, Soil and human security in the 21st century. *Science*. **348**, 1261071 (2015).
178. N. H. Batjes, Harmonized soil property values for broad-scale modelling (WISE30sec) with estimates of global soil carbon stocks. *Geoderma*. **269**, 61–68 (2016).

179. R. B. Jackson, K. Lajtha, S. E. Crow, G. Hugelius, M. G. Kramer, G. Piñeiro, The ecology of soil carbon: pools, vulnerabilities, and biotic and abiotic controls. *Annu. Rev. Ecol. Evol. Syst.* **48**, 419–445 (2017).

180. D. Harris, W. R. Horwáth, C. Van Kessel, Acid fumigation of soils to remove carbonates prior to total organic carbon or carbon-13 isotopic analysis. *Soil Sci. Soc. Am. J.* **65**, 1853–1856 (2001).

181. M. A. Arshad, B. Lowery, B. Grossman, "Physical tests for monitoring soil quality" in *Methods for Assessing Soil Quality*, J. W. Doran, A. J. Jones, Eds. (Soil Science Society of America, Madison, WI, 1997) pp. 123–141.

182. D. U. Hooper, L. Johnson, Nitrogen limitation in dryland ecosystems: responses to geographical and temporal variation in precipitation. *Biogeochemistry* **46**, 247–293 (1999).

183. P. M. Vitousek, S. Porder, B. Z. Houlton, O. A. Chadwick, Terrestrial phosphorus limitation: mechanisms, implications, and nitrogen–phosphorus interactions. *Ecol. Appl.* **20**, 5–15 (2010).

184. L. Yahdjian, L. Gherardi, O. E. Sala, Nitrogen limitation in arid-subhumid ecosystems: a meta-analysis of fertilization studies. *J. Arid Environ.* **75**, 675–680 (2011).

185. R. F. Brennan, B. Penrose, R. W. Bell, Micronutrients limiting pasture production in Australia. *Crop Pasture Sci.* **70**, 1053–1064 (2019).

186. D. L. Jones, V. B. Willett, Experimental evaluation of methods to quantify dissolved organic nitrogen (DON) and dissolved organic carbon (DOC) in soil. *Soil Biol. Biochem.* **38**, 991–999 (2006).

187. G. K. Sims, T. R. Ellsworth, R. L. Mulvaney, Microscale determination of inorganic

nitrogen in water and soil extracts. *Commun. Soil Sci. Plant Anal.* **26**, 303–316 (1995).

188. P. R. Hesse, *A Textbook of Soil Chemical Analysis* (Chemical Publishing, 1971).

189. S. Kuo, "Phosphorus" in *Methods of Soil Analysis. Part 3. Chemical methods*, D. Sparks, A. Page, P. Helmke, R. Loeppert, Eds. (Soil Science Society of America, American Society of Agronomy, Madison, WI, 1997) pp. 869–920.

190. V. H. D. Zuazo, C. R. R. Pleguezuelo, Soil-erosion and runoff prevention by plant covers: a review. *Sustain. Agric.* **16**, 785–811 (2009).

191. M. Ruiz-Colmenero, R. Bienes, D. J. Eldridge, M. J. Marques, Vegetation cover reduces erosion and enhances soil organic carbon in a vineyard in the central Spain. *Catena* **104**, 153–160 (2013).

192. R. Bartley, C. H. Roth, J. Ludwig, D. McJannet, A. Liedloff, J. Corfield, A. Hawdon, B. Abbott, Runoff and erosion from Australia's tropical semi-arid rangelands: influence of ground cover for differing space and time scales. *Hydrol. Process.* **20**, 3317–3333 (2006).

193. A. Cerdà, M. E. Lucas-Borja, I. Franch-Pardo, X. Úbeda, A. Novara, M. López-Vicente, Z. Popović, M. Pulido, The role of plant species on runoff and soil erosion in a Mediterranean shrubland. *Sci. Total Environ.* **799**, 149218 (2021).

194. B. Steinhoff-Knopp, T. K. Kuhn, B. Burkhard, The impact of soil erosion on soil-related ecosystem services: development and testing a scenario-based assessment approach. *Environ. Monit. Assess.* **193**, 274 (2021).

195. C. A. Guerra, T. Pinto-Correia, M. J. Metzger, Mapping soil erosion prevention using an ecosystem service modeling framework for integrated land management and policy. *Ecosystems* **17**, 878–889 (2014).

196. C. A. Guerra, J. Maes, I. Geijzendorffer, M. J. Metzger, An assessment of soil erosion prevention by vegetation in Mediterranean Europe: Current trends of ecosystem service provision. *Ecol. Indic.* **60**, 213–222 (2016).

197. R. B. Bryan, Soil erodibility and processes of water erosion on hillslope. *Geomorphology* **32**, 385–415 (2000).

198. A. J. Franzluebbers, Water infiltration and soil structure related to organic matter and its stratification with depth. *Soil Tillage Res.* **66**, 197–205 (2002).

199. Y. A. Pachepsky, W. J. Rawls, Soil structure and pedotransfer functions. *Eur. J. Soil Sci.* **54**, 443–452 (2003).

200. R. Lal, Soil conservation and ecosystem services. *Int. Soil Water Conserv. Res.* **2**, 36–47 (2014).

201. B. Barthès, E. Roose, Aggregate stability as an indicator of soil susceptibility to runoff and erosion; validation at several levels. *Catena* **47**, 133–149 (2002).

202. P. C. Teixeira, R. K. Misra, Erosion and sediment characteristics of cultivated forest soils as affected by the mechanical stability of aggregates. *Catena* **30**, 119–134 (1997).

203. J. Laishram, K. G. Saxena, R. K. Maikhuri, K. S. Rao, Soil Quality and Soil Health: A Review. *Int. J. Ecol. Environ. Sci.* **38**, 19-37–37 (2012).

204. C. J. Bronick, R. Lal, Soil structure and management: a review. *Geoderma* **124**, 3–22 (2005).

205. C. A. Seybold, J. E. Herrick, Aggregate stability kit for soil quality assessments. *Catena* **44**, 37–45 (2001).

206. J. Six, H. Bossuyt, S. Degryze, K. Denef, A history of research on the link between (micro) aggregates, soil biota, and soil organic matter dynamics. *Soil Tillage Res.* **79**,

7–31 (2004).

207. W. D. Kemper, R. C. Rosenau, “Aggregate stability and size distribution” in *Methods of Soil Analysis, Part 1. Physical and Mineralogical Methods* (2nd Edition), A. Klute, Ed. (Soil Science Society of America, American Society of Agronomy, Madison, WI, 1986), pp. 425-442.

208. D. J. Horne, D. R. Scotter, The available water holding capacity of soils under pasture. *Agric. Water Manag.* **177**, 165–171 (2016).

209. O. E. Sala, W. J. Parton, L. A. Joyce, W. K. Lauenroth, Primary Production of the Central Grassland Region of the United States. *Ecology* **69**, 40–45 (1988).

210. B. Grizzetti, D. Lanzanova, C. Liquete, A. Reynaud, A. C. Cardoso, Assessing water ecosystem services for water resource management. *Environ. Sci. Policy*. **61**, 194–203 (2016).

211. A. M. Helalia, The relation between soil infiltration and effective porosity in different soils. *Agric. Water Manag.* **24**, 39–47 (1993).

212. J. Lipiec, J. Kuś, A. Słowińska-Jurkiewicz, A. Nosalewicz, Soil porosity and water infiltration as influenced by tillage methods. *Soil Tillage Res.* **89**, 210–220 (2006).

213. I. Tokumoto, J. L. Heilman, S. Schwinning, K. J. McInnes, M. E. Litvak, C. L. S. Morgan, R. H. Kamps, Small-scale variability in water storage and plant available water in shallow, rocky soils. *Plant Soil* **385**, 193–204 (2014).

214. M. G. Castiglioni, M. C. Sasal, M. Wilson, J. D. Oszust, M. G. Castiglioni, M. C. Sasal, M. Wilson, J. D. Oszust, Seasonal variation of soil aggregate stability, porosity and infiltration during a crop sequence under no tillage. *Terra Latinoam.* **36**, 199–209 (2018).

215. X. Hao, B. C. Ball, J. L. B. Culley, “Soil density and porosity” in *Soil Sampling and Methods of Analysis*, M. R. Carter, E. G. Gregorich, Eds. (CRC Press, Boca Raton, FL, 2007), pp. 743–759.

216. Y. Fu, Z. Tian, A. Amoozegar, J. Heitman, Measuring dynamic changes of soil porosity during compaction. *Soil Tillage Res.* **193**, 114–121 (2019).

217. J. Shang, M. Flury, Y. Deng, Force measurements between particles and the air-water interface: Implications for particle mobilization in unsaturated porous media. *Water Resour. Res.* **45** (2009).

218. L. J. Munkholm, R. J. Heck, B. Deen, T. Zidar, Relationship between soil aggregate strength, shape and porosity for soils under different long-term management. *Geoderma* **268**, 52–59 (2016).

219. Z. Cui, G.-L. Wu, Z. Huang, Y. Liu, Fine roots determine soil infiltration potential than soil water content in semi-arid grassland soils. *J. Hydrol.* **578**, 124023 (2019).

220. Z. Gozubuyuk, U. Sahin, I. Ozturk, A. Celik, M. C. Adiguzel, Tillage effects on certain physical and hydraulic properties of a loamy soil under a crop rotation in a semi-arid region with a cool climate. *Catena* **118**, 195–205 (2014).

221. L. Tedersoo, M. Bahram, S. Põlme, U. Kõljalg, N. S. Yorou, R. Wijesundera, L. V. Ruiz, A. M. Vasco-Palacios, P. Q. Thu, A. Suija, M. E. Smith, C. Sharp, E. Saluveer, A. Saitta, M. Rosas, T. Riit, D. Ratkowsky, K. Pritsch, K. Põldmaa, M. Piepenbring, C. Phosri, M. Peterson, K. Parts, K. Pärtel, E. Otsing, E. Nouhra, A. L. Njouonkou, R. H. Nilsson, L. N. Morgado, J. Mayor, T. W. May, L. Majuakim, D. J. Lodge, S. S. Lee, K.-H. Larsson, P. Kohout, K. Hosaka, I. Hiiesalu, T. W. Henkel, H. Harend, L. Guo, A. Greslebin, G. Grelet, J. Geml, G. Gates, W. Dunstan, C. Dunk, R. Drenkhan,

J. Dearnaley, A. D. Kesel, T. Dang, X. Chen, F. Buegger, F. Q. Brearley, G. Bonito, S. Anslan, S. Abell, K. Abarenkov, Global diversity and geography of soil fungi. *Science* **346**, 1256688 (2014).

222. M. Bahram, F. Hildebrand, S. K. Forslund, J. L. Anderson, N. A. Soudzilovskaia, P. M. Bodegom, J. Bengtsson-Palme, S. Anslan, L. P. Coelho, H. Harend, J. Huerta-Cepas, M. H. Medema, M. R. Maltz, S. Mundra, P. A. Olsson, M. Pent, S. Põlme, S. Sunagawa, M. Ryberg, L. Tedersoo, P. Bork, Structure and function of the global topsoil microbiome. *Nature* **560**, 233–237 (2018).

223. M. Delgado-Baquerizo, A. M. Oliverio, T. E. Brewer, A. Benavent-González, D. J. Eldridge, R. D. Bardgett, F. T. Maestre, B. K. Singh, N. Fierer, A global atlas of the dominant bacteria found in soil. *Science* **359**, 320–325 (2018).

224. M. Delgado-Baquerizo, R. D. Bardgett, P. M. Vitousek, F. T. Maestre, M. A. Williams, D. J. Eldridge, H. Lambers, S. Neuhauser, A. Gallardo, L. García-Velázquez, O. E. Sala, S. R. Abades, F. D. Alfaro, A. A. Berhe, M. A. Bowker, C. M. Currier, N. A. Cutler, S. C. Hart, P. E. Hayes, Z.-Y. Hseu, M. Kirchmair, V. M. Peña-Ramírez, C. A. Pérez, S. C. Reed, F. Santos, C. Siebe, B. W. Sullivan, L. Weber-Grullon, N. Fierer, Changes in belowground biodiversity during ecosystem development. *Proc. Natl. Acad. Sci. U. S. A.* **116**, 6891–6896 (2019).

225. R. Zornoza, C. Guerrero, J. Mataix-Solera, V. Arcenegui, F. García-Orenes, J. Mataix-Beneyto, Assessing air-drying and rewetting pre-treatment effect on some soil enzyme activities under Mediterranean conditions. *Soil Biol. Biochem.* **38**, 2125–2134 (2006).

226. R. Zornoza, J. Mataix-Solera, C. Guerrero, V. Arcenegui, J. Mataix-Beneyto, Storage effects on biochemical properties of air-dried soil samples from southeastern Spain.

Arid Land Res. Manag. **23**, 213–222 (2009).

227. Y. Qiu, B. Fu, J. Wang, L. Chen, Spatial variability of soil moisture content and its relation to environmental indices in a semi-arid gully catchment of the Loess Plateau, China. *J. Arid Environ.* **49**, 723–750 (2001).
228. F. T. Maestre, S. Bautista, J. Cortina, G. Díaz, M. Honrubia, R. Vallejo, Microsite and mycorrhizal inoculum effects on the establishment of Quercus coccifera in a semi-arid degraded steppe. *Ecol. Eng.* **19**, 289–295 (2002).
229. Y. Cantón, A. Solé-Benet, F. Domingo, Temporal and spatial patterns of soil moisture in semiarid badlands of SE Spain. *J. Hydrol.* **285**, 199–214 (2004).
230. A. P. Castillo-Monroy, F. T. Maestre, A. Rey, S. Soliveres, P. García-Palacios, Biological soil crust microsites are the main contributor to soil respiration in a semiarid ecosystem. *Ecosystems* **14**, 835–847 (2011).
231. H. Matuschek, R. Kliegl, S. Vasishth, H. Baayen, D. Bates, Balancing Type I error and power in linear mixed models. *J. Mem. Lang.* **94**, 305–315 (2017).
232. D. J. Barr, R. Levy, C. Scheepers, H. J. Tily, Random effects structure for confirmatory hypothesis testing: Keep it maximal. *J. Mem. Lang.* **68**, 255–278 (2013).
233. R Core Team, *R: A language and environment for statistical computing* (R Foundation for Statistical Computing, Vienna, 2013). https://www.R-project.org/
234. N. Gross, Y. L. Bagousse-Pinguet, P. Liancourt, M. Berdugo, N. J. Gotelli, F. T. Maestre, Functional trait diversity maximizes ecosystem multifunctionality. *Nat. Ecol. Evol.* **1**, 0132 (2017).
235. Y. L. Bagousse-Pinguet, N. Gross, F. T. Maestre, V. Maire, F. de Bello, C. R. Fonseca, J. Kattge, E. Valencia, J. Leps, P. Liancourt, Testing the environmental filtering

concept in global drylands. *J. Ecol.* **105**, 1058–1069 (2017).

236. Y. L. Bagousse-Pinguet, S. Soliveres, N. Gross, R. Torices, M. Berdugo, F. T. Maestre, Phylogenetic, functional, and taxonomic richness have both positive and negative effects on ecosystem multifunctionality. *Proc. Natl. Acad. Sci. U.S.A.* **116**, 8419–8424 (2019).

237. M. Berdugo, M. Delgado-Baquerizo, S. Soliveres, R. Hernández-Clemente, Y. Zhao, J. J. Gaitán, N. Gross, H. Saiz, V. Maire, A. Lehmann, M. C. Rillig, R. V. Solé, F. T. Maestre, Global ecosystem thresholds driven by aridity. *Science* **367**, 787–790 (2020).

238. A. Lafuente, M. A. Bowker, M. Delgado-Baquerizo, J. Durán, B. K. Singh, F. T. Maestre, Global drivers of methane oxidation and denitrifying gene distribution in drylands. *Glob. Ecol. Biogeogr.* **28**, 1230–1243 (2019).

239. F. T. Maestre, J. Cortina, S. Bautista, J. Bellot, R. Vallejo, Small-scale environmental heterogeneity and spatiotemporal dynamics of seedling establishment in a semiarid degraded ecosystem. *Ecosystems* **6**, 630–643 (2003).

240. A. Mills, M. Fey, J. Donaldson, S. Todd, L. Theron, Soil infiltrability as a driver of plant cover and species richness in the semi-arid Karoo, South Africa. *Plant Soil* **320**, 321–332 (2009).

241. F. Qi, E. Kunihiko, C. Guodong, Soil water and chemical characteristics of sandy soils and their significance to land reclamation. *J. Arid Environ.* **51**, 35–54 (2002).

242. F. T. Maestre, M. Delgado-Baquerizo, T. C. Jeffries, D. J. Eldridge, V. Ochoa, B. Gozalo, J. L. Quero, M. García-Gómez, A. Gallardo, W. Ulrich, M. A. Bowker, T. Arredondo, C. Barraza-Zepeda, D. Bran, A. Florentino, J. Gaitán, J. R. Gutiérrez, E. Huber-Sannwald, M. Jankju, R. L. Mau, M. Miriti, K. Naseri, A. Ospina, I. Stavi, D.

Wang, N. N. Woods, X. Yuan, E. Zaady, B. K. Singh, Increasing aridity reduces soil microbial diversity and abundance in global drylands. *Proc. Natl. Acad. Sci. U.S.A.* **112**, 15684–15689 (2015).

243. G. M. Mace, K. Norris, A. H. Fitter, Biodiversity and ecosystem services: a multilayered relationship. *Trends Ecol. Evol.* **27**, 19–26 (2012).

244. B. J. Cardinale, J. E. Duffy, A. Gonzalez, D. U. Hooper, C. Perrings, P. Venail, A. Narwani, G. M. Mace, D. Tilman, D. A. Wardle, Biodiversity loss and its impact on humanity. *Nature* **486**, 59–67 (2012).

245. P. Balvanera, I. Siddique, L. Dee, A. Paquette, F. Isbell, A. Gonzalez, J. Byrnes, M. I. O'Connor, B. A. Hungate, J. N. Griffin, Linking biodiversity and ecosystem services: current uncertainties and the necessary next steps. *BioScience* **64**, 49–57 (2014).

246. C. Wagg, S. F. Bender, F. Widmer, M. G. A. van der Heijden, Soil biodiversity and soil community composition determine ecosystem multifunctionality. *Proc. Natl. Acad. Sci. U.S.A.* **111**, 5266–5270 (2014).

247. H. Deraison, I. Badenhausser, N. Loeuille, C. Scherber, N. Gross, Functional trait diversity across trophic levels determines herbivore impact on plant community biomass. *Ecol. Lett.* **18**, 1346–1355 (2015).

248. E. Kaarlejärvi, A. Eskelinen, J. Olofsson, Herbivores rescue diversity in warming tundra by modulating trait-dependent species losses and gains. *Nat. Commun.* **8**, 419 (2017).

249. K. Barton, *Mu-MIn: multi-model inference*, R package version 0.12.2 https://cran.r-project.org/web/packages/MuMIn/index.html (2009).

250. A. F. Zuur, E. N. Ieno, N. J. Walker, A. A. Saveliev, G. M. Smith, *Mixed Effects*

Models and Extensions in Ecology with R (Springer, New York, 2009).

251. D. Bates, M. Mächler, B. Bolker, S. Walker, Fitting Linear Mixed-Effects Models Using lme4. *J. Stat. Softw.* **67**, 1–48 (2015).

252. A. Tremblay, J. Ransijn, *LMERConvenience-Functions: Model selection and post-hoc analysis for (G) LMER models*, R package version 2.10, https://cran.r-project.org/web/packages/LMERConvenienceFunctions/index.html (2015).

253. R. S. Bivand, D. W. Wong, Comparing implementations of global and local indicators of spatial association. *Test* **27**, 716–748 (2018).

254. A. D. Cliff, J. K. Ord, *Spatial Processes: Models & Applications* (Pion Limited, London, 1981).

255. J.B. Grace, D.R. Schoolmaster Jr, G.R. Guntenspergen, A.M. Little, B.R. Mitchell, K.M. Miller, E.W. Schweiger, Guidelines for a graph-theoretic implementation of structural equation modeling. *Ecosphere*, **3**, 1– 44 (2012).

256. E. Laliberté, G. Zemunik, B. L. Turner. Environmental filtering explains variation in plant diversity along resource gradients. *Science* **345**, 1602-1605 (2014).

257. B. Shipley, Confirmatory path analysis in a generalized multilevel context. *Ecology* **90**, 363–368 (2009).

258. J. B. Grace, K. A. Bollen, Interpreting the Results from Multiple Regression and Structural Equation Models. The Bulletin of the Ecological Society of America. **86**, 283–295 (2005).

259. C. A. Guerra, M. Delgado-Baquerizo, E. Duarte, O. Marigliano, C. Görgen, F. T. Maestre, N. Eisenhauer, Global projections of the soil microbiome in the Anthropocene. *Global Ecol. Biogeogr.* **30**, 987–999 (2021).

260. T. Ebert, J. Belz, O. Nelles, Interpolation and extrapolation: Comparison of definitions and survey of algorithms for convex and concave hulls. *2014 IEEE Symposium on Computational Intelligence and Data Mining (CIDM)* (2014) doi:10.1109/cidm.2014.7008683.

261. D. A. Jackson, Y. Chen, Robust principal component analysis and outlier detection with ecological data. *Environmetrics* **15**, 129–139 (2004).

262. P. J. Rousseeuw, B. C. van Zomeren, Unmasking Multivariate Outliers and Leverage Points. *J. Am. Stat. Assoc*. **85**, 633–639 (1990).

263. T. Hengl, J. M. de Jesus, G. B. M. Heuvelink, M. R. Gonzalez, M. Kilibarda, A. Blagotić, W. Shangguan, M. N. Wright, X. Geng, B. Bauer-Marschallinger, M. A. Guevara, R. Vargas, R. A. MacMillan, N. H. Batjes, J. G. B. Leenaars, E. Ribeiro, I. Wheeler, S. Mantel, B. Kempen, SoilGrids250m: Global gridded soil information based on machine learning. *PLoS One* **12**, e0169748 (2017).

264. D. J. Eldridge, M. Delgado-Baquerizo, S. K. Travers, J. Val, I. Oliver, Do grazing intensity and herbivore type affect soil health? Insights from a semi-arid productivity gradient. *J. Appl. Ecol.* **54**, 976–985 (2017).

265. S. P. Wang, Y. H. Li, Effects of stocking rate and grazing period on the amounts of faeces, intake and dry matter digestibility of grazing sheep. *Acta Zoonutrimenta Sin.* **9**, 47–54 (1997).

266. K. E. Veblen, L. M. Porensky, C. Riginos, T. P. Young, Are cattle surrogate wildlife? Savanna plant community composition explained by total herbivory more than herbivore type. *Ecol. Appl.* **26**, 1610–1623 (2016).

267. S. Chatterjee, B. Price, *Regression Analysis by Example*, 2nd edition (Wiley, New

York, USA, 1991).

Acknowledgments: We acknowledge Sainbileg Undrakhbold, Munkhbat Uuganbayar, Batbold Byambatsogt, Sanchir Khaliun, Shijirbaatar Solongo, Bud Batchuluun, Michael Sloan, John Spence, Erika Geiger, Isys Souza, Richard Onoo, Thiago Araújo, Mancha Mabaso, Percy Mutseka Lunga, Louis Eloff, Pieter Eloff, Julius Sebei, Dr Jorrie Joordan, Dr Edwin Mudongo, Vincent Mokoka, Baltimore Mokhou, Thabang Maphanga, Florian Hoffmann, Rebecca Peters, Adriana Lozada, Edualdo Vidal, Franco Perrona, Roxana Ledezma, Rose Matjea, Liana Kindermann, Chris Goebel, Bruce Semple, and Bobby Tamayo for assistance with field work. We thank Bush Heritage Australia, the University of Limpopo, the Ministry of Environment and Tourism (Namibia) the Ministry of Agriculture, Water and Land Reform (Namibia), CONAF and the agricultural community Quebrada de Talca (Chile), and the South African Military for granting research permissions and/or granting access to their research farms and properties. We also thank Blas Benito for his revisions on the R code. Any use of trade, product, or firm names in this paper is for descriptive purposes only and does not imply endorsement by the U.S. Government.

Funding: This research was funded by the European Research Council (ERC Grant agreement 647038 [BIODESERT]) and Generalitat Valenciana (CIDEGENT/2018/041). F.T.M acknowledges support from a Rei Jaume I Award, the Alexander von Humboldt Foundation and the Synthesis Center (sDiv) of the German Centre for Integrative Biodiversity Research Halle–Jena–Leipzig (iDiv). C.A.G., S.C. and N.E. acknowledge support from iDiv and the Deutsche Forschungsgemeinschaft (DFG– FZT 118, 202548816; Flexpool proposal 34600850). Y.L.B.-P.

was supported by a Marie Sklodowska-Curie Actions Individual Fellowship (MSCA-IF) within the European Program Horizon 2020 (DRYFUN Project 656035). N.G. was supported by CAP 20-25 (16-IDEX-0001) and the AgreenSkills+ fellowship programme which has received funding from the EU's Seventh Framework Programme under grant agreement N° FP7-609398 (AgreenSkills+ contract). B.B. and B.E. were supported by the Taylor Family-Asia Foundation Endowed Chair in Ecology and Conservation Biology. J.D., A.R. and H.C. acknowledge support from the Fundação para a Ciência e a Tecnologia (IF/00950/2014 and 2020.03670.CEECIND, SFRH/BDP/108913/2015, and in the scope of the framework contract foreseen in the numbers 4-6 of the article 23, of the Decree-Law 57/2016, August 29, changed by Law 57/2017, July 19, respectively), as well as from the MCTES, FSE, UE, and the CFE (UIDB/04004/2020) research unit financed by Fundação para a Ciência e a Tecnologia/MCTES through national funds (PIDDAC). C.P. acknowledges support from the Spanish Ministry of Science and Innovation (ref. AGL201675762-R, AEI/FEDER, UE, and PID2020-116578RB-I00, MCIN/AEI/10.13039/501100011033) and the European Union's Horizon 2020 Research and Innovation Programme under Grant Agreement No 101000224. E.V. was funded by the 2017 program for attracting and retaining talent of Comunidad de Madrid (no. 2017-T2/ AMB-5406). M.A.B. acknowledges support from the School of Forestry and College of the Environment, Forestry and Natural Sciences of Northern Arizona University. E.H.S. acknowledges support from the Consejo Nacional de Ciencia y Tecnología (SEP-CB-2015-01-251388, PN 2017-5036 and PRONAII 319059). F.M.H. acknowledges support from the National Council for Scientific and Technological Development (CNPq - PCI/INMA) of the Brazilian Ministry of Science, Technology and Innovation (MCTI, processes number 302381/2020-1). H.L.T. acknowledges support from the US National Science Foundation (DEB 0953864). A.N. and M.K. acknowledge the support from Fundação para a Ciência e a Tecnologia (SFRH/BD/130274/2017, CEECIND/02453/2018/CP1534/CT0001, PTDC/ASP-SIL/7743/2020 and UIDB/00329/2020). A.A.C. acknowledges support from the Coordenação de Aperfeiçoamento de Pessoal de Nível Superior - Brasil (CAPES) - Finance Code 001. J.E.K. and T.P.M. gratefully acknowledge the National Research Foundation of South Africa (Grant number 114412). F.J. and N.B. acknowledge support from the German Federal Ministry of Education and Research (BMBF) in the framework of the SPACES projects OPTIMASS (FKZ: 01LL1302A) and ORYCS (FKZ: 01LL1804A). A.L. and A.S.K.F. acknowledge support from the German Federal Ministry of Education and Research (BMBF) in the framework of the SPACES projects Limpopo Living Landscapes (FKZ: 01LL1304D) and SALLnet (FKZ: 01LL1802C). L.W. acknowledges support from the US National Science Foundation (EAR 1554894). L.H.F. acknowledges support from the Natural Sciences and Engineering Research Council of Canada Industrial Research Chair Program in Ecosystem Reclamation. S.C.R. acknowledges support from the U.S. Geological Survey Ecosystems Mission Area and the U.S. Bureau of Land Management. G.M.W acknowledges support from the Australian Research Council. L.vd.B. and K.T. acknowledge support from the German Research Foundation (DFG) priority research program SPP-1803 “EarthShape: Earth Surface Shaping by Biota” (TI 338/14-1). M.D-B. acknowledges support from the Spanish Ministry of Science and Innovation for the I+D+i project PID2020-115813RA-I00 funded by MCIN/AEI/10.13039/501100011033. M.D-B. is also supported by a project of the Fondo Europeo de Desarrollo Regional (FEDER) and the Consejería de Transformación Económica, Industria, Conocimiento y Universidades of the Junta de Andalucía (FEDER Andalucía 2014-2020 Objetivo temático “01 - Refuerzo de la investigación, el desarrollo tecnológico y la innovación”) associated with the research project P20_00879 (ANDABIOMA).

P.J.R and A.J.M. acknowledge support from Fondo Europeo de Desarrollo Regional through the FEDER Andalucía operative programme, FEDER-UJA 1261180 project. A.F. thanks ANID PIA/BASAL FB210006 and Millennium Science Initiative Program NCN2021-050. A.J. acknowledges support from the Bavarian Research Alliance Germany (BayIntAn_UBT_2017_61). C.B. gratefully acknowledges the National Natural Science Foundation of China (Grant number 41971131). Biodiversity and ecosystem function research in the B.K.S. laboratory is funded by the Australian Research Council (DP210102081). Any use of trade, product, or firm names in this paper is for descriptive purposes only and does not imply endorsement by the U.S. Government. H.S. is supported by a María Zambrano fellowship funded by the Ministry of Universities and European Union-Next Generation plan. G.P. and C.V.L. acknowledge support from Universidad Nacional de Río Negro (PI 40-C-873 and 654). V. R. acknowledges support from the Regional Government of Extremadura (Spain) through a "Talento" fellowship (TA18022).

Author contributions:

Conceptualization: FTM, NG, YLB-P

Methodology: FTM, NG, YLB-P, DJE, HS

Investigation: YLB-P, DJE, HS, MB, BG, VO, MGG, EV, JJG, SA, BJM, CP, PDM, AR, AL, MCR, SC, NE, EMJ, OS,MA, NA, CLA, VA, FA, TA, RJA, KB, FBS, NB, BB, MAB, DB, CB, RC, APCM, HC, IC, PCQ, RC, AAC, CMC, ADN, BC, DAD, AJD, JD, BE, CIE, AF, MF, DF, ASKF, LHF, LAG, ACG, EGM, RMHH, NH, EHS, FMH, OJM, FJ, AJ, KFK, MK, JEK, CVL, AL, PCLR, XL, PL, JL, MAL, GMK, THP, OMI, AJM, EM, JPM, GM, SMM, AN, GO, GRO, GP, MODP, YP, REQ, SR, SCR, PJR, BR, AR, VR, JGR, JCR, AS, MAS, SS, IS, CRAS, ANS, ALT, ADT, HLT, KT, ST, JV, OV, LVDB, SVA, FV, WW, DW, LW, GMW, LY, EZ, YZ, XZ, NG

Formal analysis: NG, YLB-P, MB, DJE, EV, CAG, JTW, HWH, JZH

Resources: FTM, YLB-P, DJE, HS, MB, BG, VO, MGG, EV, JJG, SA, BJM, CP, PDM, AR, HWH, JZH, JTW, AL, MCR, SC, NE, EMJ, OS,MA, NA, CLA, VA, FA, TA, RJA, KB, FBS, NB, BB, MAB, DB, CB, RC, APCM, HC, IC, PCQ, RC, AAC, CMC, ADN, BC, DAD, AJD, JD, BE, CIE, AF, MF, DF, ASKF, LHF, LAG, ACG, EGM, RMHH, NH, EHS, FMH, OJM, FJ, AJ, KFK, MK, JEK, CVL, AL, PCLR, XL, PL, JL, MAL, GMK, THP, OMI, AJM, EM, JPM,

GM, SMM, AN, GO, GRO, GP, MODP, YP, REQ, SR, SCR, PJR, BR, AR, VR, JGR, JCR, AS, MAS, SS, IS, CRAS, ANS, ALT, ADT, HLT, KT, ST, JV, OV, LVDB, SVA, FV, WW, DW, LW, GMW, LY, EZ, YZ, XZ, BKS, NG, MDB

Funding acquisition: FTM, NG, NE, YLB-P, BB, BE, JD, AR, CP, MAB, EHS, FMH, HLT, AN, MK, JEK, TPM, FJ, NB, AL, ASKF, LW, LHF, SCR, GMW, KT, AF, CB, AJ

Project administration: FTM, NG, YLB-P, HS, EV, JMV, VO, BG

Software: NG, YLB-P

Supervision: FTM

Validation: MB, CP

Visualization: NG, YLB-P, DJE, EG, MB, EV

Writing – original draft: FTM, NG, YLB-P, DJE, HS, MDB

Writing – review & editing: FTM, NG, YLB-P, DJE, MDB, HS, MB, BG, VO, EG, JMV, MGG, EV, EG, JJG, SA, BJM, CP, PDM, AR, HWH, JZH, JTW, AL, MCR, SC, NE, EMJ, OS,MA, NA, CLA, VA, FA, TA, RJA, KB, FBS, NB, BB, MAB, DB, CB, RC, APCM, HC, IC, PCQ, RC, AAC, CMC, ADN, BC, DAD, AJD, JD, BE, CIE, AF, MF, DF, ASKF, LHF, LAG, ACG, EGM, RMHH, NH, EHS, FMH, OJM, FJ, AJ, KFK, MK, JEK, CVL, AL, PCLR, XL, PL, JL, MAL, GMK, THP, OMI, AJM, EM, JPM, GM, SMM, AN, GO, GRO, GP, MODP, YP, REQ, SR, SCR, PJR, BR, AR, VR, JGR, JCR, AS, MAS, SS, IS, CRAS, ANS, ALT, ADT, HLT, KT, ST, JV, OV, LVDB, SVA, FV, WW, DW, LW, GMW, LY, EZ, YZ, XZ, BKS

Competing interests: Authors declare that they have no competing interests.

Data and materials availability: All the data used in this article and the R scripts employed to generate the main results of the study are available through figshare (doi: 10.6084/m9.figshare.14923065). The raw sequence data generated in this study are available from figshare (doi: 10.6084/m9.figshare.20131355).

Supplementary Materials

Materials and Methods

figs. S1 to S19

Tables S1 to S28

References (31–266)

Movie S1

Figures

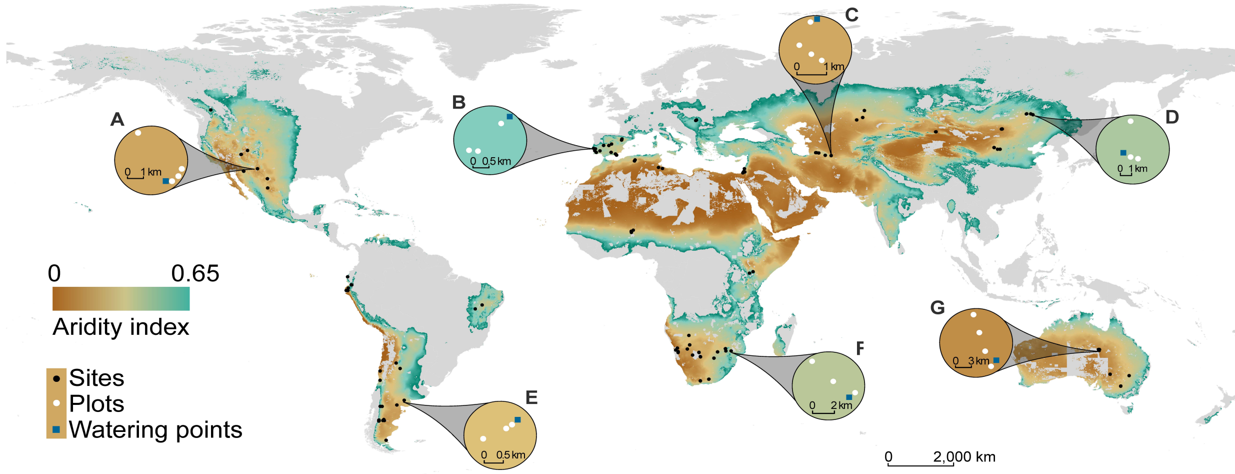

Figure 1. Location of the 98 study sites with examples (insets A-G) of the local grazing gradients surveyed at each site. Each black dot represents a site with multiple plots (white dots) of 45 × 45 m surveyed in situ; a total of 326 plots were surveyed across the 98 study sites. Watering points are ponds, impoundments, or drinking troughs that provide permanent sources of water for livestock in drylands; they are used in our study to create local grazing gradients (*13*). The background of the map indicates the extent of dryland rangeland areas. The aridity index is calculated as precipitation/potential evapotranspiration and is strongly related to mean annual precipitation in our dataset (R^2 = 0.82). See Materials and Methods (*13*) for the aridity index and rangeland area data sources used.

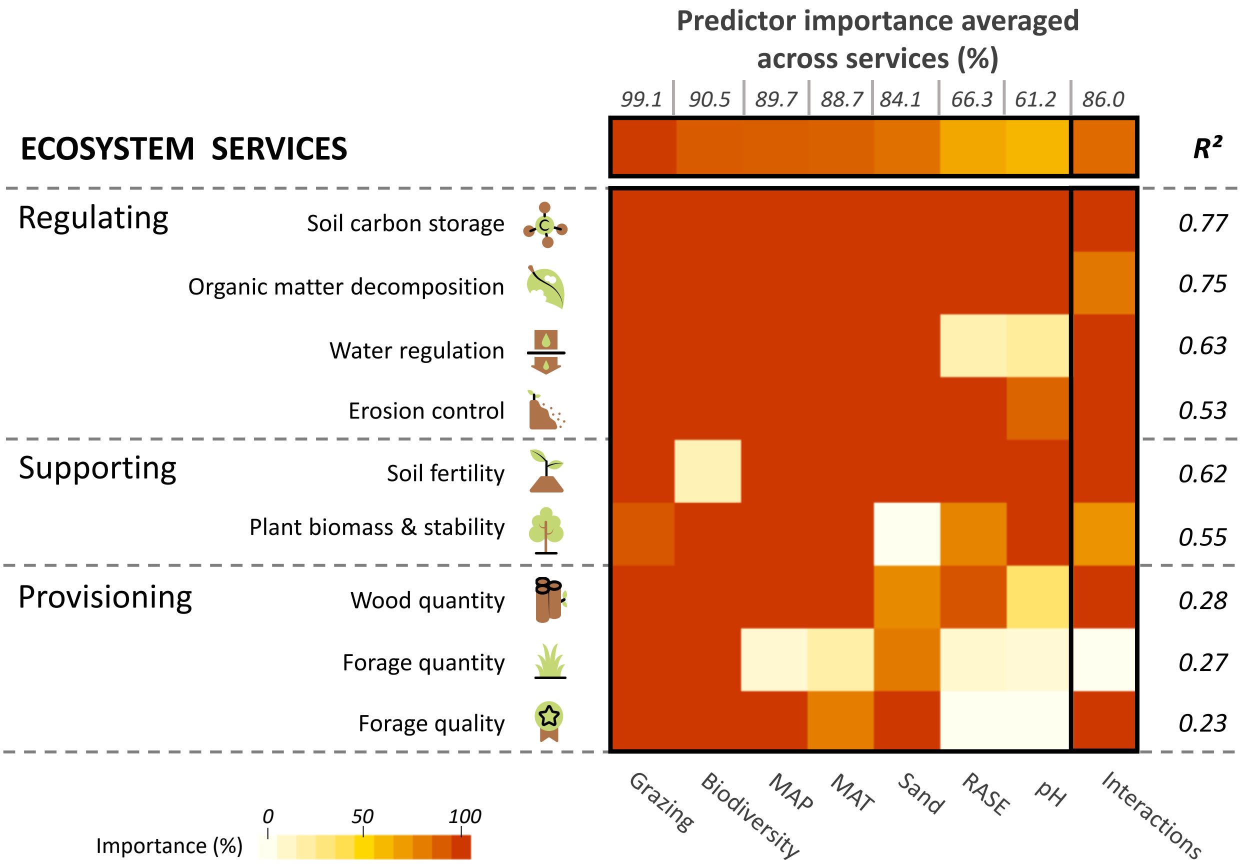

Figure 2. Relative importance (importance) of predictors (grazing pressure, climate, biodiversity, and soil variables, and their interactions) of ecosystem services selected in the best-fitting models. Importance is quantified as the sum of the Akaike weights of all models that included the predictor of interest, considering the number of models in which each predictor appears. It is proportional to the number of times a given predictor (and its interactions with other predictors) was selected in the final set of best-fitting models (*13*). Interactions include all interactions between grazing pressure and climate, biodiversity, and soil variables; the importance of each interaction type is shown in fig. S12. In the case of biodiversity, predictor importance considers the number of models that includes at least one biodiversity proxy (plant species richness, mammalian herbivore richness, or belowground diversity). Separate results for

each biodiversity proxy are shown in fig. S12. Full details on model results, including the number of best-fitting models, are available in tables S13 to S15. Plant biomass & stability = aboveground plant biomass and its temporal stability, Grazing = grazing pressure, MAT = mean annual temperature, RASE = rainfall seasonality, and MAP = mean annual precipitation.

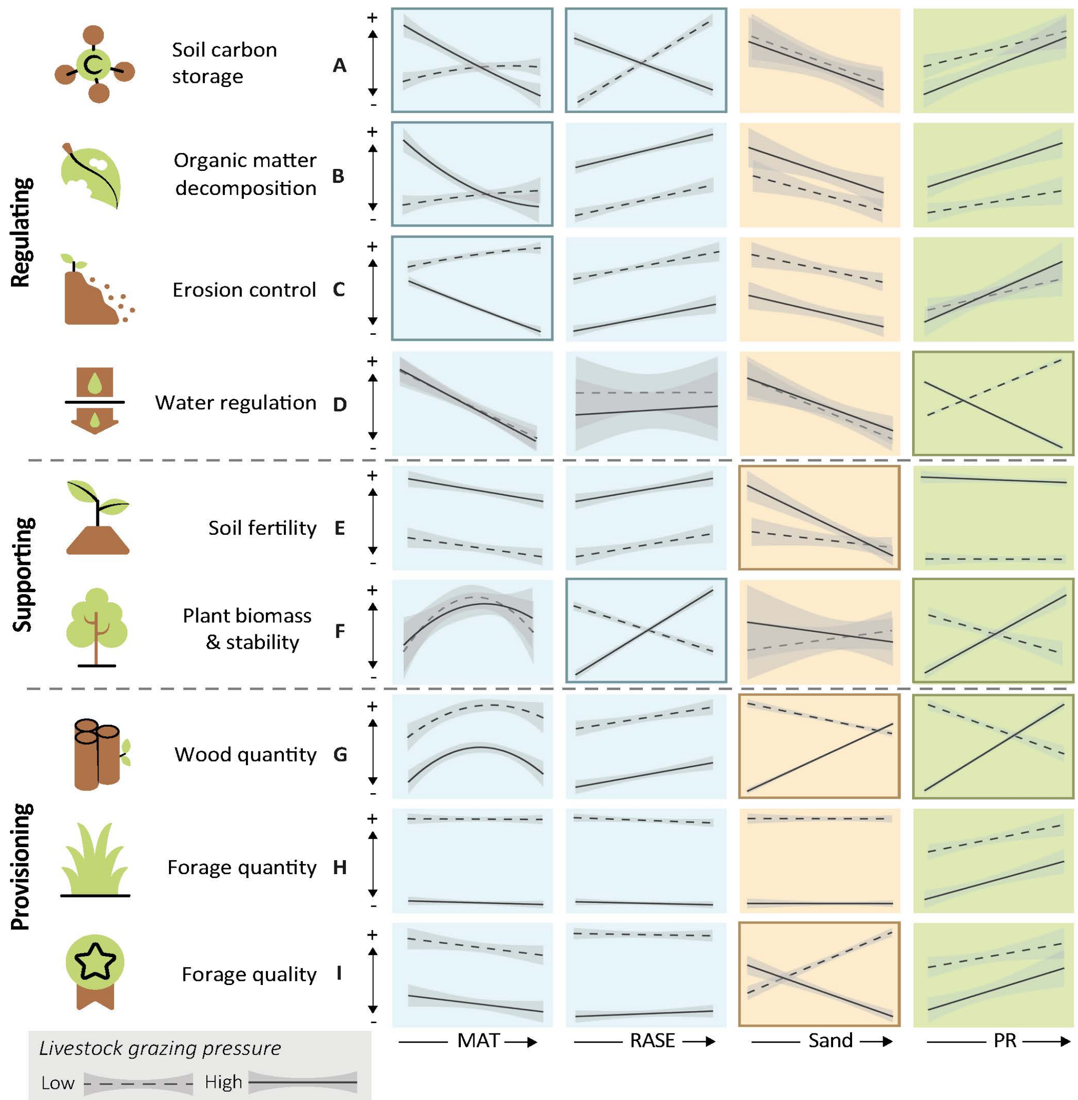

Figure 3. Predicted responses of ecosystem services to changes in climate, sand content, and plant species richness at low and high grazing pressure levels. The lines at each panel show model fits (using partial residuals) for each predictor selected in the final best-fitting models at low and high grazing pressures for each service. Panels surrounded with a border denote significant interactions between grazing and other predictors. Predicted responses of

ecosystem services to all grazing pressure levels (ungrazed, low, medium, and high) and to other model predictors are presented in figs. S12 to S14. The complete set of statistical results and model fits are available in tables S13 to S15. Plant biomass & stability = aboveground plant biomass and its temporal stability, MAT = mean annual temperature, RASE = rainfall seasonality, Sand = sand content, and PR = plant species richness.

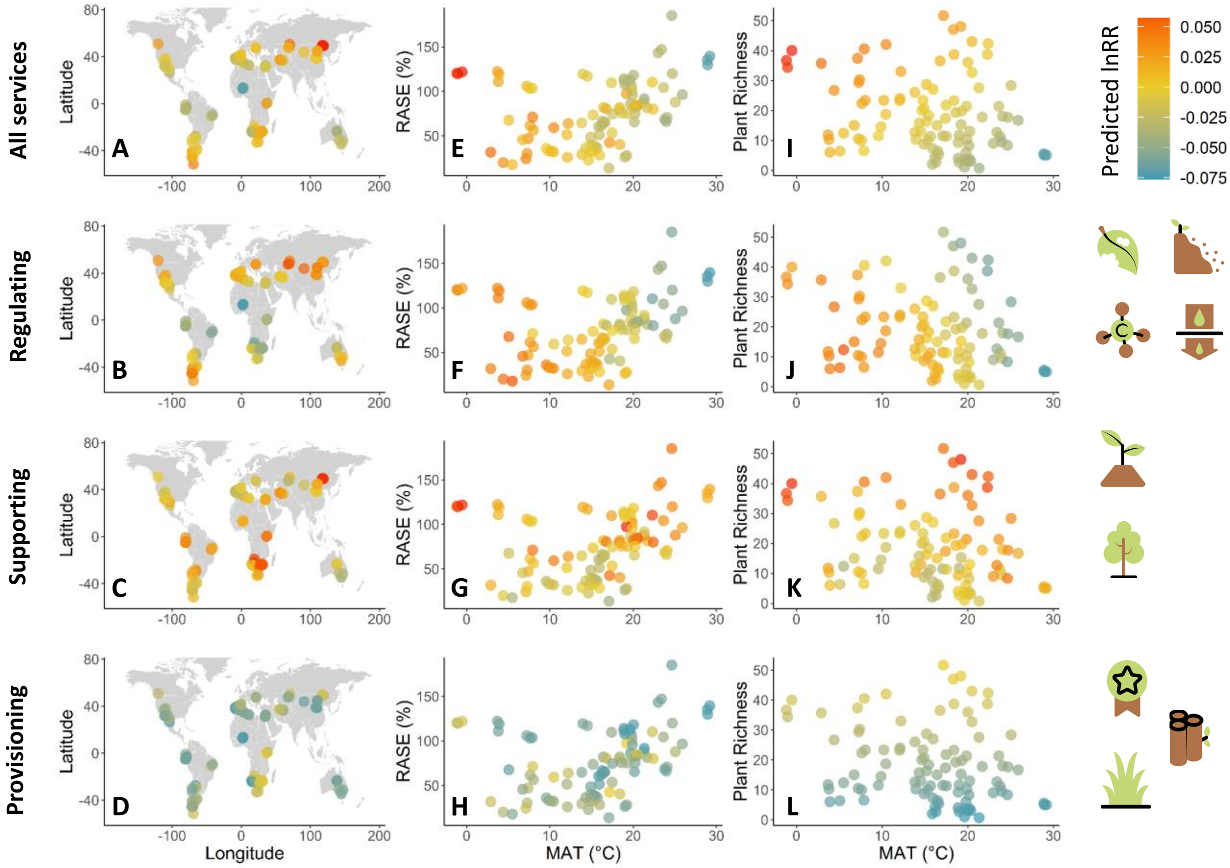

Figure 4. Geographical variation in the effect of grazing pressure on ecosystem services across global drylands. For each of the 98 sites surveyed, we plot the effect of grazing pressure on ecosystem services predicted by model parameters along the wide climatic and plant species richness gradients evaluated. To do so, we first predicted each ecosystem service at low and high grazing pressures using predictor estimates of the best-fitting models (see tables S13 to S15). Then we calculated the predicted effect of grazing at each site as the difference between high and low grazing pressure levels using a log response ratio (lnRR; *13*). Predictions were made using plant species richness, mean annual temperature (MAT), and rainfall seasonality (RASE); all other parameters were fixed at their mean value (*13*). For simplicity, we averaged grazing effects across all ecosystem services (A, E, I), and across regulating (B, F, J), supporting (C, G, K), and

provisioning (D, H, L) services. Blue and red dots indicate negative and positive effects of grazing, respectively. See figs. S16 and S17 for detailed results on each service and Fig. 2 for the meaning of the symbols depicting each ecosystem service.

Science
AAAS

Supplementary Materials for

Grazing and ecosystem service delivery in global drylands

Fernando T. Maestre, Yoann Le Bagousse-Pinguet, Manuel Delgado-Baquerizo, David J. Eldridge, Hugo Saiz, Miguel Berdugo, Beatriz Gozalo, Victoria Ochoa, Emilio Guirado, Miguel García-Gómez, Enrique Valencia, Juan J. Gaitán, Sergio Asensio, Betty J. Mendoza, César Plaza, Paloma Díaz-Martínez, Ana Rey, Hang-Wei Hu, Ji-Zheng He, Jun-Tao Wang, Anika Lehmann, Matthias C. Rillig, Simone Cesarz, Nico Eisenhauer, Jaime Martínez-Valderrama, Eduardo Moreno-Jiménez, Osvaldo Sala, Mehdi Abedi, Negar Ahmadian, Concepción L. Alados, Valeria Aramayo, Fateh Amghar, Tulio Arredondo, Rodrigo J. Ahumada, Khadijeh Bahalkeh, Farah Ben Salem, Niels Blaum, Bazartseren Boldgiv, Matthew A. Bowker, Donaldo Bran, Chongfeng Bu, Rafaella Canessa, Andrea P. Castillo-Monroy, Helena Castro, Ignacio Castro, Patricio Castro-Quezada, Roukaya Chibani, Abel A. Conceição, Courtney M. Currier, Anthony Darrouzet-Nardi, Balázs Deák, David A. Donoso, Andrew J. Dougill, Jorge Durán, Batdelger Erdenetsetseg, Carlos I. Espinosa, Alex Fajardo, Mohammad Farzam, Daniela Ferrante, Anke S.K. Frank, Lauchlan H. Fraser, Laureano A. Gherardi, Aaron C. Greenville, Carlos A. Guerra, Elizabeth Gusmán-Montalvan, Rosa M. Hernández-Hernández, Norbert Hölzel, Elisabeth Huber-Sannwald, Frederic M. Hughes, Oswaldo Jadán-Maza, Florian Jeltsch, Anke Jentsch, Kudzai F. Kaseke, Melanie Köbel, Jessica E. Koopman, Cintia V. Leder, Anja Linstädter, Peter C. le Roux, Xinkai Li, Pierre Liancourt, Jushan Liu, Michelle A. Louw, Gillian Maggs-Kölling, Thulani P. Makhalanyane, Oumarou Malam Issa, Antonio J. Manzaneda, Eugene Marais, Juan P. Mora, Gerardo Moreno, Seth M. Munson, Alice Nunes, Gabriel Oliva, Gastón R. Oñatibia, Guadalupe Peter, Marco O.D. Pivari, Yolanda Pueyo, R. Emiliano Quiroga, Soroor Rahmanian, Sasha C. Reed, Pedro J. Rey, Benoit Richard, Alexandra Rodríguez, Víctor Rolo, Juan G. Rubalcaba, Jan C. Ruppert, Ayman Salah, Max A. Schuchardt, Sedona Spann, Ilan Stavi, Colton R. A.Stephens, Anthony M. Swemmer, Alberto L. Teixido, Andrew D. Thomas, Heather L. Throop, Katja Tielbörger, Samantha Travers, James Val, Orsolya Valkó, Liesbeth van den Brink, Sergio Velasco Ayuso, Frederike Velbert, Wanyoike Wamiti, Deli Wang, Lixin Wang, Glenda M. Wardle, Laura Yahdjian, Eli Zaady, Yuanming Zhang, Xiaobing Zhou, Brajesh K. Singh, Nicolas Gross.

Correspondence to: ft.maestre@ua.es

This PDF file includes:

Materials and Methods
figs. S1 to S19
Tables S1 to S28
Caption for Movie S1

Other Supplementary Materials for this manuscript include the following:

Movie S1

Materials and Methods

Characteristics of the study sites

We carried out our study in rangelands, defined as “lands carrying natural or semi-natural vegetation that provide habitat suitable for herds of wild or domestic ungulates” (*31*), located in drylands (areas with an aridity index [precipitation/potential evapotranspiration [P/PET] below 0.65, *32*) between January 2016 and September 2019. The area of dryland rangelands shown in Fig. 1 and fig. S1 was obtained from refs. 33 and 34. Field data and plant and soil samples were gathered at 98 sites located in 25 countries from six continents (Algeria, Argentina, Australia, Botswana, Brazil, Canada, Chile, China, Ecuador, Hungary, Iran, Israel, Kazakhstan, Kenya, Mexico, Mongolia, Namibia, Niger, Palestine, Peru, Portugal, South Africa, Spain, Tunisia, and the United States of America; fig. 1, Movie S1), including remote and traditionally poorly studied dryland regions. These include the Southeast of Tunisia, the Sechura Desert in Peru, the Golestan province in Iran, and the West Bank, to name a few. Site selection aimed to capture a wide range of grazing pressure levels and of the variety of the abiotic (climate, soil type, surface inclination) and biotic (type of vegetation, total plant cover, species richness) features characterizing dryland rangelands worldwide, and to be as geographically representative as possible while keeping the survey logistically feasible.

Standardized climatic data from all the sites were obtained from WorldClim 2.0 (www.worldclim.org), a high resolution (30 arc seconds or ~ 1 km at equator) database based on many climate observations and topographical data for the 1970-2000 period (*35*). Aridity index data were obtained from the Global Aridity Index and Potential Evapotranspiration Climate Database v2 (*36*), which uses interpolations based on WorldClim. The range of the aridity index, mean annual precipitation, and mean annual temperature values covered by the study sites was 0.01 to 0.54, 26 mm/yr to 891 mm/yr, and -1.2 ºC to 29.2 ºC, respectively. All sites experienced high seasonal variability in rainfall (74.69% ± 34.61%, mean ± SD). The studied sites included 16 of the World Reference Base soil groups (*37*) and all major soil groups present in drylands worldwide (*38*). Surface inclination values ranged between 0º and 31.6º. All sites with a slope value > 2º were located on SE-SW and NE-NW faces in the Northern and the Southern Hemispheres, respectively, to minimize the potential effects of different microclimates promoted by slope aspect, which can be very important in drylands (*39–41*). Elevation varied between 12 m and 2214 m a.s.l. The sites surveyed encompass a wide variety of representative vegetation physiognomies, including grasslands, shrublands, savannas, and open woodlands with shrubs (fig. S2). Perennial plant canopy cover ranged between 0% and 99%. Detailed information about the location and main environmental characteristics of the study sites can be found in the database that accompanies this article (doi: 10.6084/m9.figshare.14923065).

Selection of local grazing gradients and characterization of grazing pressure

At each of the 98 study sites, multiple 45 m × 45 m plots were sampled once across a local grazing gradient (including the effects of vegetation removal and trampling) with different levels of grazing pressure (low, medium, and high grazing pressure plus another plot in an ungrazed area whenever possible) by livestock and native herbivores. This gradient approach, which is frequently used in large-scale studies assessing grazing impacts (*42–44*), is the most appropriate way to capture: i) potential effects of grazing, and the interactions between climate, biodiversity, and soils, on the provision of ecosystem services and ii) the large amount of environmental variability/heterogeneity across sites and to minimize this variability within sites.

To determine a grazing gradient within each site, we located plots at different distances from artificial watering points, which are ponds, impoundments, or drinking troughs that provide permanent sources of water for livestock and wild herbivores in drylands (*43*, *45*). The distance to watering points is a valuable proxy of grazing pressure (i.e., sites closer to water are more heavily grazed; *43*, *45–47*), and has been widely employed (and validated multiple times) when assessing the ecological impacts of grazing pressure in drylands worldwide (*43*, *45–50*). To ensure a correct characterization of the grazing gradient, we also conducted an expert-level heuristic assessment of plot-level grazing pressure using the best available knowledge, historical records, and prior information whenever available. While this heuristic assessment of grazing pressure combined with distance to waterpoints and expert knowledge is somewhat subjective, each survey team was familiar with current grazing intensities at their plots and sites. In eight of the 98 surveyed sites, local grazing gradients were established using paddocks grazed at different intensities, rather than distance to watering points. Nevertheless, all plots were established in areas representative of the vegetation and soil types found in the site, so the impacts of grazing pressure could be assessed at each site without confounding factors associated with differences in climate, soil type or vegetation. This is because plots within each site have identical or similar climate and parent material, so differences among them are largely due to the different grazing pressure levels they experience. Selected watering points were separated from other watering points and/or elements that could alter the movement of mammalian herbivores, such as fences, by at least 1 km to avoid confounding effects that could influence the impact of distance to water on the measured ecosystem structural and functional attributes.

Of the 98 sites surveyed, a total of 52 sites had three plots corresponding to three grazing intensities (low, medium, and high grazing pressure). In addition to these 52 sites, 35 sites had an additional ungrazed area surveyed (ungrazed, low, medium, and high grazing pressure). In eight sites, an ungrazed control plus two additional grazing levels (medium and high or low and high grazing pressure) were surveyed. Finally, in three sites, only two plots could be located because they lacked low or medium grazing pressure plots. In total, 326 plots of 45 m × 45 m (including 43 ungrazed, 88 low grazing pressure, 97 medium grazing pressure, and 98 high grazing pressure plots) were surveyed in situ as described in the following sections.

Our study needed to be standardized (so results can be comparable), and thus it was not possible to capture the wide variation in the size of fields used for managing extensive livestock grazing across dryland rangelands (*51–53*). This issue (i.e., a fixed plot size), which is shared by any global standardized experiment and survey conducted so far (e.g., BIOCOM (*18*), NutNet (*54*), DroughtNet (*55*), Darkdiv (*56*)), does not preclude the acquisition of representative results in our study for four main reasons. First, the spatial resolution [plot area] and actual extent [summed area of all plots] (sensu ref. 57) at which our field data were gathered (spatial resolution of 2025 m^2 and actual extent of 660,150 m^2 respectively) is substantially larger than that used in most ecological and grazing studies conducted so far (*57*, *58*). Furthermore, the potentially represented area of the surveyed plots at each site (i.e., that covered by these plots and the distance between them) is much larger (range 1.1 - 6096.7 ha, mean size = 25.8 ha) and resembles that of (small to medium sized) paddocks typically found across rangeland drylands worldwide (*51*, *53*, *59*).

Second, our plots were in areas representative of their landscapes. In dryland ecosystems such as those we surveyed, the spatial resolution and size of the plots we used captures information on key ecosystem properties (e.g., perennial vegetation cover) that are both representative of those found at larger spatial extents (*60*) and can be scaled up to larger regions (*61*). Third, the location of plots of different grazing pressures within each site captures the spatial heterogeneity in grazing that is typically found in larger paddocks (*62*). Finally, paddock size per se may not be a good proxy for grazing pressure at the scale of our study. For instance, a high density of herbivores in a small paddock in a subhumid environment could represent a moderate grazing pressure for that area whereas fewer herbivores in a much larger paddock in an arid landscape could equate to high grazing pressure for that area. For these reasons, paddock size is not an attribute that we considered in our study. Certainly, paddock size would be an important consideration if we were looking at the same number of animals in paddocks of different sizes.

We fully acknowledge that some grazing effects (e.g., on soil properties such as carbon) might take years to be noticeable (*63*). We consider that our approach is appropriate since we measured the response variables in paddocks subjected to grazing for many years. This is one of the advantages of our observational study vs. experiments that are usually done over short periods of time. Furthermore, the time needed for some grazing impacts to be noticeable in soil variables is not a problem to interpret our results because we are comparing the impacts of grazing pressure on ecosystem services across space, not across time, and because we are controlling for site-specific effects in our analyses (see “Statistical analyses” section below). This issue would have been a problem if we had compared, for instance, the impacts of grazing on soil properties in a single site using a short temporal data series.

Overall, our study focused on the resultant grazing pressure, which is a composite of different types of herbivores, the location of particular plots within a paddock (close to water, far from water), the length of time that grazing has occurred, and the type of herbivores, among other considerations. The resultant signature, assessed as grazing pressure (recent and historic), was linked to the different ecosystem services measured. In this way the type of grazing (e.g., set stocking, time-controlled grazing, low risk stocking, transhumance, etc.) is not particularly an issue because we are using dung and livestock tracks to ensure that our local grazing gradients are properly characterized (see “Validation of grazing pressure gradients” section below). Finally, and as shown in fig. S9, our experimental approach successfully captured the full range of grazing pressure that is typically observed across dryland rangelands worldwide. Our results are relevant, therefore, to situations where grazing pressure is greater, whether this occurs close to watering points, or under nomadic systems, or where different densities of animals are constrained within paddocks. We believe that grazing pressure, rather than the assessment methodology or how such pressure is created, is the most important aspect when interpreting the results of our study.

Validation of grazing pressure gradients

Our grazing pressure was not selected a priori, though we would expect that our plots would represent a gradient in grazing pressure within each site. To confirm that this was the case, we conducted multiple validation tests of the heuristic value of grazing pressure obtained at each plot by: i) identifying, counting and weighing the dung or pellets of all herbivores within quadrats, a standard approach to assess the abundance of livestock and wild herbivores (*64–66*),

ii) using livestock density data whenever available, iii) conducting a cluster analysis with dung/pellet data, and iv) measuring the width and depth of all livestock tracks crossing the plot to derive a total cross-sectional area of livestock tracks for each site, a surrogate of historic grazing pressure (*67*). Results from all validation tests conducted, presented in detail in the following paragraphs, indicated that dung mass accurately predicted the four-level categorical assessment of grazing pressure (ungrazed, low, medium, and high grazing pressure; figs. S4-S8). Increases in grazing pressure (from ungrazed to high grazing pressure) were associated with livestock density (fig. S6), dung mass (fig. S7) and area/density of livestock tracks (fig. S8).

We first conducted in situ assessments of recent grazing pressure by all herbivores in all plots by counting and identifying their dung and pellets. The assessment of dung production has been used widely to evaluate recent grazing pressure and abundance of large mammalian herbivores (*66*), such as cattle (*65*), sheep (*64*), deer (*68*, *69*) and kangaroos (*70*). Because our aim was to investigate the impact of grazing pressure on biodiversity and ecosystem services, we limited our assessment of herbivory to mammalian, mostly large-bodied herbivores (> 20 kg e.g., Roe deer *Capreolus capreolus*). We also included grazing by the European rabbit (*Oryctolagus cuniculus*) and hares (*Lepus* spp.) because these herbivores are typically associated with environments grazed by livestock. Further, these grazers have been shown to contribute to substantial biomass reduction in rangelands (*71*, *72*). We acknowledge, however, that smaller-bodied mammalian herbivores and omnivores, such as the Southern Mountain cavi (*Microcavia australis*) and birds such as the Greater rhea (*Rhea americana*) and Common ostrich (*Struthio camelus*), also co-occur with livestock and larger mammalian herbivores. However, we did not record the dung of these animals in field surveys because their relative grazing effects would be extremely small compared with livestock and other native herbivores, and because they are not associated with increases in grazing pressure.

To measure dung and pellets in the field, we placed a 25 m^2 (5 m × 5 m) quadrat, within which was nested a smaller 1 m^2 (1 m by 1 m) quadrat, at distances of 10 m and 30 m along each 45 m transect. Within the larger quadrat we counted the dung of large-bodied herbivores (e.g., giraffe, cattle, and horses), and in the smaller quadrat the dung or pellets of smaller-bodied herbivores (e.g., goats, sheep, lagomorphs), and classified it according to the species producing it. Experienced field operators were familiar with the dung of different herbivores and were, therefore, able to identify and separate dung in the field. This was particularly important in locations supporting high herbivore richness such as those from South Africa, where herbivore richness was the greatest ($n = 6$). Field guides are available to allow operators to identify dung in different regions (e.g., antelope spp. in Africa (*73*) or different herbivores in Australia (*74*)). However, it was not possible to successfully separate the dung of sheep and goats, except where they occurred separately, largely because of the high degree of overlap in dung morphology (*75*).

To calculate dung/pellet (dung hereafter) mass, we used one of two approaches: i) direct measurements, or ii) estimates based on dung counts. Some survey teams made direct measurements of dung by collecting, oven drying and weighing all dung found in the quadrats and expressed it as a mass per m^2 for each plot and herbivore type. Direct measurements of dung mass are typically used either where dung mass is low, or where the main herbivores do not produce clearly defined pellets, such as horses (*Equus caballus*), cattle (*Bos* spp.), donkeys (*Equus africanus asinus*), giraffe (*Giraffa camelopardalis*), elephants (*Loxodonta africana*), buffalo (*Syncerus caffer*), camels (*Camelus* sp.), hartebeest (*Alcelaphus buselaphus*), wildebeest

(*Connochaetes* sp.), and zebra (*Equus quagga*). Alternatively, field surveyors counted dung of each herbivore in all quadrats but collected it from only a subsample of the quadrats surveyed, generally four large (25 m^2) or small (1 m^2) quadrats (depending on herbivore type), to derive relationships between dung counts and mass for separate herbivore types. This estimation technique is highly effective for those herbivores that produce pellets, such as goats (*Capra hirca)*, sheep (*Ovis aries*), deer (*Capreolus capreolus, Cervus elaphus*), various antelope species including Gemsbok (*Oryx gazella*), Springbok (*Antidorcas marsupialis*) and Greater kudu (*Tragelaphus strepsiceros*), various kangaroos (*Osphranter rufus*, *Macropus* spp.), European rabbit, and the European hare (*Lepus* sp., table S2). Typical relationships between dung counts and mass varied among herbivore types and sites, but coefficients of determination were always > 0.40 (fig. S4). Although in most plots we directly measured the weight of dung, some sites relied on the calibration between dung count and mass. These ranged from very strong relationships (e.g., horses in Chile: R^2=0.89, P < 0.001, n = 27; cattle in Argentina: R^2=0.94, P < 0.001, n = 12) to relatively weak, often due to low sample size (cattle in Hungary: R^2=0.43, P = 0.003, n = 17; cattle in New Mexico USA: R^2=0.64, P = 0.054, n = 5). Thus, using either direct assessment of dung mass or estimated measures, we were able to calculate the total oven-dried mass of dung per hectare for each herbivore as one measure of recent grazing pressure.

As an initial test of the validity of herbivore dung as a measure of recent grazing pressure, we examined four sites in our study (two from Argentina, one each from Australia and Iran) that were all grazed by sheep and from which we had data on the mass of dung collected in the field and empirical data on long-term stocking rates obtained from experimental studies or from pastoralists or herders. We plotted the total dry mass of dung against livestock density, which was adjusted to a common scale of dry sheep equivalents ($DSE \cdot ha^{-1}$); the value of one non-lactating ewe without a lamb (*76*). Results for these four sites demonstrate a positive linear relationship between livestock density ($DSE \cdot ha^{-1}$) and dung mass ($kg \cdot ha^{-1}$; fig. S5). Moreover, experimental studies of sheep grazing in arid South Australia show a strong relationship between the time that livestock spend grazing and the amount of dung produced (*77*). Other studies from Zimbabwe (*78*), Kenya (*79*), South Africa (*80*) and southern Mongolia (*81*) have linked dung counts to herbivore grazing pressure. We are confident, therefore, that greater time spent grazing equates with more livestock dung and thus a greater amount of recent grazing.

We then examined whether the reported grazing pressure ($DSE \cdot ha^{-1}$) was related to our heuristic measure of grazing pressure (ungrazed, low, medium, high) using data from the Australian, Iranian and the combined Argentinian sites described previously (fig. S6). Our results clearly show a significant increase in grazing pressure along a grazing gradient from ungrazed to high grazing pressure in Argentina (One-way ANOVA: $F_{3,7}$ = 4.8, P = 0.04), Australia ($F_{3,10}$ = 4.51, P = 0.045) and Iran ($F_{3,7}$ = 22.3, P = 0.001).

As a final test of the links between our dung measurements and current grazing pressure, we examined the relationship between the total mass of dung from each study ($kg \cdot ha^{-1}$) and our heuristic measure of grazing pressure (ungrazed and low, medium, and high grazing pressure) using two analyses. First, we tested the relationship between these grazing pressure levels and dung measurements using a general linear model that considered study sites as a random effect. Increases in grazing pressure were associated with increasing levels of dung production (F = 37.0, df = 3, P < 0.001, on $\log_{10}(x+1)$ data; fig. S7a). Tukey's *post-hoc* LSD test indicated a significant difference among all grazing pressure levels except medium and high, which did not differ significantly. When dung data were separated into livestock and wild herbivores (fig. S1), this pattern was reproduced for livestock species but not for wild herbivores, as their dung mass did not increase among the different grazing levels evaluated. These results further suggest that increases in grazing pressure along our local grazing gradient were largely driven by livestock, and not by wild herbivores. Second, we performed a cluster analysis validation. In this analysis, we first standardized the dung density values by dividing them by the maximum dung density found within each site. Standardization yielded a value ranging from 1 (maximum density within a site) to 0 (minimum possible dung density). We then performed a cluster analysis, using the Elbow method (*82*), to identify the optimum number of clusters that can be obtained using dung data only. This analysis identified four clusters as being optimum, which is consistent with our assignment of four categorical classes under the expert-derived heuristic method (fig. S7b). To test the veracity and accuracy of this clustering approach, we assigned clusters to the plots based on the mass of dung (labeled U, L, M and H in fig. S7c) and compared the match with the classification made by individual experts (ungrazed and low, medium, and high grazing pressure). Total accuracy of expert assignment was 39.2%, with a significant association between dung-based and expert-based grazing levels ($\chi^2 = 95.05$, df= 9, $P < 0.001$). Low accuracy was driven mainly by a similarity among low and ungrazed plots, which are not well distinguished in terms of dung clusters. When this process was repeated without ungrazed plots, the match between expert-based assignment and dung-based assignment increased to 53.2% (fig. S7d; $\chi^2 = 46.01$, df = 4, $P < 0.001$). For this reduced analysis, the greatest mismatch between expert-based and dung-based approaches occurred under medium grazing pressure plots, which sometimes had dung levels close to high grazing pressure and others close to low grazing pressure plots (fig. S7d).

The dung data gathered across all our plots showed a very wide range of variation (fig. S9), suggesting that our survey effectively captured a large range in grazing pressure levels. The comparison of these dung data with those obtained from the literature (including studies assessing a wide range of grazing pressure, from ungrazed to very high grazing, in drylands from Australia, China and Kenya) shows how the range of variation reported in these studies is very similar to that observed in our survey (fig. S9).

We also used the size and density of livestock tracks as a measure of historic grazing by livestock. These tracks are semi-permanent landscape features that are formed when livestock traverse the same path to and from water (*83*). These compacted tracks are clearly visible over many decades, and tracks become wider and deeper as the pressure of livestock grazing increases. The density and size of livestock tracks are therefore useful indicators of the history of livestock grazing (*46*, *66*). These tracks, however, fail to form or persist on sandy soils, which lack the compaction created by trampling (*84*), so historic grazing could not be assessed at all sites.

To assess the level of historic grazing pressure, we measured the width and depth of all livestock tracks crossing each of the 45 m transects to derive a total cross-sectional area of tracks for each site. These values were then scaled to a total area per 100 m of transect. We also calculated the total number of tracks per 100 m of transect (fig. S8). Using a general linear model that considered study site as a random effect, we found a strong and significant difference in the area of livestock tracks among the four levels of grazing pressure (ungrazed and low, medium, and high grazing pressure; $F_{3,163} = 14.95$, $P < 0.001$ on $\log_{10}(x+1)$-transformed data; fig. S8). For track density, we found a significant difference in density between ungrazed and the three levels of grazing pressure ($F_{3,166} = 9.28$, $P < 0.001$; $\log_{10}(x+1)$-transformed data).

Overall, the comprehensive analyses conducted showed very similar trends, irrespective of whether we used dung mass as a measure of recent grazing pressure, track area/density as a measure of long-term grazing pressure or the expert heuristic site classification. This gives us a high degree of confidence that the grazing gradients we observed are true gradients in grazing pressure, and thus were well-suited to achieve the objectives of our study. Furthermore, the range of variation in dung mass observed across the surveyed sites was very similar to that observed in previous studies carried out in multiple dryland regions (fig. S9), suggesting that our survey successfully captured the full range of grazing pressure levels that is typically observed in grazed drylands across the globe.

Vegetation and soil sampling

Vegetation and soil surveys were conducted following a standardized sampling protocol, described in full in ref. 85. The coordinates and elevation of each 45 m × 45 m plot were recorded in situ with a portable Global Positioning System and were standardized to the WGS84 ellipsoid for visualization and analyses. We located four 45 m transects oriented downslope within each plot, spaced 10 m apart across the slope, for the vegetation surveys. To minimize potential impacts of seasonal variability within and across sites, vegetation and soil surveys took place just after the main vegetation growth period and in the peak of the dry season, respectively. This ensured that the data obtained across sites were as standardized and comparable as possible. When required by local authorities, permissions were obtained for conducting field work. Our study did not involve handling or collection of endangered species.

Perennial plant presence and cover were measured in each transect using the line-point intercept method (*86*). Specifically, we surveyed points located every 20 cm for a total of 225 points per transect (900 points per plot). Also, we placed 25 contiguous quadrats (1.5 m × 1.5 m) in each transect (100 quadrats per plot) and visually estimated the cover of each perennial vascular plant present as the percentage of the quadrat covered (0-100). The cover for each species was calculated as the sum of the species cover for all quadrats. In addition, all identified species per plot were classified into three functional categories associated with their life strategy/biological type: forbs, grasses, and woody species. The cover of each category was calculated as the proportion of total vegetation cover (sum of the cover for all species) that was associated with that category (e.g., $cover_{grass}$ = sum [cover of all grass species]/sum [cover all species]). We restricted our study to perennial plants because they are instrumental in maintaining the functioning of drylands (*18*, *87*). Moreover, annual plant composition in drylands shows high intra- and inter-annual variability (*87*, *88*). Thus, we did not survey annual species to avoid confounding effects in the differences in plant species richness among study sites caused primarily by the timing of sampling.

We measured maximum plant height, specific leaf area, and leaf dry mass content (LDMC) on 21,106 individuals from 1,918 species, and foliar nitrogen content on 2,570 individuals from 1,034 species following standard protocols (*89*). Maximum plant height (in m) measures the height of a plant from the ground up to the highest leaves belonging to the vegetative part of the plant. Specific leaf area ($cm^2 \cdot g^{-1}$) was calculated as the ratio between leaf area (cm^2) and dry leaf mass (g), while LDMC (unitless) was estimated as the ratio between oven-dry and water-saturated fresh mass of leaves. The selected traits were measured on the tallest individual of each perennial plant species present in 20 quadrats randomly selected among the 100 quadrats surveyed at each plot (5 quadrats per transect). For each selected plant individual, we sampled the youngest mature and undamaged leaves at the top of the plant (sampled leaf surface was always > 2 cm^2). Leaves were then stored in moistened plastic bags and brought to the laboratory for rehydration. Leaf area was quantified on each individual by taking photographs of the collected leaves and analyzing them using the freeware ImageJ (*90*) (https://imagej.nih.gov/ij/index.html; see ref. 85 for additional details on the procedure followed). Leaf fresh and dry mass were obtained by weighing before and after oven drying at 60 ºC for 48 h. To obtain foliar nitrogen content, leaves were grouped by species within each plot for chemical analysis. Then, oven-dried leaves were ground in a homogenizer (Precellys® 24; Bertin Technologies, Montigny-le-Bretonneux, France) and analyzed for total nitrogen on a EuroEA3000 elemental analyser (EuroVector, Pavia, Italy).

Soils were sampled using a stratified random procedure. At each plot, five 50 cm × 50 cm quadrats were randomly placed under the canopy of the dominant (in terms of % cover) perennial vegetation element and in open areas devoid of perennial vegetation (10 quadrats in total). A composite topsoil sample consisting of five 145 cm^3 soil cores (0-7.5 cm depth) was collected from each quadrat, bulked, and homogenized in the field. After field collection, the soil samples were taken to the laboratory, where they were sieved (2 mm mesh). Once sieved, a fraction was air-dried for one month and stored for physico-chemical analyses; another was immediately frozen at -20 ºC for microbial analyses (depending upon the availability of a freezer close to the field site). Dried plant and soil samples, and frozen soil samples from all the countries were shipped to the laboratory of Rey Juan Carlos University in Móstoles (Spain). These shipments were carried out according to national and international regulations; exporting permits were obtained for each country (when required) and importing permits to Spain were obtained for every shipment by the Spanish Ministry of Agriculture, Fisheries and Food. Once in the laboratory, we created a composite soil sample per microsite (vegetated and open areas) and plot using equal amounts of all the replicate soil samples collected in the field. All the laboratory analyses were carried out on these composite samples (two composite samples per plot, 648 samples in total), either at Rey Juan Carlos University or in other laboratories. By doing so, every variable was analyzed in the same laboratory by the same personnel and using the same protocol.

Soil properties measured

Soil pH was measured in all the soil samples with a pH meter, in a 1: 1 soil to water (w:v) suspension. Soil texture (sand, clay, and silt content) was measured according to ref. 91. The three textural variables measured (sand, clay, and silt) were highly intercorrelated at both open (Spearman $\rho_{sand\text{-}silt} = -0.969$, $P < 0.001$; Spearman $\rho_{sand\text{-}clay} = -0.796$, $P < 0.001$; Spearman $\rho_{silt\text{-}clay} = 0.677$, $P < 0.001$) and vegetated (Spearman $\rho_{sand\text{-}silt} = -0.987$, $P < 0.001$; Spearman $\rho_{sand\text{-}clay} = -0.851$, $P < 0.001$; Spearman $\rho_{silt\text{-}clay} = 0.766$, $P < 0.001$) microsites. Thus, we selected just one of these fractions (sand), to use in our data analyses because this fraction is less prone to measurement errors given the method used (*91*). These physico-chemical properties widely differed among the 326 plots surveyed: sand content and pH ranged from 14% to 99% and from 3.73 to 9.93, respectively.

Characterization of above- and belowground biodiversity

Plant diversity - The total plant species richness of each plot was calculated as the total number of perennial plant species found using at least one of the survey methods (transects or quadrats). Plant species richness was highly correlated with other diversity metrics such as Shannon's and Simpson's indices ($r > 0.65$, $P < 0.001$), so we focused on species richness for this study because it represents the most widely studied component of biodiversity to date (*23*, *92–94*), and shows positive relationships with ecosystem functions related to multiple ecosystem services in global drylands (*18*).

Herbivore diversity - We used data from the in situ dung/pellet survey (see "Validation of grazing pressure gradients" section above) to estimate the richness of domestic and wild mammalian herbivores present at each site as described above. Across all sites, we recorded a total of 31 different herbivores (table S2), ranging in body size from the European rabbit encountered in Europe, Australia, and the Americas (~1.2 kg) to the African elephant in Namibia (~2,500 kg). Dung/pellet data were not available from 26 plots, so the final data set for herbivore richness includes 300 plots.

Belowground diversity - To quantify belowground diversity, we measured the richness of soil bacteria, fungi, protists, and invertebrates by amplicon sequencing on the 16S and 18S rRNA genes, respectively. Soil DNA was extracted from 0.5 g of defrosted soil samples from vegetated microsites using the Powersoil® DNA Isolation Kit (Mo Bio Laboratories, Carlsbad, CA, USA) according to the instructions provided by the manufacturer. The extracted DNA samples were frozen and shipped to the Next Generation Genome Sequencing Facility of the University of Western Sydney (Australia). There, they were defrosted and analyzed using the Illumina MiSeq platform. Prokaryotic 16S and eukaryotic 18S rRNA genes were amplified using the 341F/805R (*95*) and Euk1391f/EukBr (*96*, *97*) primer sets, respectively. Raw reads quality control, merging and chimera detection were performed using USEARCH (*98*), and phylotypes (i.e., ASVs) were identified at the 100% identity level using UNOISE3 (*99*, *100*). Representative sequences of the ASVs were annotated against the SILVA-132 SSU database for bacteria, and SILVA LSU (*101*) and PR2 (*102*) databases for eukaryotes, respectively. The ASV abundance tables were generated using QIIME (*103*), and then rarefied at 10,000 (16S rRNA gene) and 2,000 (18S rRNA gene) reads *per* sample to ensure even sampling depth before diversity calculation. Frozen samples were obtained for 80 sites encompassing 264 of the 326 plots surveyed. The amplification procedure failed for some samples, leaving the total number of plots available for belowground diversity analyses to 242. The richness of soil bacteria, fungi, protists, and invertebrates were scaled using the Z-score transformation and averaged to obtain a synthetic index of belowground diversity (*104*).

Assessment of ecosystem services

In all plots, we measured a total of 36 ecosystem variables linked to nine ecosystem services (four regulating, two supporting, and three provisioning services; see table S1). The four regulating ecosystem services assessed were: i) water regulation, measured using soil porosity and water holding capacity, ii) soil carbon storage, evaluated by measuring soil organic carbon stocks, iii) organic matter decomposition, quantified using five soil extracellular enzyme activities related to the degradation of organic matter (β-glucosidase, phosphatase, cellobiase, β-

N-acetylglucosaminidase and xylanase) and measurements of soil carbon and nitrogen mineralization and microbial biomass, and iv) erosion control, assessed by measuring total plant cover, soil aggregation, and the stability of soil macro-aggregates (aggregates >250 µm). The two supporting ecosystem services evaluated included: i) aboveground plant biomass and its temporal stability, estimated using the average plant biomass (APB) measured using satellite data and the inverse of the CV of APB, and ii) soil fertility, evaluated using multiple proxies of soil nutrient availability (contents of total N, NH_4^+, NO_3^-, dissolved organic N, total P, K, Cu, Mg, Fe, Mn, and Zn). The three provisioning services included: i) forage quantity, estimated as the biovolume of perennial grasses and forbs, ii) forage quality, evaluated using the SLA, the LDMC, and the leaf nitrogen content of perennial grasses and forbs weighted by their relative cover, and iii) wood quantity, quantified using the biovolume of woody vegetation. These soil and vegetation variables have often been used as proxies of the ecosystem services evaluated (*105–110*), which are essential for sustaining dryland livelihoods and their livestock (*15*, *111*, *112*). A detailed description of how each ecosystem service was quantified is given below.

Aboveground plant biomass and its temporal stability. This service, which is particularly important for extensive livestock production that is dependent upon native forage (*113–115*), was quantified using two variables: the average APB and the inverse of the coefficient of variation (CV) of APB during the 1999-2019 period. To quantify APB, we used the Normalized Difference Vegetation Index (NDVI), obtained using images from the Landsat 7 Enhanced Thematic Mapper Plus (ETM+) sensor (*116*). Multiple studies have shown that NDVI is a good proxy of APB, particularly in areas with sparse vegetation such as drylands (*117-119*). Since the removal of vegetation by grazing changes the amount of photosynthetically active biomass, it also modifies NDVI accordingly (*120*). In a similar way, NDVI may also be affected by differences in APB that may depend on species composition (*121*). However, NDVI has been found to be a good proxy of APB in dryland rangelands subject to different grazing levels (*121*, *122*). Finally, the resolution of Landsat data is 30 m x 30 m/pixel, thus it is suitable for quantifying NDVI at our plots, which have a size of 45 m x 45 m. Indeed, Landsat data have been frequently used to quantify NDVI in field plots of a size similar to that used in our study (*123*, *124*).

Landsat ETM+ images (pixel size of 30 m x 30 m) were atmospherically corrected using the Landsat Ecosystem Disturbance Adaptive Processing System (*124*), and included a cloud, shadow, water, and snow mask produced using the C Function of Mask, and a per-pixel saturation mask (*125*). The NDVI was calculated as:

$$NDVI = \frac{(R_{NIR} - (R_{red})}{(R_{NIR} + (R_{red})}$$

where R_{NIR} and R_{red} are the spectral reflectance near-infrared (0.77–0.90 µm) and in the red (0.63–0.69 µm) bands of Landsat ETM+. The NDVI calculation produces values between -1 to 1, where positive values indicate areas with vegetation, and negative values are typically areas devoid of vegetation cover, such as bare soil. Using NDVI data, we calculated the mean NDVI (NDVIµ) and its variability (*126*) as:

$$NDVI\mu = \frac{\sum NDVI}{n}$$

$$NDVIvariability = \mathrm{NDVI}_{CV}$$

where *n* is the number of NDVI data available with the above quality criteria (n = 141,863) and NDVI_{CV} is the coefficient of variation of NDVI for the 1999-2019 period.

It is worth highlighting that we considered the average value of 20 years when evaluating APB, perhaps the most dynamic variable among those used to quantify the ecosystem services measured. This makes variation in APB across sites/plots due to the different sampling years among the 3.7 yr window of our survey unlikely to have biased our results and conclusions.

Dryland rangeland vegetation dynamics, and consequently livestock production and human livelihoods, are highly sensitive to changes in both average APB and its yearly variability (see ref. 127 and references therein). Thus, we used $NDVI\mu$ and the inverse of $NDVIvariability$ to quantify a synthetic index of APB and its temporal stability. The inverse of the coefficient of variation is commonly used when estimating the temporal stability of a given ecological variable (*128–131*). For our calculations, we scaled and averaged $NDVI\mu$ and $1/NDVIvariability$ observed within each plot. A high value of this service is indicative of productive and stable dryland ecosystems, something that is highly valued by dryland inhabitants and makes these ecosystems more functional (*132*) and less prone to degradation (*133*).

Forage quantity. This service was quantified using the biovolume of grasses and forbs present at each plot, a variable often used as a proxy for forage available for livestock in drylands (*134–137*). The biovolume of each plot was calculated by multiplying the average cover of each species across all quadrats in a plot and the averaged maximum plant height of each species (m), obtained from field measurements, and then grouped and summed by plant life form (grasses and forbs). This metric is provided in $m^3 \cdot m^{-2}$.

Forage quality. This ecosystem service was quantified using the specific leaf area (SLA), leaf dry mass content (LDMC) and leaf nitrogen content of grasses and forbs and weighted by their relative abundance within each plot. Both SLA and LDMC are functional markers describing one of the major axes of plant diversification observed in terrestrial systems (*138*). They discriminate between acquisitive and conservative growth strategies associated with leaf nutrient contents (*139*). The nitrogen content of plant leaves is commonly used to estimate leaf protein contents (*140–143*) and is strongly linked to the nutritive value of forage plants (*144–146*). Overall, these three plant traits are good proxies for plant palatability -leaves with higher SLA and lower LDMC are more palatable than leaves with low SLA and high LDMC (*147*)- and nutritional content, and thus for forage quality (*147–155*).

To measure this service, we first averaged individual SLA, leaf nitrogen and LDMC measurements at the species level. We then quantified plot-level estimates of these variables by calculating, for grasses and forbs, the community mean trait (Mean *j*) values as:

$$Mean_j = \sum_{i}^{n} piTi$$

where *pi* and *Ti* are the relative abundance and the trait value of species *i* in plot *j*, respectively. We then calculated the leaf water content (LWC) as 1 / LDMC.

The community mean trait values for SLA, nitrogen content and LWC were scaled and averaged to obtain a synthetic index of leaf palatability and nutritional value. This index was then multiplied by the cover of grass and forb species to obtain plot-level estimates of forage quality. A high value of this service corresponds to plots dominated by grass and forb species characterized by high SLA, high nitrogen content and low LDMC, a marker of a high forage quality (*147*, *148*, *151*, *156*).

Wood quantity. To quantify this ecosystem service, we used the biovolume of woody vegetation, which is frequently used as a proxy for fuelwood and wood resources available for construction and other uses in dryland areas (*157–159*). The biovolume of woody species was quantified following the same procedure described for grasses and herbs above (but using data from woody species).

Organic matter (OM) decomposition. To quantify this ecosystem service, we measured five soil extracellular enzyme activities related to the degradation of OM [β-glucosidase, phosphatase, cellobiase, β-N-acetylglucosaminidase and xylanase], soil C and nitrogen mineralization, and microbial biomass. These variables are either direct measurements of OM decomposition (e.g., C and N mineralization) (*160–163*) or are involved in the degradation of compounds such as sugars, chitin, cellulose, and hemicellulose (soil enzymatic activities) (*164*, *165*). Therefore, they are good proxies for the capacity of a given ecosystem to decompose OM and return available nutrients from organic sources to the soil (*166*).

The activity of phosphatase was measured by determination of the amount of p-nitrophenol (PNF) released from 0.5 g soil after incubation at 37 ºC for 1 h with the substrate p-nitrophenyl phosphate in MUB buffer (*167*) (pH 6.5). The activity of β-glucosidase was assayed according to ref. 168, following the procedure for phosphatase, but using p-nitrophenyl-β-D-glucopyranoside as substrate and Trishydroxymethyl aminomethane instead of NaOH. The activities of β-N-acetylglucosaminidase, cellobiase and xylanase were measured from 1 g of soil using fluorometry as described in ref. 169.

Carbon mineralization rate (µg CO_2-C·g^{-1} dry soil·day^{-1}) was measured as CO_2 evolved after 48 h of incubation at 25 ºC and 60% of water holding capacity in soil samples from each plot. We waited 48 h to make sure that an equilibrium in the soil atmosphere was reached after disruption and water adjustment to achieve 60% of WHC (*170*). We measured soil CO_2 exchange by placing 10.5 g of each soil sample inside a 30 mL plastic jar with a tightly sealed lid connected to a portable, closed-chamber soil respiration system (EGM-4, PP systems, MA, USA) during 60 s. We monitored CO_2 concentration every second and fitted these data to a linear model (R^2 > 0.95 in all cases). Afterwards, the ideal gas law equation was used to convert and calculate the net CO_2 increase (ppm) to mass of C (m) in the headspace of the jar:

$$m = \frac{ppm\ \times\ P\ \times\ V\ \times\ M}{R\ \times\ T}$$

where P (atm) and V (L) are, respectively, the air pressure and the known headspace volume in the jar, M is the atomic mass of carbon (g mol^{-1}), R is the universal gas constant (0.08206 ATM l mol^{-1} K^{-1}) and T is the temperature (ºK) at the measurement time. The headspace volume in the jar (L) was measured as the total volume of the jar minus the volume of the soil. The mass of CO_2 evolved from each flask was calculated according to ref. 171 and expressed as µg CO_2-C s^{-1}. Finally, we expressed soil carbon mineralization on a dry mass basis (µg CO_2-C g^{-1} soil day^{-1}).

Potential N mineralization rate was measured by determination of total K_2SO_4-extractable NO_3^- before and after soil incubation in the laboratory at 80% of water holding capacity and 30 ºC for 14 days (*172*).

Soil microbial biomass was assessed using an automated O_2 micro-compensation system (*173*) by substrate-induced respiration, i.e., the respiratory response of microorganisms to glucose addition (*174*). To saturate catabolic microbial enzymes, 4 mg glucose g^{-1} dry soil was added as aqueous solution to the soil samples. Prior to the measurement, and to prevent a respiration peak due to water addition, the dry soil samples were rewetted 24 h before so that they reached 40% water holding capacity. The final measurements were done at 60% water holding capacity by adding a specific amount of water and glucose to reach 4 mg glucose g^{-1} soil dry weight. The mean of the three lowest hourly measurements was taken as the maximum initial respiratory response (MIRR) – a period where microbial growth has not started - to calculate microbial biomass C. Microbial biomass C (mg C·g^{-1}) was calculated as 38 × MIRR (ml O_2 g^{-1} dry soil) according to ref. 175. All these measurements were conducted at 20 °C in an air-conditioned laboratory using the same analytical devices.

Soil extracellular enzyme activities related to the degradation of organic matter, soil carbon and nitrogen mineralization, and microbial biomass were scaled and averaged to obtain a synthetic index of OM decomposition.

Soil carbon storage. We used organic soil C stocks as a proxy for this ecosystem service (*106*, *108*). We did so because soil organic C is a major terrestrial C reservoir and a major sink of atmospheric CO_2 (*176–179*). Soil organic C stocks were calculated as the product of soil organic C concentration, bulk density, and sampling depth. Organic C concentration was determined on ball-milled soils by dry combustion, gas chromatography and thermal conductivity detection Thermo Flash 2000 NC soil analyzer (ThermoFisher Scientific, Waltham, Massachusetts, USA), after removing carbonates by acid fumigation (*180*). Bulk density was measured at each plot following the cylindrical core method (*181*). Changes in grazing pressure did not affect bulk density across the plots surveyed (Tukey's HSD test, $P > 0.85$).

Soil fertility. We quantified this ecosystem service by measuring the contents of total N, NH_4^+, NO_3^-, dissolved organic N, total P, K, Cu, Mg, Fe, Mn, and Zn, which are commonly used indicators of soil fertility because they are strongly related to plant growth and productivity in drylands (*182–185*). Total N was determined on ball-milled soils by dry combustion, gas chromatography and thermal conductivity detection using a Thermo Flash 2000 NC soil analyzer. Dissolved organic N, ammonium and nitrate concentrations were measured from a subsample of a K_2SO_4 0.5 M soil extracts in a ratio 1:5 (soil: K_2SO_4). Soil extracts were shaken in an orbital shaker at 200 rpm for 1 h at 20 ºC and filtered to pass a 0.45-µm Millipore filter (*186*). The filtered extract was kept at 4 ºC until colorimetric analyses, which were conducted within the 24 h following the extraction. Ammonium concentration was directly estimated by the indophenol blue method using a microplate reader (*187*). Nitrate was first reduced to NH_4^+-N with Devarda alloy, and its concentration was determined by the indophenol blue method.

Dissolved organic N was first oxidized to NO_3^--N with $K_2S_2O_8$ in an autoclave at 121ºC for 55 min (*171*), then reduced to NH_4^+-N with Devarda alloy, and its concentration was determined by the indophenol blue method. Total P, K, Mg, Fe, Mn, Cu and Zn were extracted by open-vessel nitric-perchloric acid wet digestion, re-suspended in water, and measured by inductively coupled plasma optical emission spectrometry (*188*, *189*) with a Perkin Elmer Optima 4300 DV (Perkin Elmer, Waltham, Massachusetts, USA).

The different nutrient concentrations were scaled and averaged to obtain a synthetic index of soil fertility.

Erosion control. We quantified this ecosystem service by measuring perennial plant cover, soil aggregation and the water stability of soil aggregates. The cover of perennial vegetation is strongly (and negatively) related to soil erosion in drylands (*190–193*), and is a variable commonly used as a proxy of erosion control (*194–196*). Soil aggregation and the water stability of soil aggregates are good proxies for erosion control, as they largely determine the resistance of soils to erosive forces (*197–202*) and are strongly linked to soil quality (*203–206*).

The cover of perennial vegetation (in %) was derived from the transects (line-point intercept data) laid out at each plot (see "Vegetation and soil sampling" section above). Soil aggregation was determined by measuring both the mean weight diameter of the whole sample and the water stability of the macro-aggregate fraction > 250 µm. Each sample was passed through a stack of sieves (1 mm, 212 µm, 53 µm, <53 µm) to separate the sample into five fractions of decreasing particle size. The fraction weights were used to calculate the mean weight diameter (in mm) as:

$$\mathrm{MWD} = \sum_{i=1}^{n} \underline{x_l}\, w_i$$

where $\underline{x_l}$ is the mean diameter of size fraction *i* and w_i is the weight of the fraction *i* standardized by the overall sample mass. Water stability of aggregates was tested following a modified protocol from ref. 207. Following the MWD measurements, samples were carefully mixed, and 4.0 g placed on small sieves of 250 µm mesh size. Samples were first wetted through capillary wetting before being introduced to the sieving machine (Agrisearch Equipment, Eijkelkamp, Giesbeek, Netherlands). They were then moved vertically for 3 min in deionized water to separate samples into their water-stable and water-unstable fractions. The water-stable fraction was then washed to extract sand particles and organic debris (i.e., the coarse matter fraction). The percentage of water-stable aggregates was calculated as follows:

$$\mathrm{WSA}\ (\%) = (\text{water stable fraction-coarse matter}) / (4.0\ \text{g-coarse matter}) * 100.$$

Perennial vegetation cover, soil aggregation and the water stability of soil aggregates were scaled and averaged to obtain a synthetic index of erosion control.

Water regulation. This ecosystem service was quantified by assessing the soil water holding capacity (the amount of water that a given soil can hold), and soil porosity (the percentage of the soil volume occupied by pore spaces). Water holding capacity is relevant to many aspects of soil water management (*208*), is an important determinant of aboveground primary productivity in rangelands (*209*) and is linked to essential water-related ecosystem services such as plant-water provision (*210*). Soil porosity is also an important physical variable that controls multiple key soil hydrological properties, including infiltration and water storage capacity (*211–214*).

To measure water holding capacity, we weighed 10 g of dry soil per sample and added them to a funnel with moist filter paper. We then added 10 mL of deionized water to each sample and covered every funnel with parafilm to avoid evaporation. The soils were allowed to drain for 24 h into a test tube. After 24 h, we weighed the soils to calculate their water holding capacity.

Soil porosity was estimated as 1 - (Db/Dp), where Db and Dp are bulk density and particle density, respectively (*215*). Bulk density was estimated for every plot as described above (see description of the soil carbon storage ecosystem service). Particle density was estimated using a constant value of 2.65 g/cm^3, a typical value used when estimating soil porosity and/or soil particle properties in soils such as those surveyed here (*216–220*).

All soil-based analyses were conducted with dry samples, as commonly carried out with global surveys conducted in drylands and mesic ecosystems (*18*, *221–224*). Previous studies have shown that in drylands such as those we studied, air drying, and further storage of soils does not appreciably alter functions such as those studied here (*225*, *226*). It is also important to note that our sampled soils would have remained dry for a large portion of the year (*227–230*), and that most samples were collected when the soil was in this very dry state. Thus, the potential bias induced by our drying treatment is expected to be minimal.

For all soil variables used to quantify ecosystem services, we first obtained a plot-level estimate from samples collected under the canopy of vegetation and on bare ground devoid of vascular vegetation (*18*). These estimates were obtained using a weighted average of the values observed in bare ground and vegetated areas, weighted by their respective cover at each plot (quantified using the line-point intercept survey). All the ecosystem services were standardized between 0 and 1 before statistical analyses to facilitate the comparison between them.

Soil aggregate stability analyses were carried out at the laboratories of the Institute of Biology at Free University Berlin (Germany). Microbial biomass and C mineralization analyses were conducted in the laboratories of the Institute of Biology at Leipzig University (Germany). C mineralization, soil organic C and total N, P, K, Mg, Fe, Mn, Cu and Zn analyses were conducted at the laboratories of the Institute of Agricultural Sciences-CSIC (Madrid). The rest of analyses were carried out at the laboratory of the Biology and Geology Department, Rey Juan Carlos University (Móstoles, Spain).

Statistical analyses

Our overarching objectives were to evaluate the relationships between grazing pressure and the capacity of drylands to deliver key ecosystem services and to evaluate how grazing pressure interacts with climate, biodiversity, and soil properties, which are known to impact the delivery of ecosystem services across drylands worldwide. To do so, we used linear mixed effect models to evaluate how grazing pressure relates to ecosystem services, accounting for the effects of key climatic variables, soil properties, and biodiversity. Site was considered as a random factor (random effect: 1|site) allowing model intercept to vary among sites since plots belonging to the same site correspond to a local grazing gradient that has been repeated across the 98 sites surveyed. Grazing was treated as a continuous variable in all models ranging 0 to 3 (0 = ungrazed, 1 = low grazing pressure, 2 = medium grazing pressure, and 3 = high grazing pressure). As grazing gradients were nested within sites, we also considered an alternative approach with a random effect nesting grazing within site (random effect: grazing|site) allowing both intercepts and slopes to vary across sites. However, this approach may lead to model overfitting and singularity in some cases, i.e., a form of multicollinearity that often occurs when using mixed models (*231*, *232*). Our results were robust to the approach employed (either 1|site or grazing|site) as both provided very similar results (see tables S13-S18). Thus, we only present and discuss in the main text results from the simplest approach considering site as a random factor (random effect: 1|site). Other predictors were fixed in our models; the rationale for using them is described below. We conducted all statistical analyses using the statistical software R v.4.0.5 (*233*).

Predictors included in ecosystem service models - We used MAT, MAP, and rainfall seasonality (coefficient of variation of 12 monthly rainfall totals; RASE) obtained from WorldClim 2.0 (*35*) to characterize the climate of all plots surveyed. We selected these variables because they: i) are important drivers of plant diversity in drylands (*234*, *235*), ii) are key predictors of the global variation observed in dryland ecosystem functioning and stability (*132*, *234*, *236*), and iii) describe largely independent features of climate across the study sites (bivariate correlations had $r < 0.4$ in all cases). We did not consider temperature seasonality (standard deviation of monthly temperatures * 100) because it was highly correlated with MAT in our dataset ($r = 0.79$). We considered quadratic terms for MAT and MAP because: i) we sampled global abiotic gradients for these variables (e.g., ranging from cold environments with freezing temperatures to hyper-arid and hot regions), and ii) ecosystem responses to changes in climate do not necessarily change linearly along global drylands (*237*).

We selected for our analyses soil variables (sand content and pH) measured in samples from open areas to ensure that their effects on the ecosystem services measured were as independent from those of organisms as possible. Soil sand content plays a key role in controlling water availability, the performance and community structure of perennial vascular plants and soil microorganisms, and ecosystem functioning in drylands (*18*, *238–241*). Soil pH is also a major driver of plant and soil diversity in drylands (*19*, *235*, *242*). A quadratic term was considered for pH in all models.

While biodiversity is sometimes viewed as a supporting service (*243*), we consider it in our study as a driver of ecosystem functioning and associated services across dryland ecosystems (*18*, *23*, *93*, *132*, *234*, *236*, *244*, *245*). We thus included in our framework the richness of perennial plants occurring in each of the 326 studied plots. We also considered the diversity of soil organisms (bacteria, fungi, protists, and invertebrates) known to influence ecosystem functions linked to key ecosystem services, such as OM decomposition and soil carbon storage (*19*, *105*, *246*). We then considered in our analyses the richness of mammalian herbivores in each plot, which has been shown to largely impact vegetation and ecosystem functioning in drylands (*25*, *247*, *248*).

Finally, we included in our models a series of covariates that may influence the relationship between grazing and ecosystem services. We considered the latitude and longitude of our study sites, as well as their elevation and topography (slope angle) in our analyses to control for these potential confounding effects. We used the sine and cosine of the longitude to avoid any bias due to intrinsic circularity of longitude in the statistical models (i.e., Longitude (sin) and Longitude (cos) hereafter, respectively) (*235*). All the predictors considered were weakly correlated (table S3).

Model selection procedure - We considered a full model for each ecosystem service *i* as:

lmer (ecosystem service$_i$ ~ (1|site) + latitude + longitude (sin) + longitude (cos) + slope + elevation + MAP*grazing + MAT*grazing + RASE*grazing + MAP^2 + MAT^2 + sand*grazing + pH*grazing + pH^2 + Biodiversity*grazing).

Using this full model considering all predictors, we ran a model averaging procedure to select the set of predictors that best explained variations in ecosystem services. To do this, we applied a multimodel inference procedure using the "MuMIn" R package (*249*). This method allowed us to create a set of models with all possible combinations of the initial variables, which were fitted using a Maximum Likelihood procedure (*250*) and sorted according to the Akaike Information Criterion (AIC). The AIC of each model was then transformed to ΔAIC, which is the difference between AIC of each model and the minimum AIC obtained. We retained all models with an AIC difference (ΔAIC) < 2, which we defined as best-fitting models.

During the model selection procedure, we maintained site as a random factor in all models and kept model covariates (latitude, longitude [sine and cosine], slope, and elevation) to account for their potential confounding effects on ecosystem services. We also forced the model selection procedure to retain the main effect when an interaction was selected in the final best-fitting model (i.e., the model with the lowest AIC value). We did so for two reasons: i) we used continuous variables to model interactions, and ii) two independent variables *x* and *y* (e.g., grazing and other predictor) will be correlated with the interaction term *xy*. By including *x*, *y*, and *xy*, we evaluated how much the interaction involving grazing can explain beyond what grazing does as a main effect. Similarly, when a quadratic term was selected for a given predictor, we retained the linear term in the best-fitting model.

For each service, we finally averaged predictor estimates selected across best-fitting models (those models selected within a ΔAIC < 2) using the conditional averaging approach in the function model.avg from the "MuMIn" R package. We fitted all models with the R package "lme4" using the LMER function (*251*). The full results of the model averaging procedure, including model estimates, standard errors, *P* values, variable importance values, and variance inflation factors, are available in tables S13-S15.

All predictors were standardized before analyses using the Z score to interpret parameter estimates on a comparable scale. Response variables were log-transformed when necessary to normalize data distribution prior to analyses to meet the assumptions of the tests used, i.e., normal distribution of residuals. For each model, we inspected the distribution of residuals and checked for the presence of potential outliers using the Cook's distance in the function romr.fnc from the package "LMERConvenienceFunctions" (*252*). If outliers were detected, they were removed as they may bias model estimates. Models were then rerun using the same model averaging procedure. Across the nine services considered, we detected the presence of nine, eight and four outliers for water regulation, soil fertility, and aboveground plant biomass and its temporal stability, respectively, representing 0.007% of the whole data set. We also tested for model multicollinearity using Variance Inflation Factors, checked the distribution of residuals, and tested for the presence of spatial autocorrelation in the residuals using Moran tests (*253*, *254*). Multicollinearity and spatial autocorrelation were absent in model residuals for all response variables considered (tables S13-S15).

For each service, we calculated the relative importance of each predictor in the model selection procedure using the sum of weights calculated for each predictor. This sum was calculated using the sw function from the "MuMIn" R package (*249*). This function uses Akaike's weights to define the relative importance of each predictor across the final set of best-fitting models (i.e., those with a ΔAIC < 2 from the best-fitting model) by summing the Akaike weights values of all models that include the predictor of interest, considering the number of models in which each predictor appears. Predictor importance is proportional to the number of times a given predictor (and its interactions with other predictors) was selected in the final set of best-fitting models, and ranges from 0 (when a given predictor is not selected in any of the best-fitting models) to 100 (when a given predictor was selected in all of the best-fitting models). The relative importance of predictors was also averaged across the nine ecosystem services measured to compare their overall importance on ecosystem service delivery (Fig. 2).

Finally, and to ensure the robustness of our results, we repeated all analyses described above but considering dung mass and livestock track area instead of our continuous variable of grazing pressure (from ungrazed [0] to high grazing pressure [3]). Data of dung mass and livestock track areas were scaled within each site prior to analyses to reflect local grazing gradients. Dung mass provided very similar results to those obtained using our continuous variable for all services except for wood quantity and APB and its temporal stability (tables S19-S21). Interestingly, the analyses conducted with track area well explained those two services and in a similar way to our continuous gradient (tables S22-S24). Therefore, our results are not only robust to the approach employed to characterize the grazing gradient, but also show that our local grazing gradient encompasses complex effects of grazing on ecosystem services such as short- and long-term effects. Because of this, we only present and discuss in the main text results from the approach considering grazing as a continuous variable ranging from 0 (ungrazed) to 3 (high grazing pressure).

Use of biodiversity data in our statistical models - We considered the richness of perennial plants, mammalian herbivores (herbivore richness) and belowground organisms as biodiversity predictors in our models. While data for plant species richness were available for the 326 plots surveyed, herbivore richness and belowground diversity data were available for 300 and 242 plots, respectively. Because models with a different number of observations cannot be compared using AIC, we conducted a model preselection procedure to select the best set of biodiversity predictors to be included in the model selection procedure described above. To do so, we considered a subset data of 242 plots where both belowground diversity and plant species richness were available. We compared a full model including both belowground diversity and plant species richness together to a model including plant richness only. If models including belowground diversity showed lower AIC values, we considered the subset of 242 plots to perform the model selection procedure. If the best models only included plant species richness, we considered the full data set of 326 plots to perform the model averaging procedure. We performed the same preselection for the data subset that includes the 300 plots with both plant and herbivore richness information. If mammalian herbivore richness improved model quality compared to models with plant species richness only, we considered the subset data with herbivore richness for the model selection procedure. If herbivore richness did not improve model AIC, we considered the full data set with plant species richness only. Results of the model pre-selection procedure are available in table S25 for analyses using 1|site as random effect, in table S26 for analyses using grazing|site as random effect, and in tables S27 and S28 for analyses using dung mass and livestock tracks as surrogates of grazing pressure, respectively.

Plotting the interactive effect of grazing with climate, soils, and biodiversity- We graphically represented the results from best fitting models (tables S13-S15) in two different ways. First, we used model partial residuals to show how each predictor influenced ecosystem services according to all grazing pressure levels evaluated (Fig. 3, figs. S13-S15). Second, we calculated the predicted values for each service in each site at low and high grazing pressure levels using model estimates of best-fitting models. Predictions were made using observed variability between sites in plant species richness, mean annual temperature (MAT), and rainfall seasonality (RASE); all other parameters were fixed at their mean value. Then we calculated the predicted effect of grazing at each site as the difference between high and low grazing pressures using a log response ratio [lnRR; Predicted lnRR = ln (predicted service at high grazing pressure/predicted service at low grazing pressure)]. Finally, we plotted the relationships between the effect of grazing pressure (Predicted lnRR) and ecosystem services across sites and along the global gradient of abiotic conditions and plant species richness surveyed (Fig. 4).

Indirect effect of grazing on ecosystem services - We also tested whether grazing could impact ecosystem services through indirect pathways. We did so because grazing may not only impact ecosystem services through direct and interactive effects but also through indirect pathways, e.g. if grazing affected local species richness or soil conditions in our models. To explore these potential indirect effects of grazing, we conducted a confirmatory path analysis, a form of structural equation modeling (*255*), using a d-sep approach (*256, 257*). This approach is based on an acyclic graph that depicts the hypothetical relationships among predictors (links represented by arrows) and independence claims among variables (missing links), where the latter are tested using the C statistic. Based on the correlation matrix of our predictors (table S3), we tested the a priori model that grazing pressure does not have indirect effects on ecosystem services through changes in soil properties and biodiversity (fig. S10). Please note that we did not test indirect effects of grazing mediated by plant cover because this variable was used in the calculation of erosion control (see the “Assessment of ecosystem services” section), and thus we could not include it as a predictor of ecosystem services in the d-sep analyses. These analyses had the following steps (*257*): i) we express the hypothesized relationships between the variables in the form of a directed acyclic graph (fig. S10). In our case, we hypothesized that there was no linkage between grazing and plant species/herbivore richness and between grazing and soils; ii) we list each of the k pairs of variables in the graph that do not have an arrow between them. This list defines the missing links in our path analyses; iii) we test each missing link by comparing the models with and without the missing links; each link was tested using linear mixed models similar to those explained in the “Model selection procedure” section above. When a P value is not significant it means that there is an independence between a given pair of variables (i.e., they are not related); and iv) we finally combined the k probabilities using the C statistic (*257*) and compared the resulting C value to a chi-squared distribution with 2k degrees of freedom. The path model is valid when the result of this test is not significant ($P > 0.05$).

Model formulas employed to test each missing link, C statistics and significance test for each path analysis are available in tables S4-S12. Standardized path coefficients were calculated following ref. 258 to measure the direct, and indirect effect of predictors for each service. For all services evaluated, we did not detect any indirect effect of grazing through changes in soil properties or richness conditions (fig. S11 and tables S4-S12). These results indicate that grazing pressure impacted the different ecosystem services measured only through direct and interactive effects.

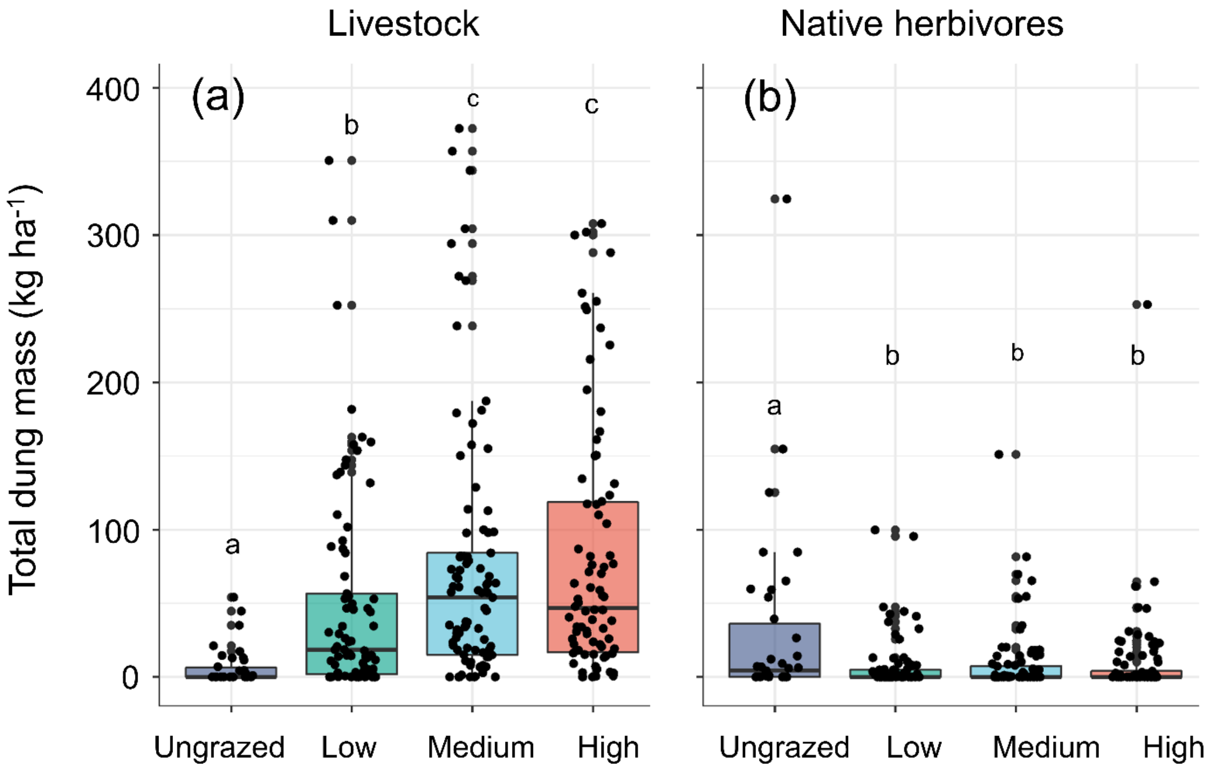

Fig. S1. Box plots of the mass of dungs of livestock (a) and wild (b) herbivores for the four levels of grazing pressure evaluated. Boxes show the median, 25^{th} and 75^{th} percentiles. Distinct lowercase letters indicate significant differences ($p < 0.05$) between grazing pressure levels (Tukey's HSD test). The total number of plots used for these analyses was 300.

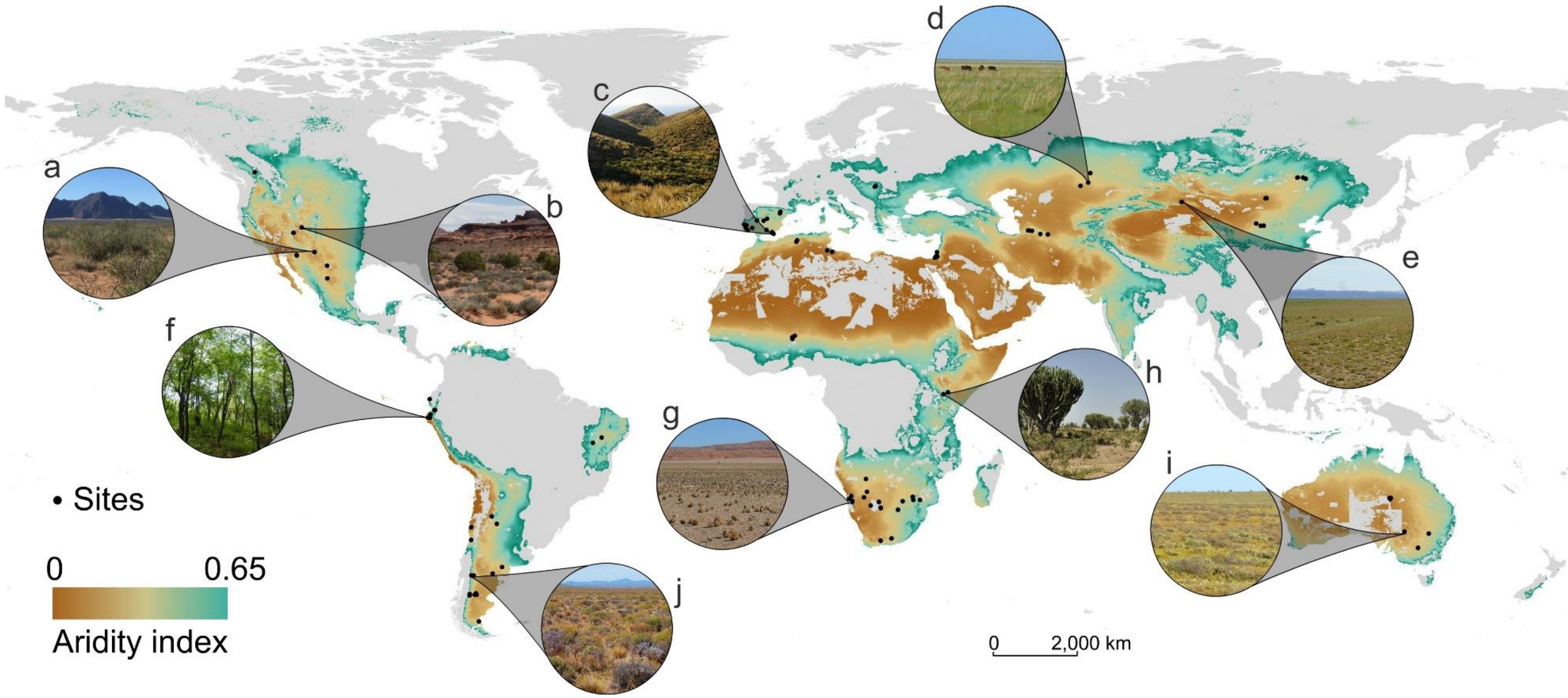

Fig. S2. Examples of the vegetation present at plots surveyed in the USA (a, b), Spain (c), Kazakhstan (d), Mongolia (e), Ecuador (f), Namibia (g), Kenya (h), Australia (i) and Argentina (j). The background map represents the extent of dryland rangelands. The aridity index (AI) is calculated as precipitation/potential evapotranspiration. See Materials and Methods for the AI and rangeland area data sources used.

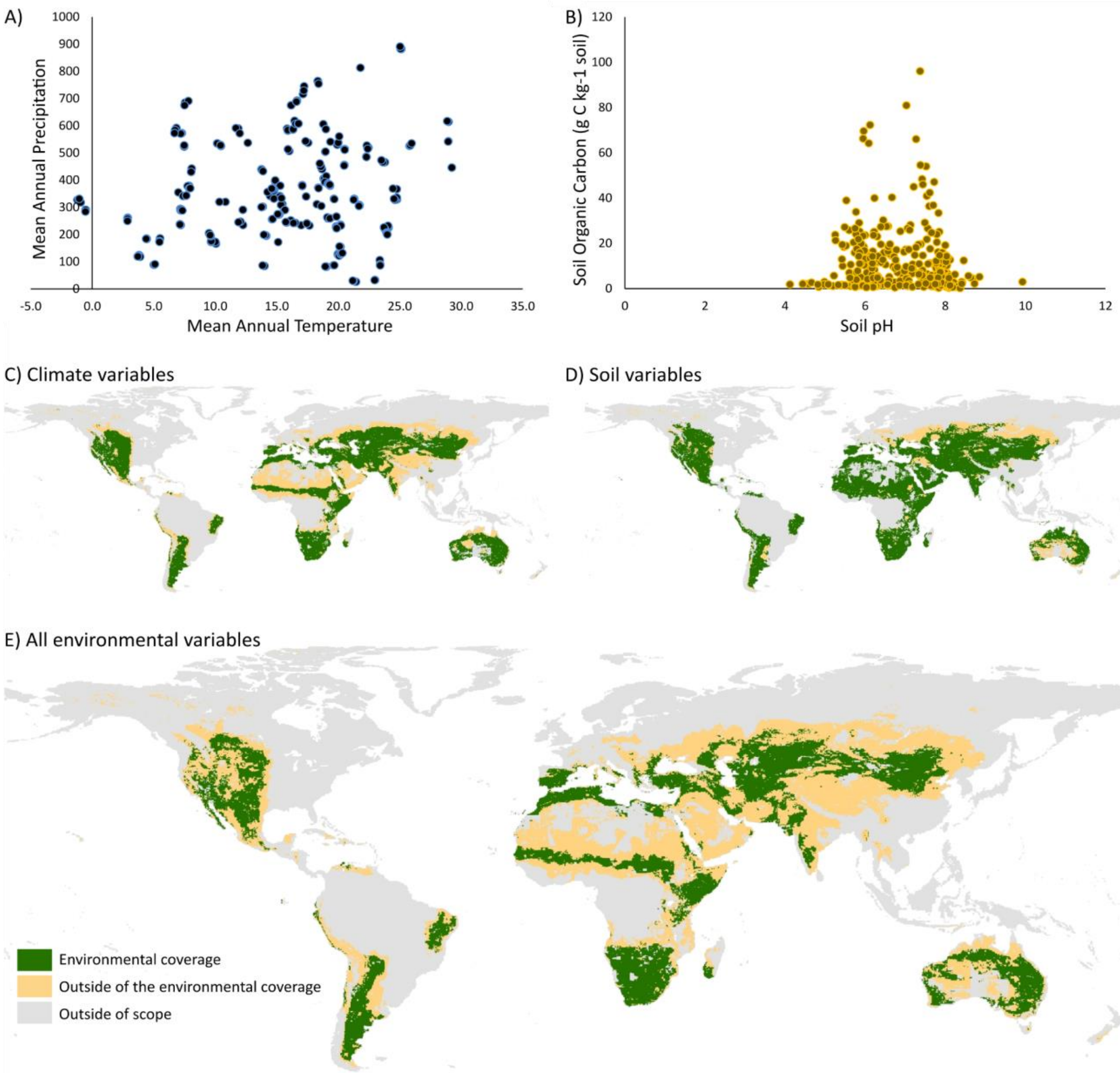

Fig. S3. Range of environmental conditions covered by the surveyed drylands. Bivariate relationships between key environmental variables (mean annual temperature and mean annual precipitation and soil pH and organic carbon) are shown in panels A and B. Panels C-E show the spatial distribution of the Mahalanobis distance regarding the environmental characteristics covered (<0.975 Chi-squared threshold for outliers) by the surveyed drylands. To obtain these panels, we determined how much the parameter space of the predictors (e.g., mean annual temperature, soil organic carbon, elevation) differed from that of global drylands (*259*). We used the Mahalanobis distance of any multidimensional point to the center of the known distribution (calculated based on the 98 locations from the original dryland dataset) (*260–262*) For panel C we considered the spatial coverage of climatic conditions (number of dimensions = 7; mean annual temperature, mean annual precipitation, temperature seasonality, precipitation seasonality, temperature mean diurnal range, aridity index and evapotranspiration) using data from refs. 35 and 36. For panel D, we considered the spatial coverage of soil conditions (number of dimensions = 5; nitrogen, carbon, soil texture [% of clay and silt], soil pH and C/N ratio) using data from ref. 263. For panel E, we considered the overall environmental coverage (number of dimensions = 14; vegetation [NDVI], elevation, nitrogen, carbon, soil texture [% of clay and silt], soil pH, C/N ratio, mean annual temperature, mean annual precipitation, temperature seasonality, precipitation seasonality, temperature mean diurnal range, aridity index, and evapotranspiration).

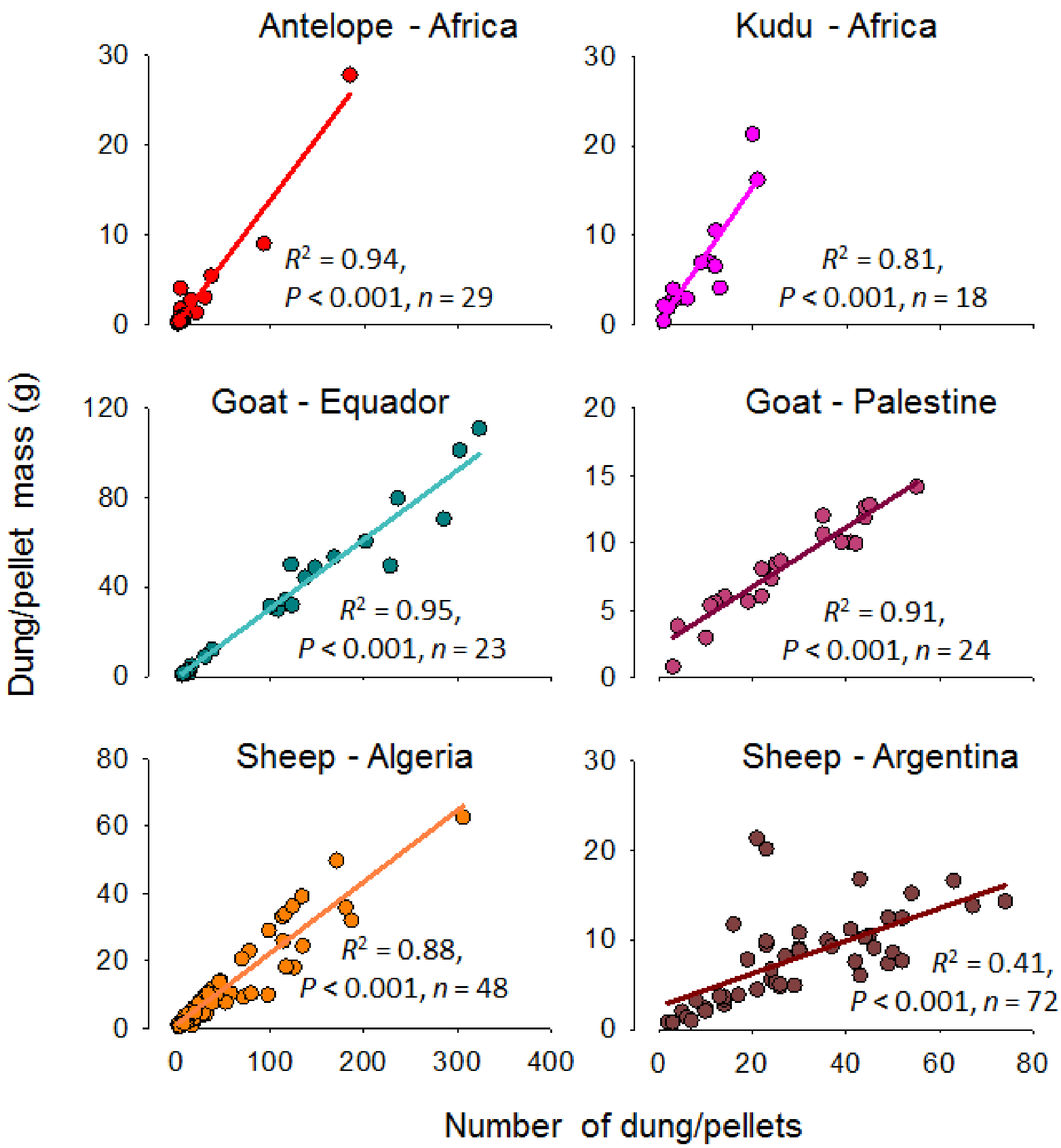

Fig. S4. Relationship between the number of dung/pellets of grazing animals and their mass (g) for six surveyed sites from Argentina, Algeria, Ecuador, Palestine, and South Africa. Each data point represents data from a quadrat surveyed in the field. Antelope records are from Namibia (n = 6), Botswana (n = 7) and South Africa (n = 16). Kudu records are from Namibia (n = 13) and South Africa (n = 5).

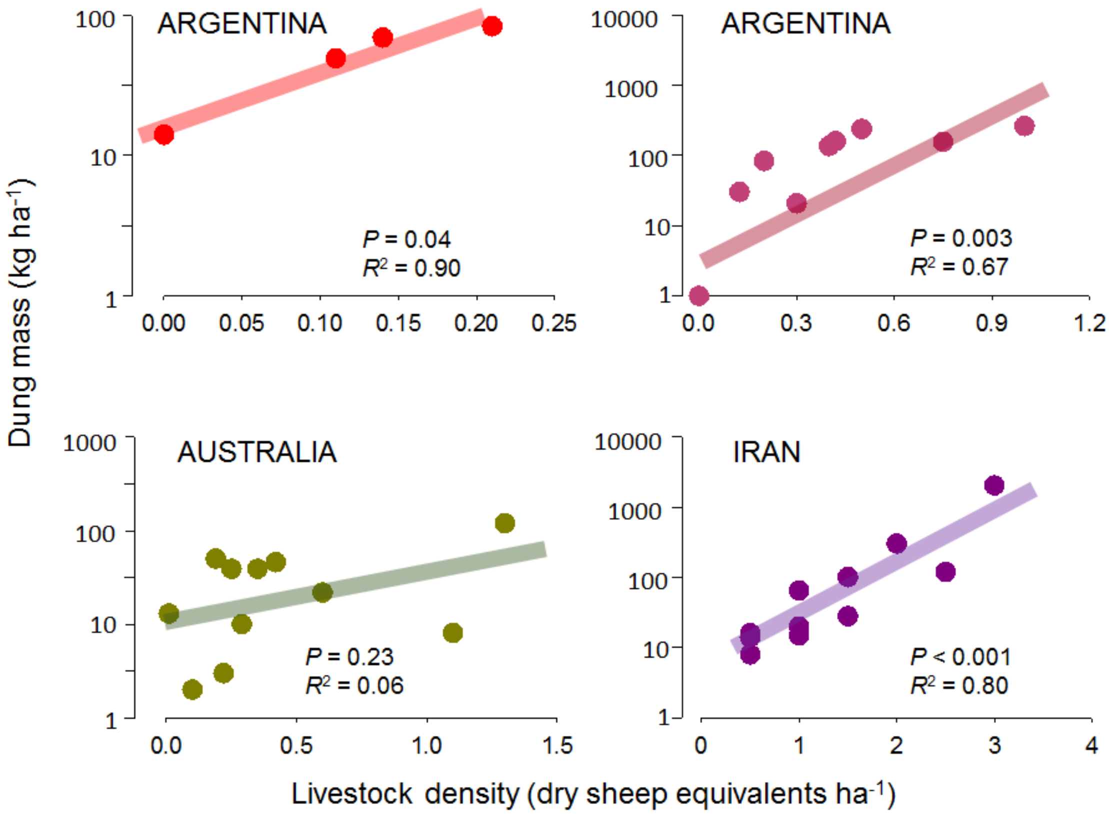

Fig. S5. Relationships between livestock density and oven-dried mass of dung for four of the surveyed countries where we had access to long-term livestock density data. Each data point represents a plot.

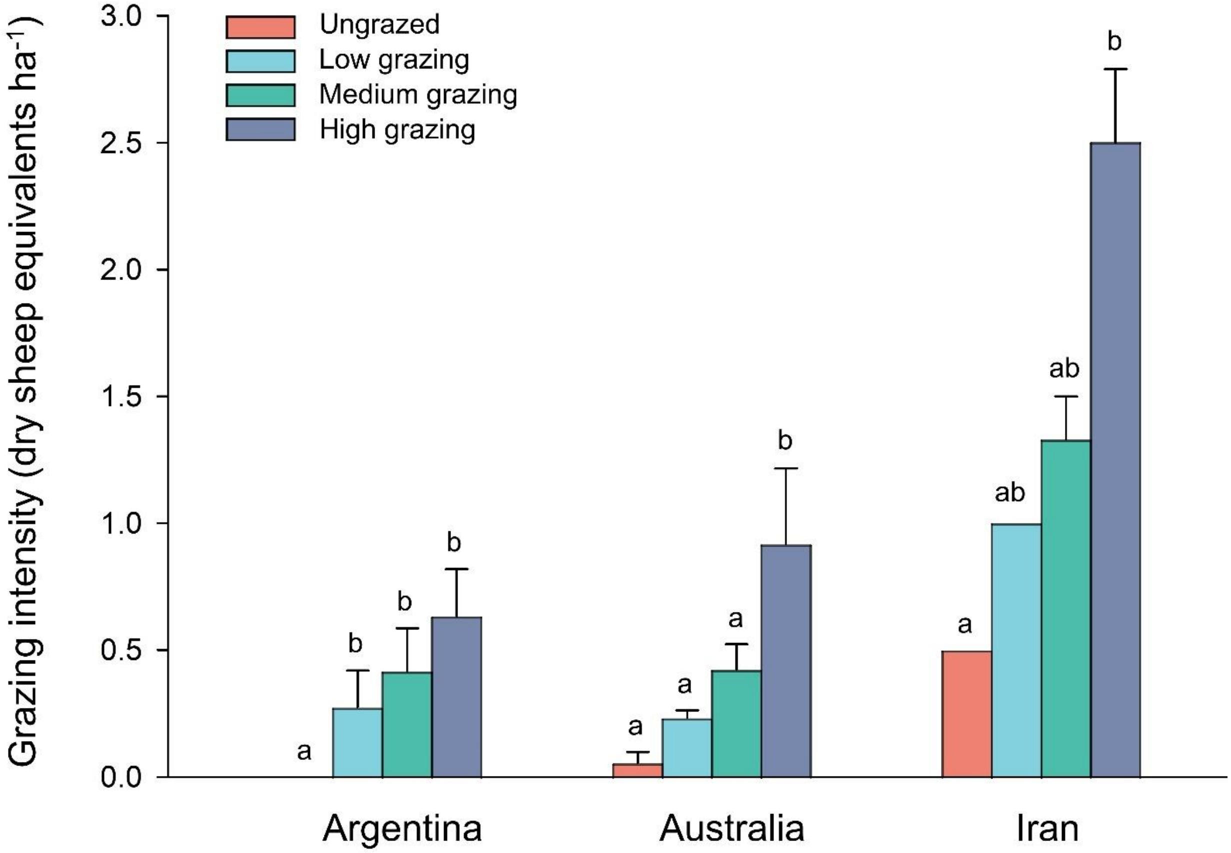

Fig. S6. Mean (± SE) livestock density, adjusted to a common scale of dry sheep equivalents, observed in ungrazed and low, medium, and high grazing pressure plots in Argentina (*n* = 15), Australia (*n* = 11) and Iran (*n* = 11). Different lowercase letters indicate significant ($P < 0.05$) differences between grazing pressure levels using a linear model (One-way ANOVA).

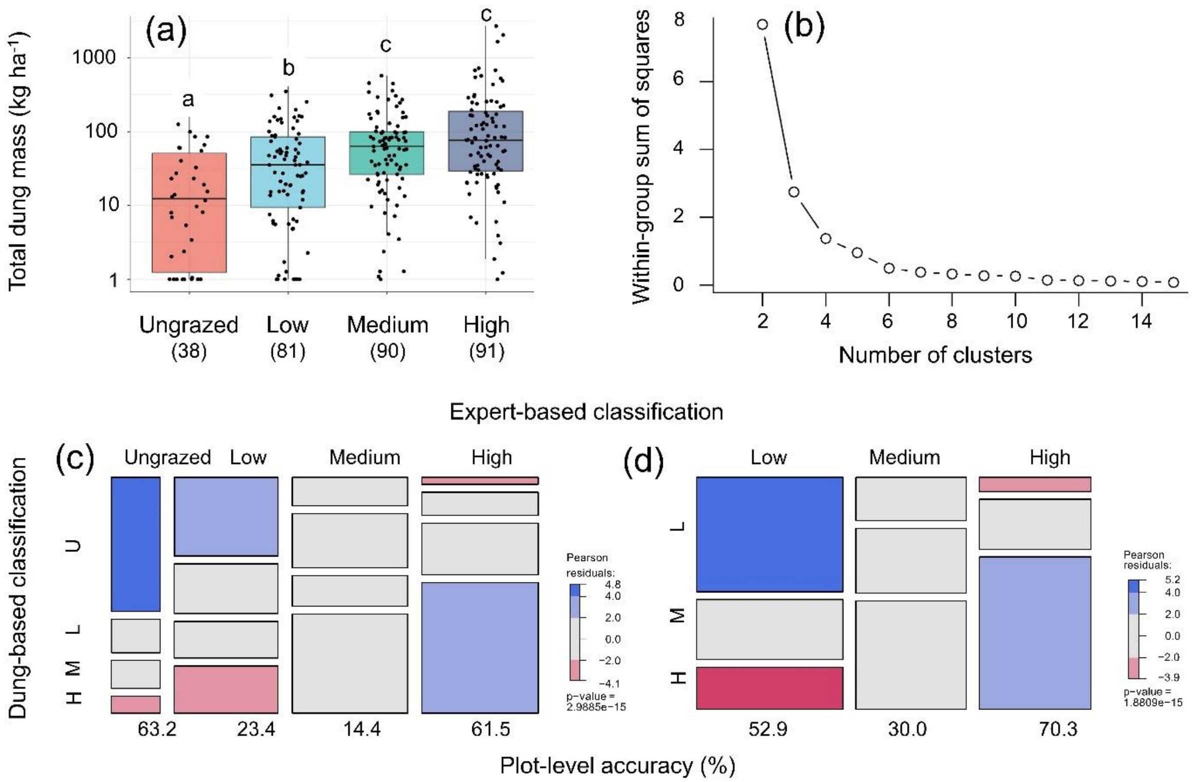

Fig. S7. Results of a cluster analysis of dung/pellet data. (a) Box plots of average dung mass ($kg{\cdot}ha^{-1}$) for the four levels of grazing pressure evaluated. Boxes show the median, 25^{th} and 75^{th} percentiles. Distinct lowercase letters indicate significant ($p < 0.05$) differences between grazing pressure levels (Tukey's HSD test); (b) Plot of within-group sum of squares in relation to the number of clusters. The optimal number of clusters is that from which additional clusters results in similar variance explained (here four clusters); (c) Mosaic plots illustrating the results of contingency tables between pre-inspection level of grazing pressure (ungrazed to high) in relation to the post-inspection assessment of dung mass on the four clusters identified in (b) above. Panel (c) uses all the classifications, but panel (d) is based on the three-group cluster. Edge length is proportional to the number of cases, and thus the area of each square is proportional to the degree of match between the two methods of classifying grazing pressure. Colour of mosaics represents over (blue) or under (red) representation of each combination of classifications, measured as Pearson's residuals obtained from chi-squared tests. For a perfect match, the diagonal of these mosaics (ungrazed-ungrazed; low-low; medium-medium; high-high) should exhibit significant overrepresentation and the other either non-significance or underrepresentation. The overall match, i.e., the sum of high to high, medium to medium, low to low and ungrazed to ungrazed, is 37.3% in panel c; and 51.3% in panel d. Plot level accuracy is calculated as correct matches (low-low, high-high, medium-medium, ungrazed-ungrazed) divided by the total of plots classified as each grazing level according to expert classification. The total number of plots used for these analyses was 300.

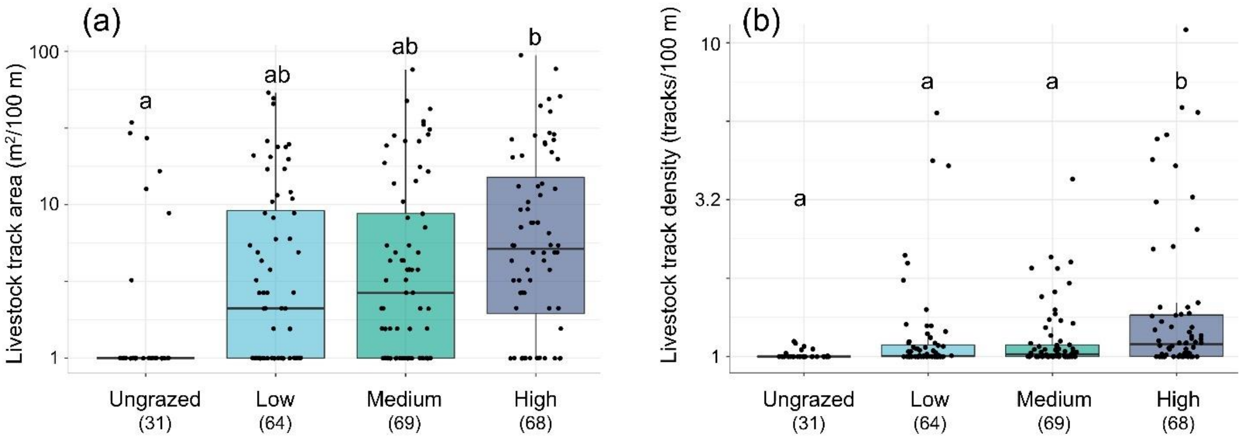

Fig. S8. Box plots of the area (a) and density (b) of livestock tracks for the four levels of grazing pressure evaluated. Boxes show the median, 25th and 75th percentiles. Distinct lowercase letters indicate significant differences ($p < 0.05$) between grazing pressure levels (Tukey's HSD test). The total number of plots used for these analyses was 232.

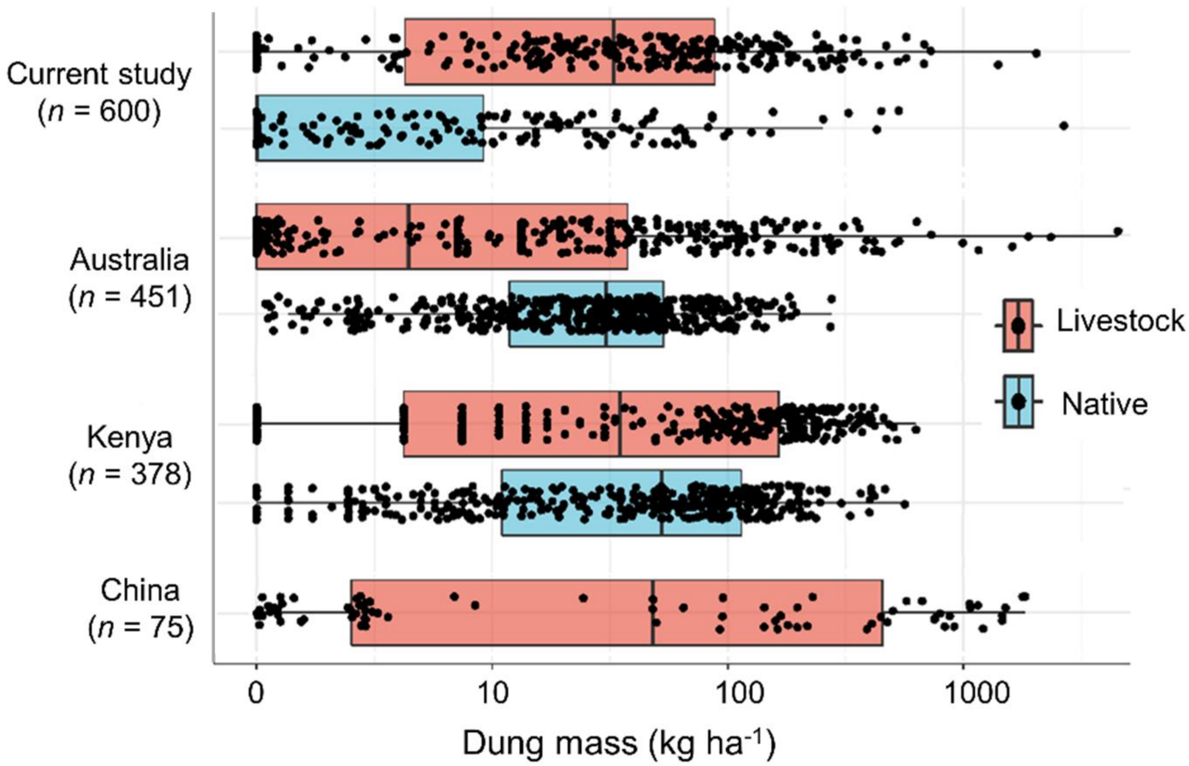

Fig. S9. Comparison of the amount of dung from livestock and native herbivores found across the surveyed plots (Current study) and in other surveys conducted in dryland rangelands from Australia, Kenya and China encompassing a wide variation in grazing pressure. Data from Australia and China come from refs. 264 and 265, respectively; data from Kenya come from refs. 266 and 78.

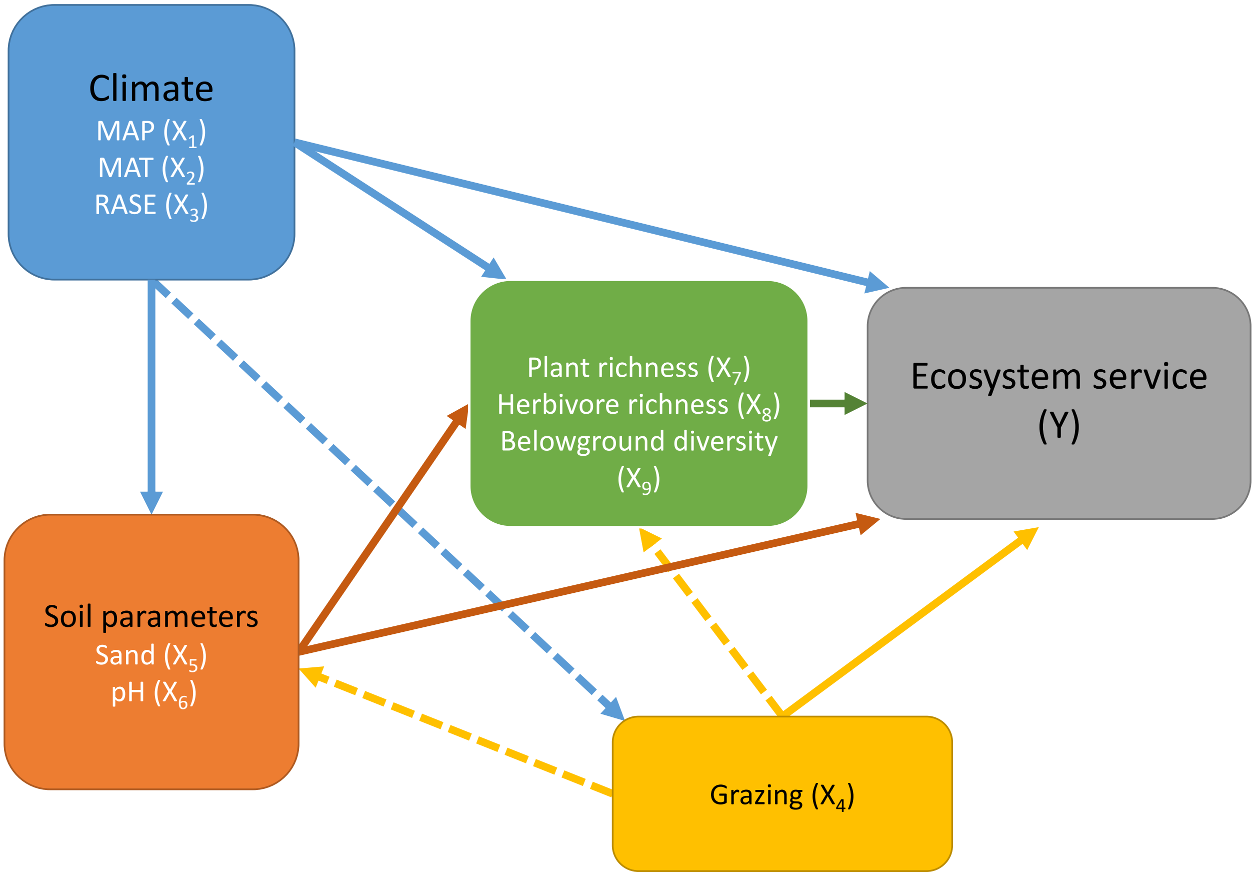

Fig. S10. *A priori* model used to evaluate direct and indirect effects of grazing pressure through changes in soil properties and biodiversity on the ecosystem services studied. Our *a priori* path model considers that grazing does not have indirect effects through changes in soil properties and biodiversity (null hypothesis). We explicitly tested conditional independence claims ("missing links") using a confirmatory path analysis (*13*). These independence claims (dashed lines), include potential indirect effects of grazing on ecosystem services mediated by biodiversity and soil parameters. We considered quadratic effects for mean annual precipitation (MAP), mean annual temperature (MAT) and soil pH. Sand = sand content, and RASE = rainfall seasonality.

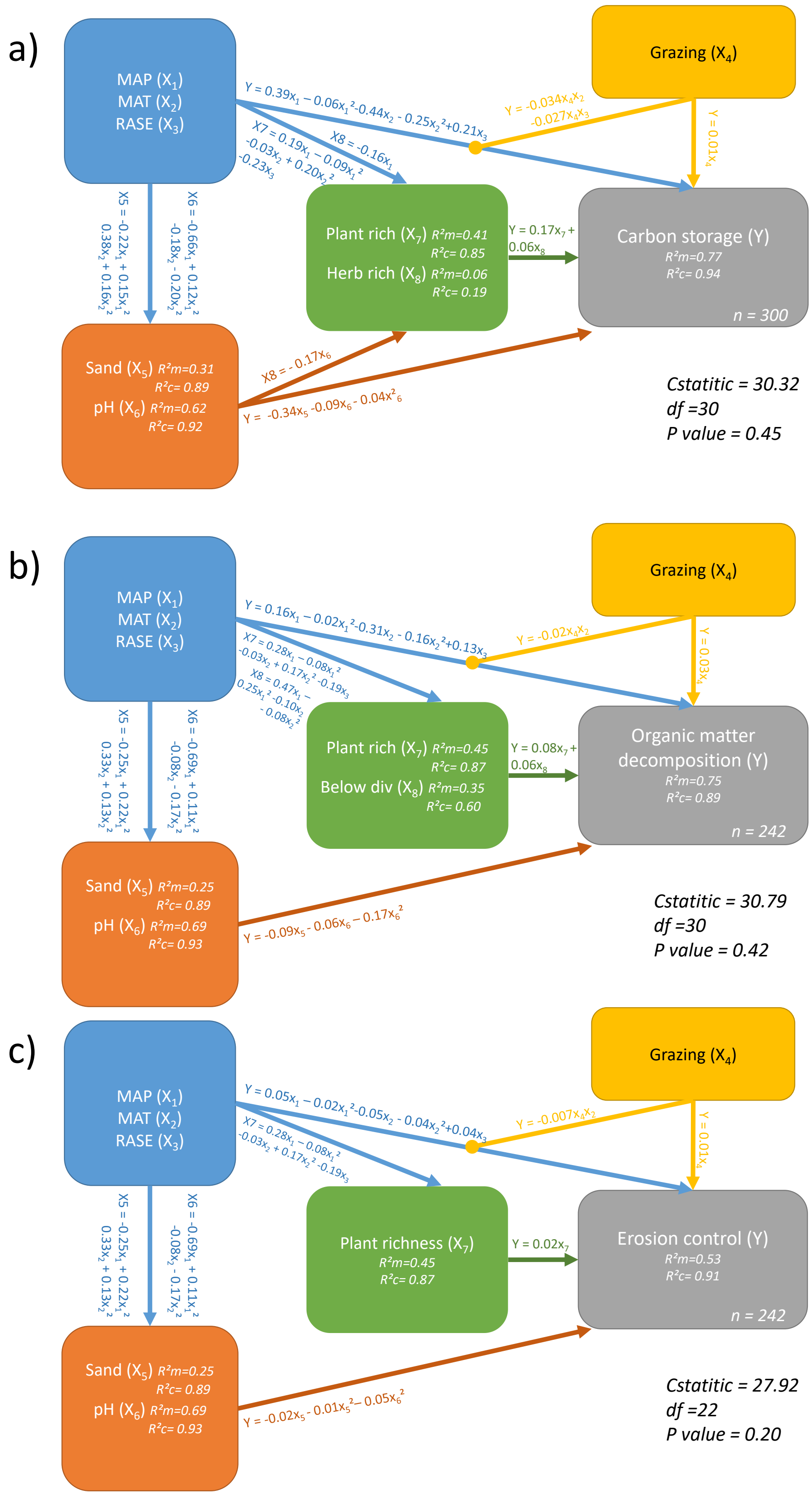

a)
MAP (X1)
MAT (X2)
RASE (X3)
Grazing (X4)
Plant rich (X7) R²m=0.41
R²c= 0.85
Herb rich (X8) R²m=0.06
R²c= 0.19
Carbon storage (Y)
R²m=0.77
R²c= 0.94
n = 300
Sand (X5) R²m=0.31
R²c= 0.89
pH (X6) R²m=0.62
R²c= 0.92
Y = 0.39x1 – 0.06x1²-0.44x2 - 0.25x2²+0.21x3
Y = -0.034x4x2
-0.027x4x3
Y = 0.01x4
Y = 0.17x7 + 0.06x8
X8 = -0.17x6
Y = -0.34x5 -0.09x6 - 0.04x²6
Cstatitic = 30.32
df =30
P value = 0.45
b)
MAP (X1)
MAT (X2)
RASE (X3)
Grazing (X4)
Plant rich (X7) R²m=0.45
R²c= 0.87
Below div (X8) R²m=0.35
R²c= 0.60
Organic matter decomposition (Y)
R²m=0.75
R²c= 0.89
n = 242
Sand (X5) R²m=0.25
R²c= 0.89
pH (X6) R²m=0.69
R²c= 0.93
Y = 0.16x1 – 0.02x1²-0.31x2 - 0.16x2²+0.13x3
Y = -0.02x4x2
Y = 0.03x4
Y = 0.08x7 + 0.06x8
Y = -0.09x5 - 0.06x6 – 0.17x6²
Cstatitic = 30.79
df =30
P value = 0.42
c)
MAP (X1)
MAT (X2)
RASE (X3)
Grazing (X4)
Plant richness (X7)
R²m=0.45
R²c= 0.87
Erosion control (Y)
R²m=0.53
R²c= 0.91
n = 242
Sand (X5) R²m=0.25
R²c= 0.89
pH (X6) R²m=0.69
R²c= 0.93
Y = 0.05x1 – 0.02x1²-0.05x2 - 0.04x2²+0.04x3
Y = -0.007x4x2
Y = 0.01x4
Y = 0.02x7
Y = -0.02x5 - 0.01x5²– 0.05x6²
Cstatitic = 27.92
df =22
P value = 0.20

d)

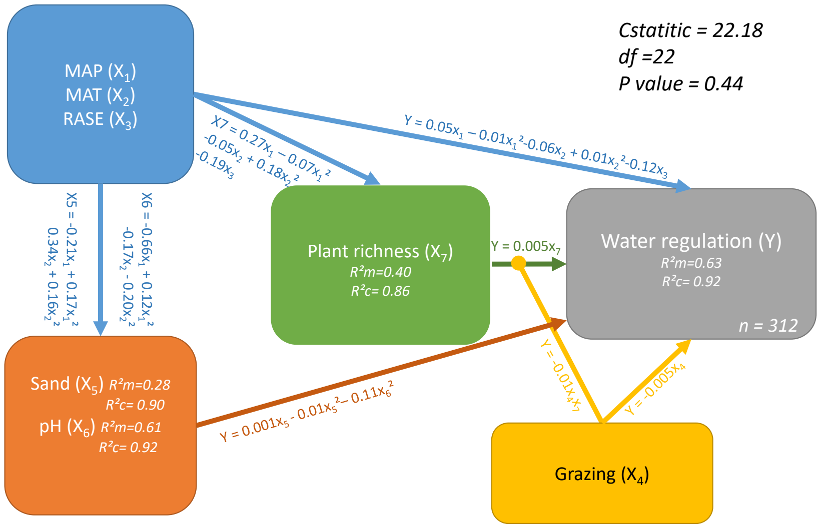

Cstatitic = 22.18
df =22
P value = 0.44
MAP (X_1)
MAT (X_2)
RASE (X_3)
Y = $0.05x_1 - 0.01x_1^2 - 0.06x_2 + 0.01x_2^2 - 0.12x_3$
X7 = $0.27x_1 - 0.07x_1^2$ $-0.05x_2 + 0.18x_2^2$ $-0.19x_3$
X5 = $-0.21x_1 + 0.17x_1^2$ $0.34x_2 + 0.16x_2^2$
X6 = $-0.66x_1 + 0.12x_1^2$ $-0.17x_2 - 0.20x_2^2$
Plant richness (X_7)
R^2m=0.40
R^2c= 0.86
Y = $0.005x_7$
Water regulation (Y)
R^2m=0.63
R^2c= 0.92
n = 312
Sand (X_5) R^2m=0.28
R^2c= 0.90
pH (X_6) R^2m=0.61
R^2c= 0.92
Y = $0.001x_5 - 0.01x_5^2 - 0.11x_6^2$
Y = $-0.01x_4x_7$
Y = $-0.005x_4$
Grazing (X_4)

e)

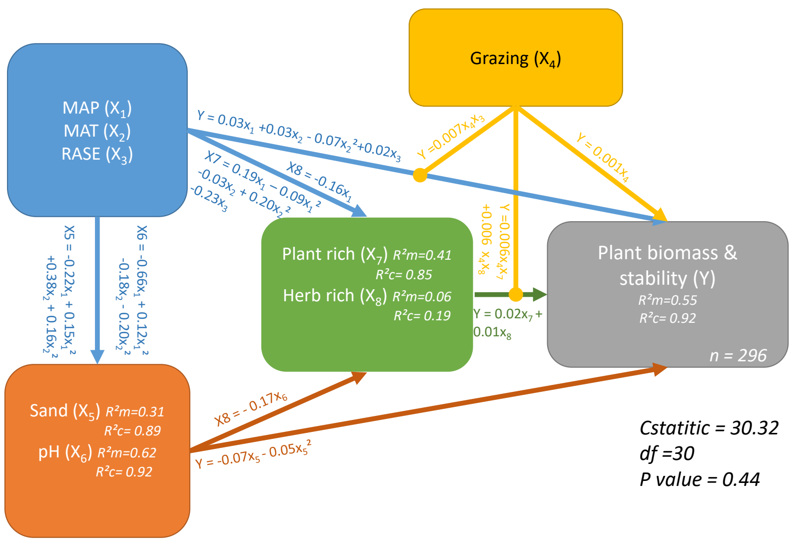

Grazing (X_4)
MAP (X_1)
MAT (X_2)
RASE (X_3)
Y = $0.03x_1 + 0.03x_2 - 0.07x_2^2 + 0.02x_3$
Y = $0.007x_4x_3$
Y = $0.001x_4$
X7 = $0.19x_1 - 0.09x_1^2$ $-0.03x_2 + 0.20x_2^2$ $-0.23x_3$
X8 = $-0.16x_1$
Y = $0.006x_4x_7$ $+0.006x_4x_8$
X5 = $-0.22x_1 + 0.15x_1^2$ $+0.38x_2 + 0.16x_2^2$
X6 = $-0.66x_1 + 0.12x_1^2$ $-0.18x_2 - 0.20x_2^2$
Plant rich (X_7) R^2m=0.41
R^2c= 0.85
Herb rich (X_8) R^2m=0.06
R^2c= 0.19
Y = $0.02x_7$ + $0.01x_8$
Plant biomass & stability (Y)
R^2m=0.55
R^2c= 0.92
n = 296
Sand (X_5) R^2m=0.31
R^2c= 0.89
pH (X_6) R^2m=0.62
R^2c= 0.92
X8 = $-0.17x_6$
Y = $-0.07x_5 - 0.05x_5^2$
Cstatitic = 30.32
df =30
P value = 0.44

f)

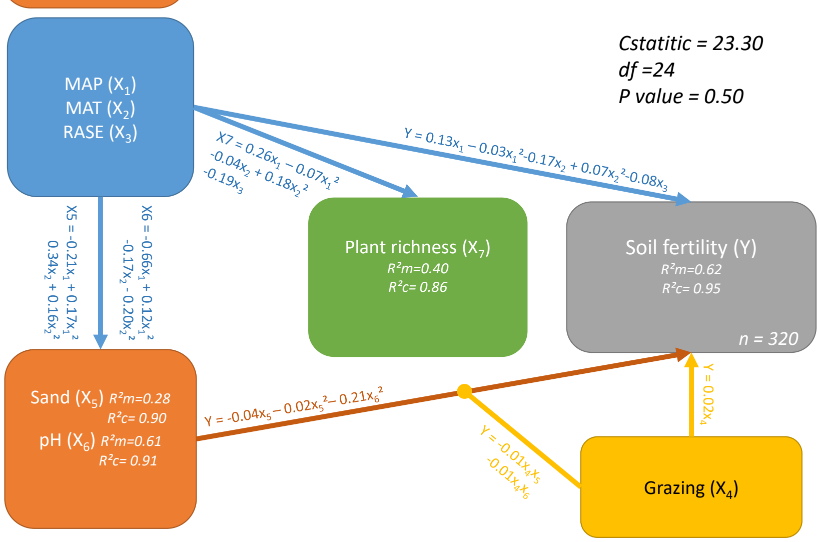

Cstatitic = 23.30
df =24
P value = 0.50
MAP (X_1)
MAT (X_2)
RASE (X_3)
Y = $0.13x_1 - 0.03x_1^2 - 0.17x_2 + 0.07x_2^2 - 0.08x_3$
X7 = $0.26x_1 - 0.07x_1^2$ $-0.04x_2 + 0.18x_2^2$ $-0.19x_3$
X5 = $-0.21x_1 + 0.17x_1^2$ $0.34x_2 + 0.16x_2^2$
X6 = $-0.66x_1 + 0.12x_1^2$ $-0.17x_2 - 0.20x_2^2$
Plant richness (X_7)
R^2m=0.40
R^2c= 0.86
Soil fertility (Y)
R^2m=0.62
R^2c= 0.95
n = 320
Sand (X_5) R^2m=0.28
R^2c= 0.90
pH (X_6) R^2m=0.61
R^2c= 0.91
Y = $-0.04x_5 - 0.02x_5^2 - 0.21x_6^2$
Y = $-0.01x_4x_5$ $-0.01x_4x_6$
Y = $0.02x_4$
Grazing (X_4)

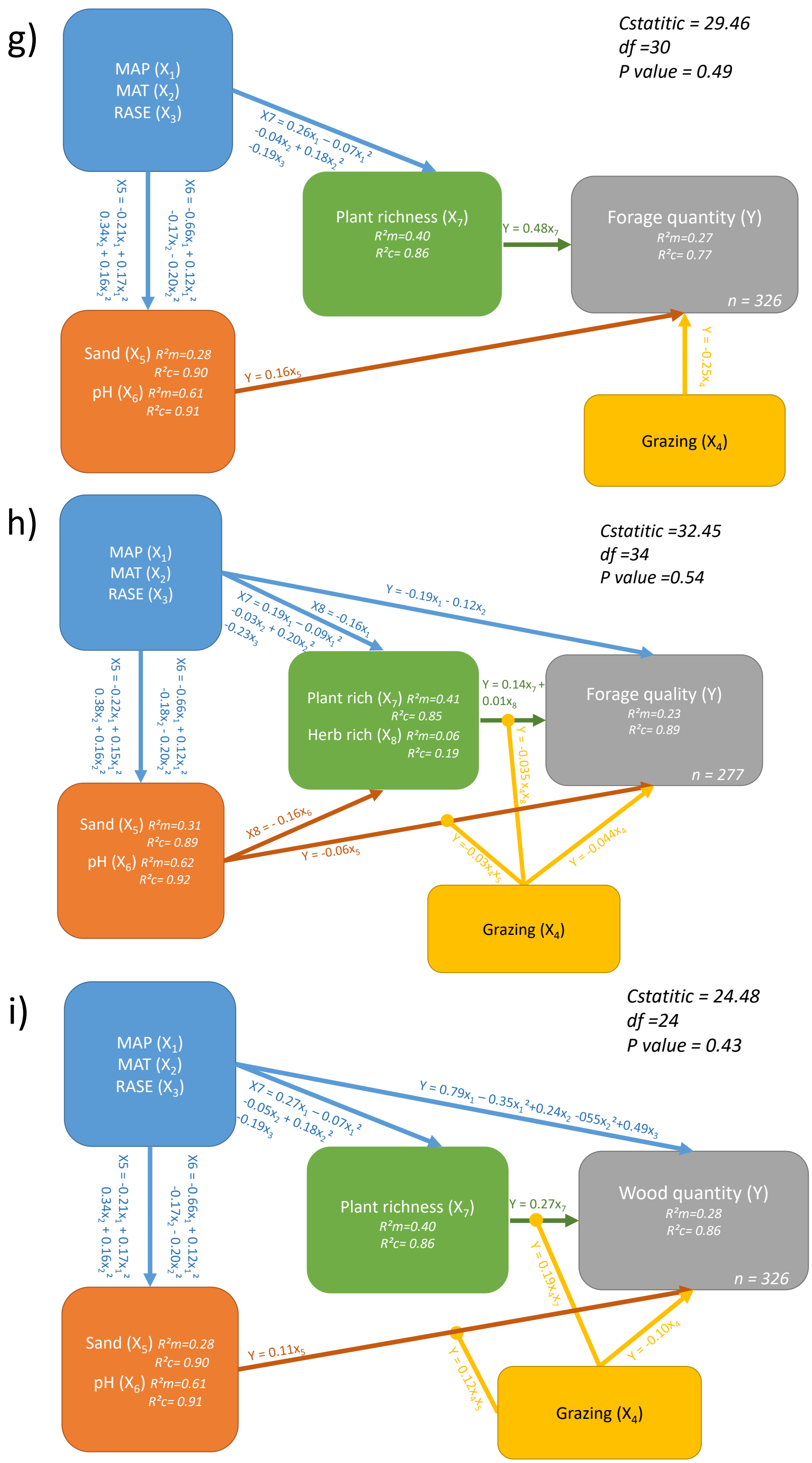
g)
MAP (X1)
MAT (X2)
RASE (X3)
X7 = 0.26x1 – 0.07x1 2 -0.04x2 + 0.18x2 2 -0.19x3
X5 = -0.21x1 + 0.17x1 2 0.34x2 + 0.16x2 2
X6 = -0.66x1 + 0.12x1 2 -0.17x2 - 0.20x2 2
Plant richness (X7)
R2m=0.40
R2c= 0.86
Y = 0.48x7
Forage quantity (Y)
R2m=0.27
R2c= 0.77
n = 326
Cstatitic = 29.46
df =30
P value = 0.49
Sand (X5) R2m=0.28
R2c= 0.90
pH (X6) R2m=0.61
R2c= 0.91
Y = 0.16x5
Y = -0.25x4
Grazing (X4)
h)
MAP (X1)
MAT (X2)
RASE (X3)
Cstatitic =32.45
df =34
P value =0.54
Y = -0.19x1 - 0.12x2
X7 = 0.19x1 – 0.09x1 2 -0.03x2 + 0.20x2 2 -0.23x3
X8 = -0.16x1
X5 = -0.22x1 + 0.15x1 2 0.38x2 + 0.16x2 2
X6 = -0.66x1 + 0.12x1 2 -0.18x2 - 0.20x2 2
Plant rich (X7) R2m=0.41
R2c= 0.85
Herb rich (X8) R2m=0.06
R2c= 0.19
Y = 0.14x7 + 0.01x8
Y = -0.035 x4x8
Forage quality (Y)
R2m=0.23
R2c= 0.89
n = 277
Sand (X5) R2m=0.31
R2c= 0.89
pH (X6) R2m=0.62
R2c= 0.92
X8 = - 0.16x6
Y = -0.06x5
Y =-0.03x4x5
Y = -0.044x4
Grazing (X4)
i)
MAP (X1)
MAT (X2)
RASE (X3)
Cstatitic = 24.48
df =24
P value = 0.43
Y = 0.79x1 – 0.35x1 2+0.24x2 -055x2 2+0.49x3
X7 = 0.27x1 – 0.07x1 2 -0.05x2 + 0.18x2 2 -0.19x3
X5 = -0.21x1 + 0.17x1 2 0.34x2 + 0.16x2 2
X6 = -0.66x1 + 0.12x1 2 -0.17x2 - 0.20x2 2
Plant richness (X7)
R2m=0.40
R2c= 0.86
Y = 0.27x7
Wood quantity (Y)
R2m=0.28
R2c= 0.86
n = 326
Y = 0.19x4x7
Sand (X5) R2m=0.28
R2c= 0.90
pH (X6) R2m=0.61
R2c= 0.91
Y = 0.11x5
Y = 0.12x4x5
Y = -0.10x4
Grazing (X4)

Fig. S11. Results of the conditional path analyses to test for indirect effects of grazing pressure. The panels show selected path models linking climate (blue arrows), soil (orange arrows), biodiversity (green arrows), and grazing (yellow arrows) with soil carbon storage (a), organic matter decomposition (b), erosion control (c), water regulation (d), soil fertility (e), aboveground plant biomass and its temporal stability (f), wood quantity (g), forage quantity (h), and forage quality (i). For each arrow, we indicated the equations associated with each significant path. Since all predictors were Z-scored prior analyses, coefficient paths represent effect sizes. We included grazing interactive effects when selected in the final best models (see supplementary tables S13-S15) represented by circle-ended arrows. Plant biomass & stability = aboveground plant biomass and its temporal stability, Sand = sand content, Plant rich = plant species richness, Herb rich = mammalian herbivore richness, Below div = belowground diversity, MAT = mean annual temperature, RASE = rainfall seasonality, and MAP = mean annual precipitation.

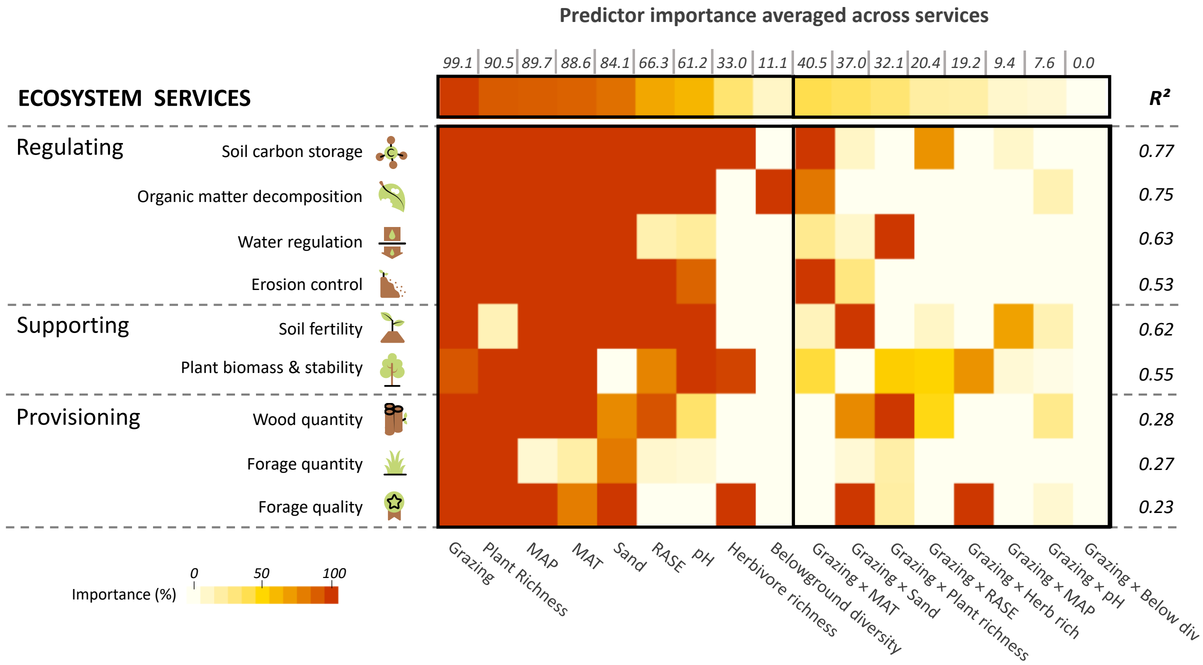

Fig. S12. Relative importance of predictors (grazing pressure, climate, biodiversity, and soil variables, and their interactions) of ecosystem services selected in best-fitting models. Importance is quantified as the sum of the Akaike weights of all models that included the predictor of interest, considering the number of models in which each predictor appears. It is proportional to the number of times a given predictor (and its interactions with other predictors) was selected in the final set of best-fitting models (*13*). In the case of biodiversity, predictor importance considers the number of models that includes at least one biodiversity proxy (plant species richness, mammalian herbivore richness or belowground diversity). Full details on model results, including the number of best-fitting models, are available in tables S13-S15. Plant biomass & stability = aboveground plant biomass and its temporal stability, Grazing = grazing pressure, Herb rich = mammalian herbivore richness, Below div = belowground diversity MAT = mean annual temperature, RASE = rainfall seasonality, and MAP = mean annual precipitation.

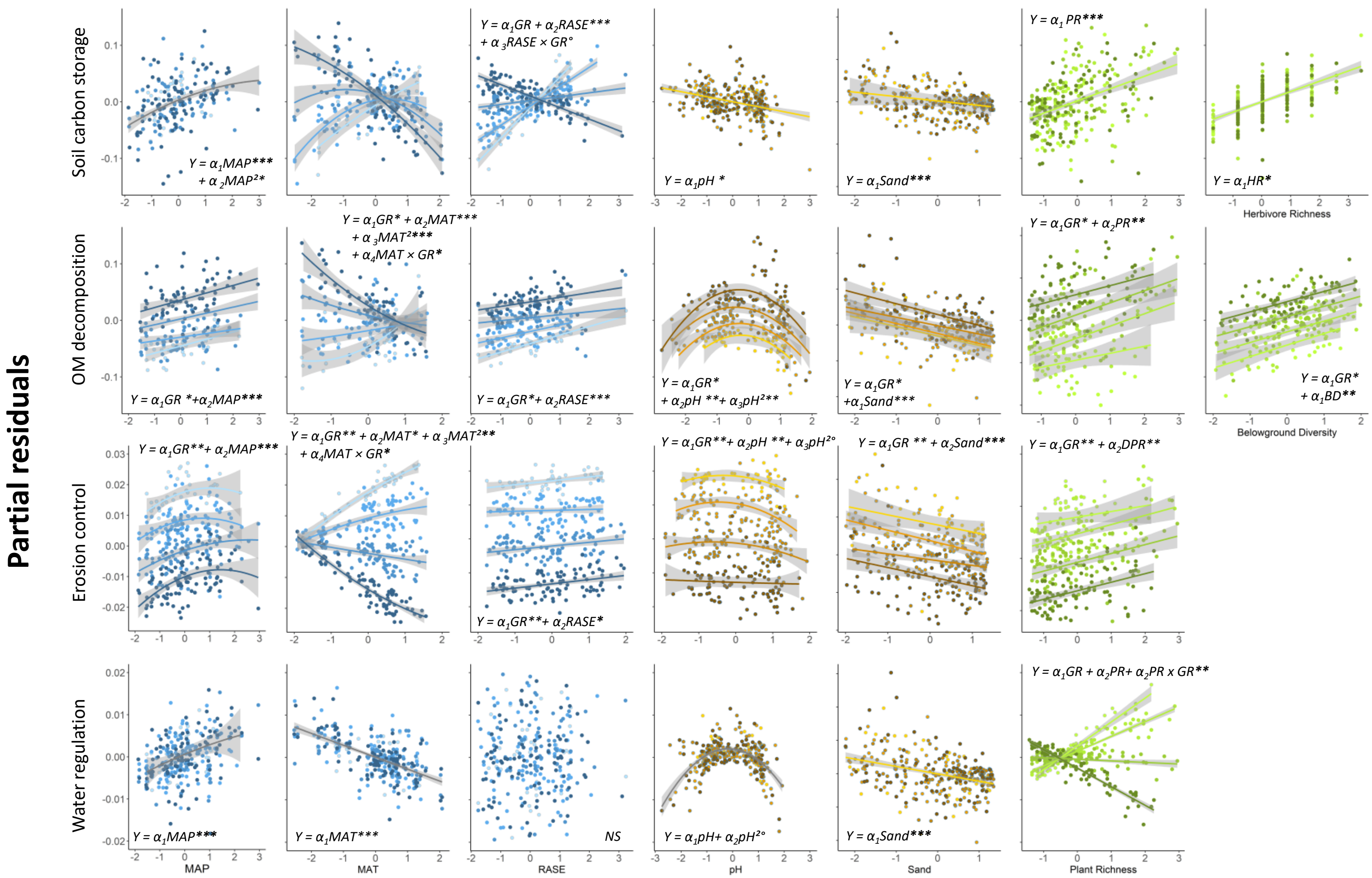

Fig. S13. Predicted responses of regulating ecosystem services to climate, sand content, and plant species richness at different levels of grazing pressure. Dots show partial residuals and lines show model fits (using partial regressions) for each significant predictor in the final best models (ΔAIC < 2, *13*). Climatic, soil, and biodiversity predictors are represented in blue, brown, and green, respectively. When significant main or interactive effects of grazing were observed in the final set of best models, we plotted predictions for the four levels of grazing pressure separately. The darkest dots represent partial residuals at high grazing pressure plots, while the brightest dots represent partial residuals at ungrazed plots. Similarly, the darkest lines represent model fits for high grazing pressure plots, the brightest lines represent model fits for ungrazed plots. In both cases, the colour increases from lightest to darkest in this order: ungrazed, low grazing pressure, medium grazing pressure, and high grazing pressure. Details on model parameters are available on tables S13-S15. OM = organic matter, NS = non-significant predictors, GR = grazing pressure, MAP = mean annual precipitation, MAT = mean annual temperature, RASE = rainfall seasonality, Sand = sand content, pH = soil pH, PR = plant species richness, HR = mammalian herbivore richness, and BD = belowground diversity. Significance of predictors as follows: ° $P < 0.10$, *, $P < 0.05$; **, $P < 0.01$; ***, $P < 0.001$.

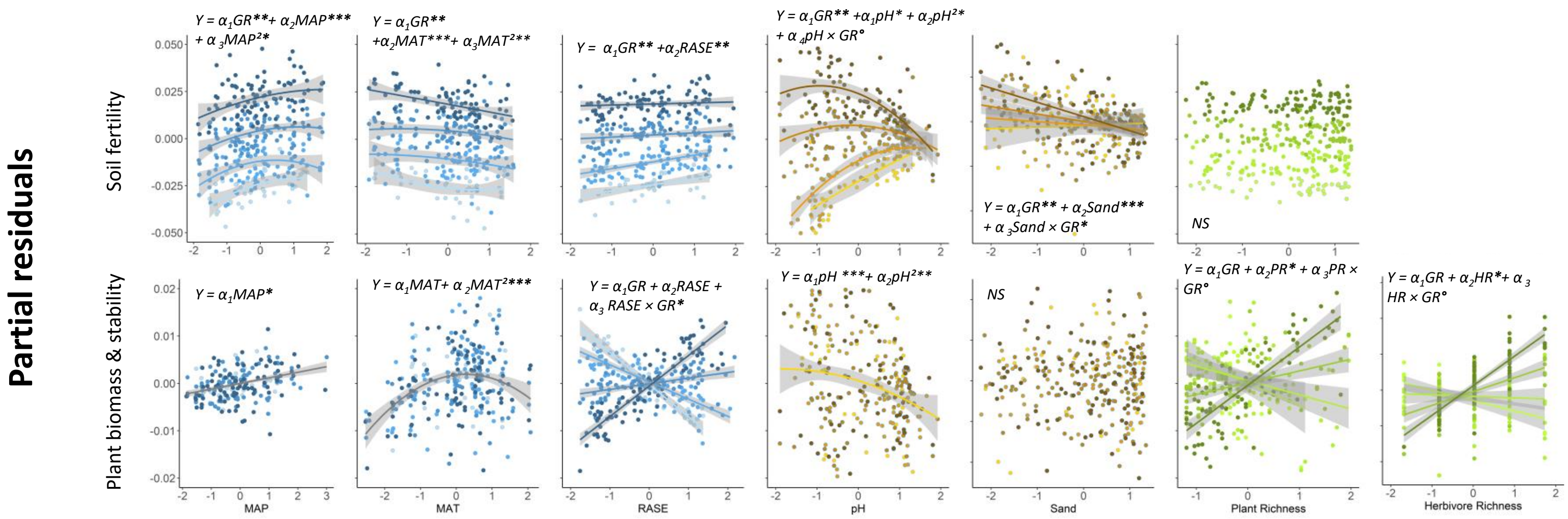

Fig. S14. Predicted responses of supporting ecosystem services to climate, sand content, and plant species richness at different levels of grazing pressure. Plant biomass & stability = aboveground plant biomass and its temporal stability. Remainder of legend as in fig. S13.

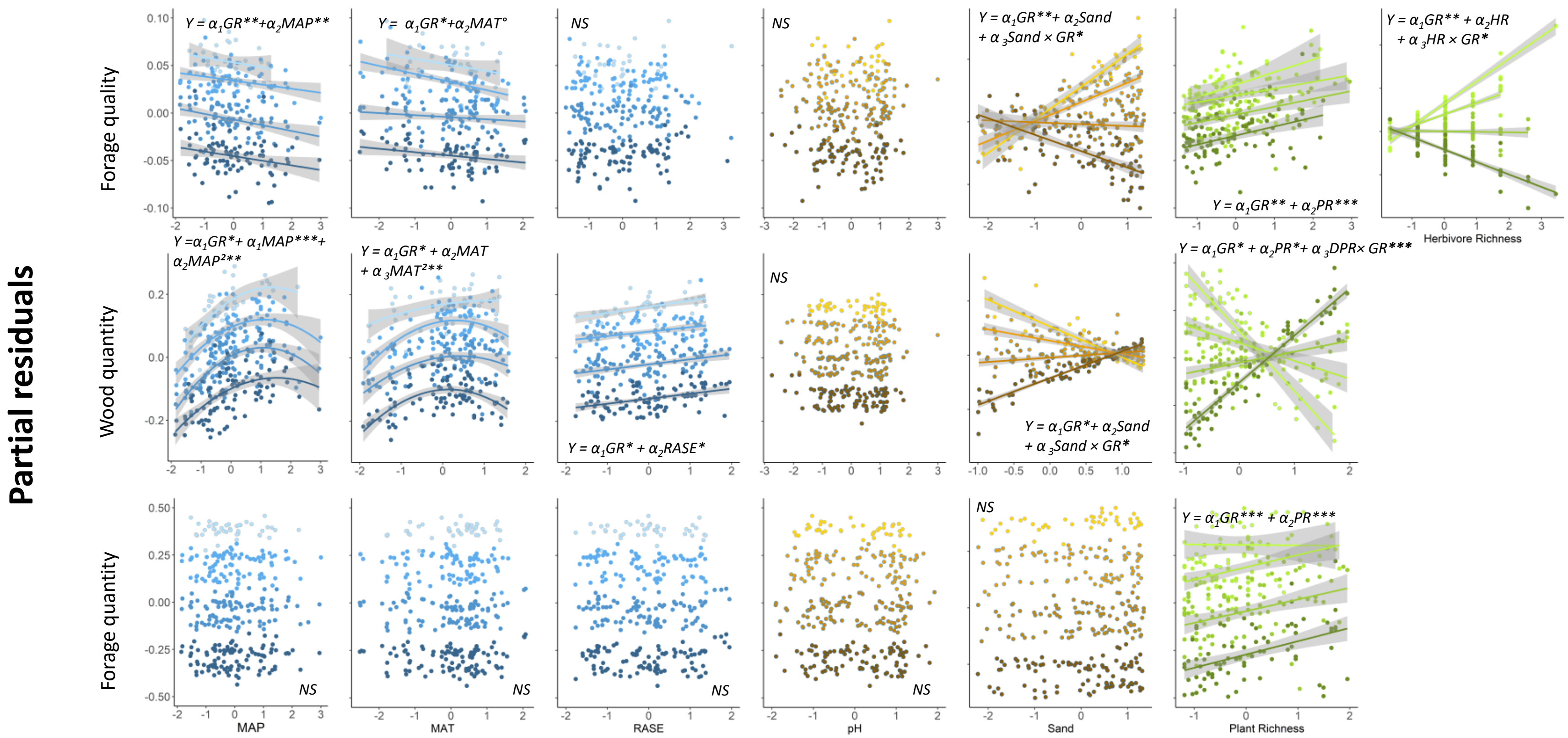

2403 **Fig. S15. Predicted responses of provisioning ecosystem services to climate, sand content, and plant species richness at different levels of grazing pressure.** Remainder of legend as in fig. S13.

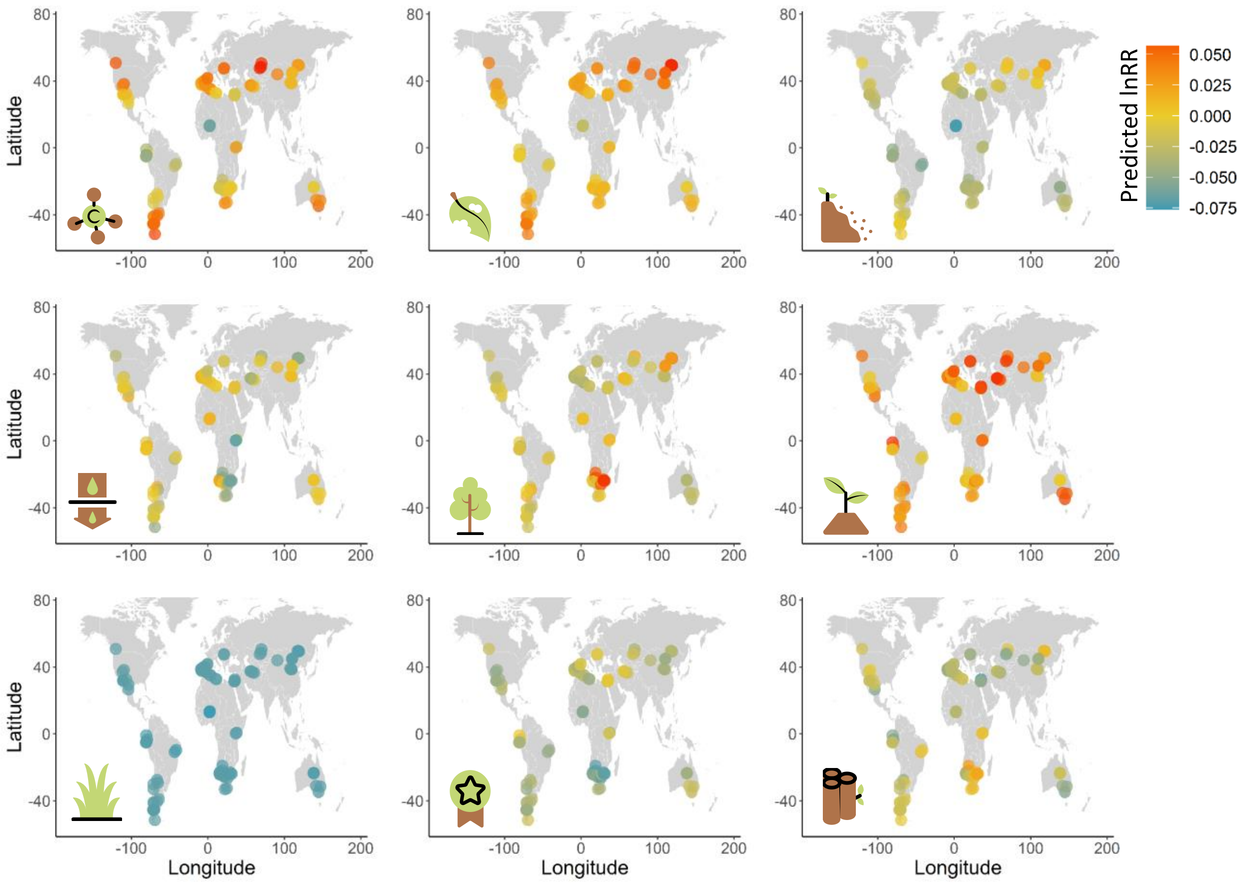

Fig. S16. Geographical variation in the effect of grazing on each ecosystem service measured across global drylands. For each of the 98 sites surveyed, we plot the effect of grazing predicted by model parameters along the wide climatic and plant species richness gradients evaluated. This effect was calculated using the predicted response ratio (lnRR) at each site, calculated as the lnRR between model predictions at high vs. low grazing pressure levels (see "Statistical analyses" section) and considering site parameters. These parameters included plant and mammalian herbivore richness, belowground diversity, mean annual temperature and rainfall seasonality; all other parameters were fixed at their mean value (see full model parameters in tables S13-S15)**.** See fig. S12 for the meaning of the symbols depicting each ecosystem service.

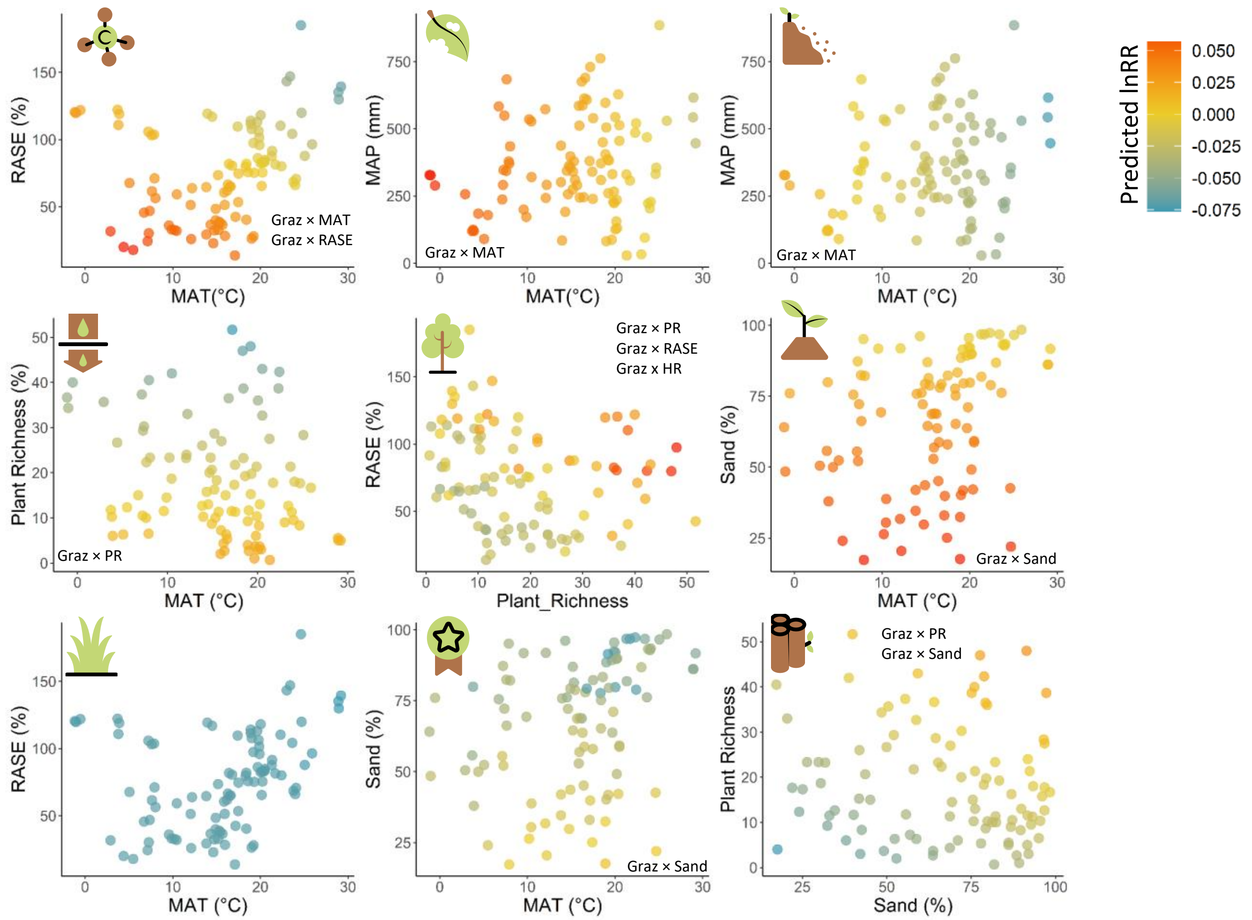

Fig. S17. Variation in the effect of grazing on each ecosystem service measured across global climatic, soil, and plant richness gradients in the drylands surveyed. For each service, we plot the effect of grazing predicted by model parameters for the 98 sites surveyed along the wide climatic and plant species richness gradients evaluated. This effect was calculated using the predicted response ratio (lnRR) at each site, calculated as the lnRR between model predictions at high vs. low grazing pressure levels (see "Statistical analyses" section) and considering site parameters. These parameters included plant species richness (PR), mammalian herbivore richness (HR), belowground diversity, mean annual temperature (MAT), mean annual rainfall (MAP) and rainfall seasonality (RASE); all other parameters were fixed at their mean value. We plot significant interactions for each service in each panel (see full model parameters in tables S13-S15). See fig. S12 for the meaning of the symbols depicting each ecosystem service. Graz = grazing and Sand = sand content.

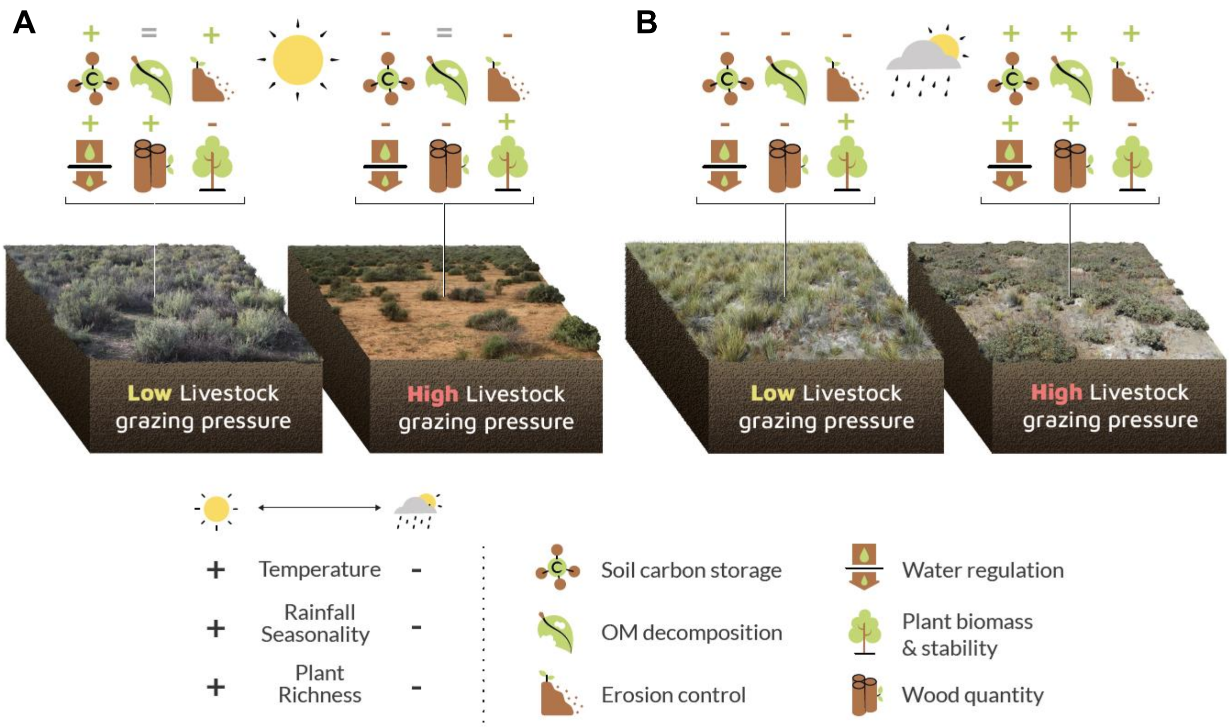

Fig. S18. The effects of increased grazing pressure on ecosystem services vary across contrasting environmental contexts. While increases in grazing pressure reduce forage quantity and quality and enhance soil fertility regardless of climatic conditions, such increases interact with temperature, rainfall seasonality and/or plant species richness to determine multiple ecosystem services. Panel A shows the situation in dryland areas with high temperature, rainfall seasonality and/or plant species richness. Panel B shows the situation in dryland areas with low temperature, rainfall seasonality and/or plant species richness. OM = organic matter and Plant biomass & stability = aboveground plant biomass and its temporal stability. This figure is based on results shown in Fig. 2 and figs. S13-S15 and S17.

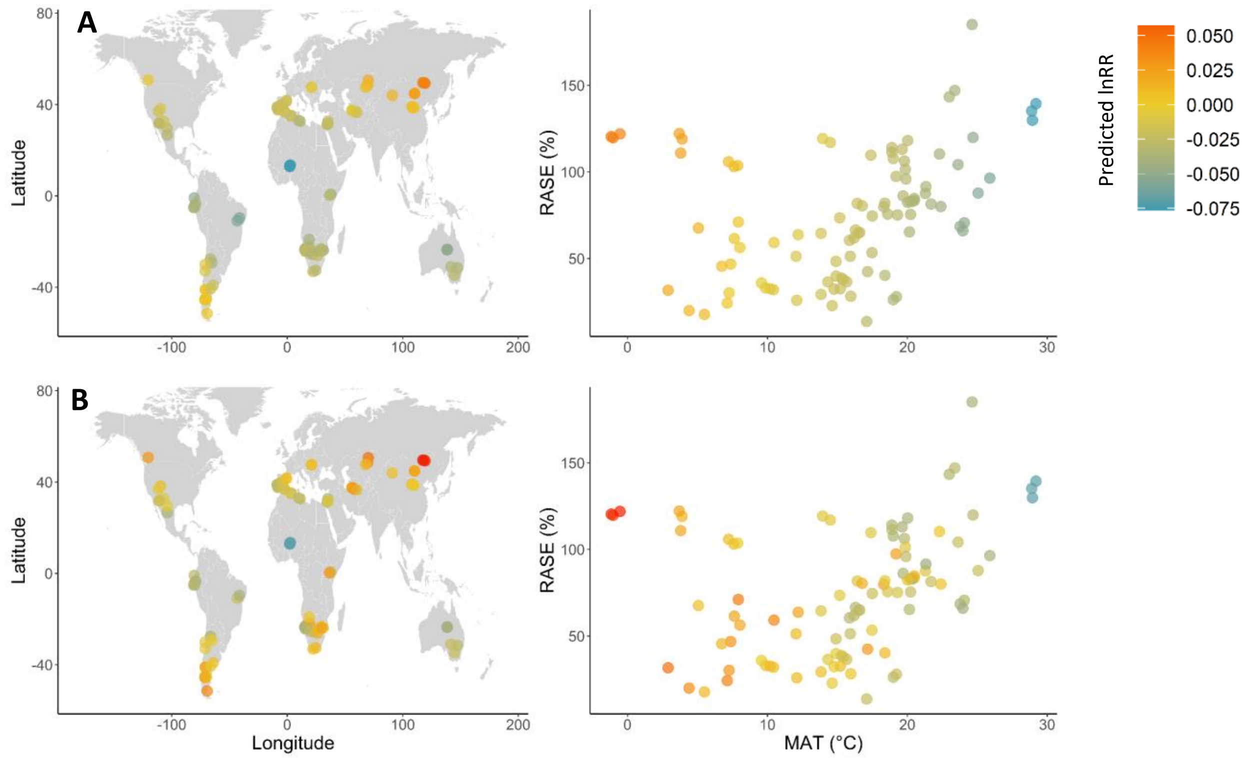

Fig. S19. Geographical variation in the effect of grazing on ecosystem services when only climate (A) and both climate and plant richness (B) are considered. This effect was calculated using the predicted response ratio (lnRR) at each site, calculated as the lnRR between model predictions at high vs. low grazing pressure levels. The climatic parameters selected (mean annual temperature [MAT] and rainfall seasonality [RASE]) interacted with grazing. Diversity components used include plant species and mammalian herbivore richness. For simplicity, we averaged the grazing effect at the site level across all services. The size of dots is proportional to the species richness observed at each site. Predicted grazing effects using climatic parameters ranged from neutral to mostly positive for most sites (a). When we accounted for the effects of plant and mammalian herbivore richness in addition to those of climate (b), grazing effects became negative according to model predictions in sites with a low plant species richness (small dots in b) while it remained positive in sites with a high plant and herbivore species richness (large dots in b). These results show that biodiversity both limits negative and promotes positive impacts of increasing grazing pressure on ecosystem services across global drylands.

Table S1. Ecosystem variables used to quantify regulating, supporting, and provisioning ecosystem services.

Type	Ecosystem service	Ecosystem variable	Units
Regulating	Water regulation	Soil water holding capacity	%
		Soil porosity	%
	Soil carbon storage	Soil organic C stock	kg C·m^{-2} soil
	Organic matter decomposition	Activity of β-glucosidase	μmol PnP·g soil^{-1}·h^{-1}
		Activity of phosphatase	μmol PnP·g soil^{-1}·h^{-1}
		Activity of cellobiase	nmol MUF·g soil^{-1}·h^{-1}
		Activity of β-N-acetylglucosaminidase	nmol MUF·g soil^{-1}·h^{-1}
		Activity of xylanase	nmol MUF·g soil^{-1}·h^{-1}
		Soil carbon mineralization	μg CO_2-C·g soil^{-1}·day^{-1}
		Soil nitrogen mineralization	mg N·kg soil^{-1}·day^{-1}
		Soil microbial biomass	μg C mic·g soil^{-1}
	Erosion control	Perennial plant cover	%
		Mean weight diameter of soil aggregates	mm
		Stability of macro-aggregates >250 μm	%
Supporting	Soil fertility	Total N content	g N·kg soil^{-1}
		NH_4^+ content	mg N·kg soil^{-1}
		NO_3^- content	mg N·kg soil^{-1}
		Dissolved organic N content	mg N·kg soil^{-1}
		Total P content	mg P·kg soil^{-1}
		K content	mg K·kg soil^{-1}
		Cu content	mg Cu·kg soil^{-1}
		Mg content	mg Mg·kg soil^{-1}
		Fe content	mg Fe·kg soil^{-1}

		Mn content	mg Mn·kg soil^{-1}
		Zn content	mg Zn·kg soil^{-1}
	Aboveground plant biomass and its temporal stability	Average aboveground plant biomass [APB]	Unitless
		Inverse of the CV of APB	Unitless
Provisioning	Wood quantity	Biovolume of woody vegetation	m^{3}·m^{-2}
	Forage quantity	Biovolume of grasses	m^{3}·m^{-2}
		Biovolume of forbs	m^{3}·m^{-2}
	Forage quality	Specific leaf area of grasses	cm^{2}·g^{-1}
		Specific leaf area of herbs	cm^{2}·g^{-1}
		Foliar nitrogen content of grasses	%
		Foliar nitrogen content of herbs	%
		Leaf dry matter content of grasses	Unitless
		Leaf dry matter content of herbs	Unitless

Table S2. Mammalian herbivores recorded at the sites surveyed and the number of sites where the different species were found.

Family/Subfamily	Animal	Type	Number of sites
Antelope	Gemsbok	*Oryx gazella*	14
	Roe deer	*Capreolus capreolus*	8
	Steenbok	*Raphicerus campestris*	7
	Common duiker	*Sylvicapra grimmia*	6
	Red deer	*Cervus elaphus*	5
	Greater kudu	*Tragelaphus strepsiceros*	4
	Springbok	*Antidorcas marsupialis*	3
	Hartebeest	*Alcelaphus buselaphus*	3
	Gazelle	*Gazella* spp.	2
	Blue wildebeest	*Connochaetes taurinus*	2
	Waterbuck	*Kobus ellipsiprymnus*	1
Rodents	South African Springhare	*Pedetes capensis*	4
Macropod	Kangaroo	*Macropus* spp., *Osphranter rufus*	5
Leporids	Rabbit	*Oryctolagus cuniculus*	33
	Hare	*Lepus* sp.	11
	African savanna hare	*Lepus victoriae*	5
Equine	[#]Horse	*Equus caballus*	34
	[#]Donkey	*Equus asinus*	8
	Common zebra	*Equus quagga*	4
	Grevy's zebra	*Equus grevyi*	3
Suidae	Common warthog	*Phacochoerus africanus*	1
Bovinae	[#]Cattle	*Bos taurus, Bos indicus*	58
	African buffalo	*Syncerus caffer*	1
Camelids	Dromedary	*Camelus dromedarius*	2
	Bactrian camel	*Camelus bactrianus*	1
	Guanaco	*Lama guanicoe*	2
Ovids	[#]Sheep	*Ovis aries*	57
Caprids	[#]Goat	*Capra hirca*	35
Giraffid	Giraffe	*Giraffa camelopardalis*	5
Elephantidae	Elephant	*Loxodonta africana*	1

[#]livestock species

Table S3. Correlation matrix among all studied predictors (n = 326). We show Spearman correlation coefficients for correlations involving grazing pressure and Pearson correlation coefficients for the rest of predictors. Graz = grazing pressure, Plant rich = plant species richness, Herb rich = mammalian herbivore richness, Below Div = belowground diversity, MAT = mean annual temperature, RASE = rainfall seasonality, and MAP = mean annual precipitation.

	Graz	MAP	MAT	RASE	Sand	Soil pH	Plant rich	Herb rich	Below div
Graz	1								
MAP	0,006	1							
MAT	0,03	0,17	1						
RASE	0	-0,12	0,23	1					
Sand	0,02	-0,14	0,28	0,21	1				
Soil pH	-0,005	-0,56	-0,33	-0,03	-0,25	1			
Plant rich	-0,03	0,28	-0,17	-0,19	-0,08	-0,20	1		
Herb rich	0,17	-0,09	-0,09	0,12	0,09	-0,10	0,12	1	
Below div	-0,20	0,32	-0,07	-0,28	0,23	-0,28	0,21	-0,05	1

Table S4. Conditional independence claims applied in the different hypotheses of the d-sep model implied by the hypothesized path models for soil carbon storage. We modeled each link using linear mixed models. Model types (lmer = linear mixed effect regression; glmer = generalized mixed effect regression) and formula are provided for each link. In each model, we controlled for the latitude, cos_longitude, sin_longitude, elevation, and slope (covariables), and used the site as a random factor (see "Statistical analyses" section). We present all independent claims considered in the model, provide the *P* value of each independent claim, and the *P* value of the different path analyses. Variables: X1 = mean annual rainfall, X2 = mean annual temperature, X3 = rainfall seasonality, X4 = Grazing, X5 = Sand, X6 = PH, X7 = plant species richness, X8 = mammalian herbivore richness, X9 = belowground diversity. Y = ecosystem service, and Cov = covariables. Value of C statistic (*P* value) = 30.70 (0.42), df = 30

<table>
<tr><th>Link</th><th>D-sep independence claims</th><th>Formula</th><th>Model</th><th>H0</th><th>P value</th></tr>
<tr><td>1</td><td>(X3,X2)|{Cov}</td><td>X3 ~ Cov + X2</td><td>lmer</td><td>||X2 = 0</td><td>0.16</td></tr>
<tr><td>2</td><td>(X4,X1)|{Cov}</td><td>X4 ~ Cov + X1</td><td>lmer</td><td>||X1 = 0</td><td>0.20</td></tr>
<tr><td>3</td><td>(X4,X2)|{Cov}</td><td>X4 ~ Cov + X3</td><td>lmer</td><td>||X3 = 0</td><td>0.68</td></tr>
<tr><td>4</td><td>(X4,X3)|{Cov}</td><td>X4 ~ Cov + X3</td><td>lmer</td><td>||X3 = 0</td><td>0.79</td></tr>
<tr><td>5</td><td>(X5,X3)|{Cov,X1,X2}</td><td>X5 ~ Cov+ X1+I(X1^2)+X2+I(X2^2)+X3</td><td>lmer</td><td>||X3 = 0</td><td>0.89</td></tr>
<tr><td>6</td><td>(X6,X3)|{Cov,X1,X2,X5}</td><td>X6 ~ Cov+ X1+I(X1^2)+X2+I(X2^2)+X5+X3</td><td>lmer</td><td>||X3 = 0</td><td>0.98</td></tr>
<tr><td>7</td><td>(X5,X4)|{Cov,X1,X2}</td><td>X5 ~Cov+ X1+I(X1^2)+X2+I(X2^2)+X4</td><td>lmer</td><td>||X4 = 0</td><td>0.28</td></tr>
<tr><td>8</td><td>(X6,X4)|{Cov,X1,X2,X5}</td><td>X6 ~ Cov+ X1+I(X1^2)+X2+I(X2^2)+X5+X4</td><td>lmer</td><td>||X4 = 0</td><td>0.96</td></tr>
<tr><td>9</td><td>(X7,X4)|{Cov,X1,X2,X3}</td><td>X7 ~ Cov+ X1+I(X1^2)+X2+I(X2^2)+X3+X4</td><td>lmer</td><td>||X4 = 0</td><td>0.56</td></tr>
<tr><td>10</td><td>(X7,X5)|{Cov,X1,X2,X3}</td><td>X7 ~ Cov+ X1+I(X1^2)+X2+I(X2^2)+X3+X5</td><td>lmer</td><td>||X5 = 0</td><td>0.68</td></tr>
<tr><td>11</td><td>(X7,X6|{Cov,X1,X2,X3}</td><td>X7 ~ Cov+ X1+I(X1^2)+X2+I(X2^2)+X3+X6</td><td>lmer</td><td>||X6 = 0</td><td>0.11</td></tr>
<tr><td>12</td><td>(X8,X2)|{Cov,X1,X6}</td><td>X7 ~ Cov+ X1+X6+X2</td><td>glmer (poisson)</td><td>||X2 = 0</td><td>0.26</td></tr>
<tr><td>13</td><td>(X8,X3)|{Cov,X1,X6}</td><td>X7 ~ Cov+ X1+X6+X3</td><td>glmer (poisson)</td><td>||X3 = 0</td><td>0.59</td></tr>
<tr><td>14</td><td>(X8,X4)|{Cov,X1,X6}</td><td>X7 ~ Cov+ X1+X6+X4</td><td>glmer (poisson)</td><td>||X4 = 0</td><td>0.02</td></tr>
<tr><td>15</td><td>(X8,X5)|{Cov,X1,X6}</td><td>X7 ~ Cov+ X1+X6+X5</td><td>glmer (poisson)</td><td>||X5 = 0</td><td>0.43</td></tr>
</table>

Table S5. Conditional independence claims applied in the different hypotheses of the d-sep model implied by the hypothesized path models for organic matter decomposition. Value of C statistic (*P* value) = 30.79 (0.42), df = 30. Remainder of legend as in table S4.

Link	D-sep independence claims	Formula	Model	H0	*P value*
1	(X3,X2)|{Cov}	X3 ~ Cov + X2	lmer	||X2 = 0	0.15
2	(X4,X1)|{Cov}	X4 ~ Cov + X1	lmer	||X1 = 0	0.36
3	(X4,X2)|{Cov}	X4 ~ Cov + X3	lmer	||X3 = 0	0.51
4	(X4,X3)|{Cov}	X4 ~ Cov + X3	lmer	||X3 = 0	0.84
5	(X5,X3)|{Cov,X1,X2}	X5 ~ Cov+ X1+I(X1^2)+X2+I(X2^2)+X3	lmer	||X3 = 0	0.12
6	(X6,X3)|{Cov,X1,X2,X5}	X6 ~ Cov+ X1+I(X1^2)+X2+I(X2^2)+X5+X3	lmer	||X3 = 0	0.48
7	(X5,X4)|{Cov,X1,X2}	X5 ~Cov+ X1+I(X1^2)+X2+I(X2^2)+X4	lmer	||X4 = 0	0.10
8	(X6,X4)|{Cov,X1,X2,X5}	X6 ~ Cov+ X1+I(X1^2)+X2+I(X2^2)+X5+X4	lmer	||X4 = 0	0.09
9	(X7,X4)|{Cov,X1,X2,X3}	X7 ~ Cov+ X1+I(X1^2)+X2+I(X2^2)+X3+X4	lmer	||X4 = 0	0.57
10	(X7,X5)|{Cov,X1,X2,X3}	X7 ~ Cov+ X1+I(X1^2)+X2+I(X2^2)+X3+X5	lmer	||X5 = 0	0.45
11	(X7,X6|{Cov,X1,X2,X3}	X7 ~ Cov+ X1+I(X1^2)+X2+I(X2^2)+X3+X6	lmer	||X6 = 0	0.33
12	(X9,X3)|{Cov,X1,X2,X7}	X9 ~ Cov+ X1+I(X1^2)+X2+I(X2^2)+X7+X3	lmer	||X3 = 0	0.94
13	(X9,X4)|{Cov,X1,X2,X7}	X9 ~ Cov+ X1+I(X1^2)+X2+I(X2^2)+X7+X4	lmer	||X4 = 0	0.84
14	(X9,X5)|{Cov,X1,X2,X7}	X9 ~ Cov+ X1+I(X1^2)+X2+I(X2^2)+X7+X5	lmer	||X5 = 0	0.89
15	(X9,X6)|{Cov,X1,X2,X7}	X9 ~ Cov+ X1+I(X1^2)+X2+I(X2^2)+X7+X6	lmer	||X6 = 0	0.22

Table S6. Conditional independence claims applied in the different hypotheses of the d-sep model implied by the hypothesized path models for erosion control. Value of C statistic (*P* value) = 27.08 (0.20), df = 22. Remainder of legend as in table S4.

<table>
<tr><th>Link</th><th>D-sep independence claims</th><th>Formula</th><th>Model</th><th>H0</th><th>P value</th></tr>
<tr><td>1</td><td>(X3,X2)|{Cov}</td><td>X3 ~ Cov + X2</td><td>lmer</td><td>||X2 = 0</td><td>0.15</td></tr>
<tr><td>2</td><td>(X4,X1)|{Cov}</td><td>X4 ~ Cov + X1</td><td>lmer</td><td>||X1 = 0</td><td>0.36</td></tr>
<tr><td>3</td><td>(X4,X2)|{Cov}</td><td>X4 ~ Cov + X3</td><td>lmer</td><td>||X3 = 0</td><td>0.51</td></tr>
<tr><td>4</td><td>(X4,X3)|{Cov}</td><td>X4 ~ Cov + X3</td><td>lmer</td><td>||X3 = 0</td><td>0.84</td></tr>
<tr><td>5</td><td>(X5,X3)|{Cov,X1,X2}</td><td>X5 ~ Cov+ X1+I(X1^2)+X2+I(X2^2)+X3</td><td>lmer</td><td>||X3 = 0</td><td>0.12</td></tr>
<tr><td>6</td><td>(X6,X3)|{Cov,X1,X2,X5}</td><td>X6 ~ Cov+ X1+I(X1^2)+X2+I(X2^2)+X5+X3</td><td>lmer</td><td>||X3 = 0</td><td>0.48</td></tr>
<tr><td>7</td><td>(X5,X4)|{Cov,X1,X2}</td><td>X5 ~Cov+ X1+I(X1^2)+X2+I(X2^2)+X4</td><td>lmer</td><td>||X4 = 0</td><td>0.10</td></tr>
<tr><td>8</td><td>(X6,X4)|{Cov,X1,X2,X5}</td><td>X6 ~ Cov+ X1+I(X1^2)+X2+I(X2^2)+X5+X4</td><td>lmer</td><td>||X4 = 0</td><td>0.09</td></tr>
<tr><td>9</td><td>(X7,X4)|{Cov,X1,X2,X3}</td><td>X7 ~ Cov+ X1+I(X1^2)+X2+I(X2^2)+X3+X4</td><td>lmer</td><td>||X4 = 0</td><td>0.57</td></tr>
<tr><td>10</td><td>(X7,X5)|{Cov,X1,X2,X3}</td><td>X7 ~ Cov+ X1+I(X1^2)+X2+I(X2^2)+X3+X5</td><td>lmer</td><td>||X5 = 0</td><td>0.45</td></tr>
<tr><td>11</td><td>(X7,X6|{Cov,X1,X2,X3}</td><td>X7 ~ Cov+ X1+I(X1^2)+X2+I(X2^2)+X3+X6</td><td>lmer</td><td>||X6 = 0</td><td>0.33</td></tr>
</table>

Table S7. Conditional independence claims applied in the different hypotheses of the d-sep model implied by the hypothesized path models for water regulation. Value of C statistic (*P* value) = 22.18 (0.44), df = 22. Remainder of legend as in table S4.

<table>
<tr><th>Link</th><th>D-sep independence claims</th><th>Formula</th><th>Model</th><th>H0</th><th>P value</th></tr>
<tr><td>1</td><td>(X3,X2)|{Cov}</td><td>X3 ~ Cov + X2</td><td>lmer</td><td>||X2 = 0</td><td>0.06</td></tr>
<tr><td>2</td><td>(X4,X1)|{Cov}</td><td>X4 ~ Cov + X1</td><td>lmer</td><td>||X1 = 0</td><td>0.41</td></tr>
<tr><td>3</td><td>(X4,X2)|{Cov}</td><td>X4 ~ Cov + X3</td><td>lmer</td><td>||X3 = 0</td><td>0.79</td></tr>
<tr><td>4</td><td>(X4,X3)|{Cov}</td><td>X4 ~ Cov + X3</td><td>lmer</td><td>||X3 = 0</td><td>0.93</td></tr>
<tr><td>5</td><td>(X5,X3)|{Cov,X1,X2}</td><td>X5 ~ Cov+ X1+I(X1^2)+X2+I(X2^2)+X3</td><td>lmer</td><td>||X3 = 0</td><td>0.65</td></tr>
<tr><td>6</td><td>(X6,X3)|{Cov,X1,X2,X5}</td><td>X6 ~ Cov+ X1+I(X1^2)+X2+I(X2^2)+X5+X3</td><td>lmer</td><td>||X3 = 0</td><td>0.82</td></tr>
<tr><td>7</td><td>(X5,X4)|{Cov,X1,X2}</td><td>X5 ~Cov+ X1+I(X1^2)+X2+I(X2^2)+X4</td><td>lmer</td><td>||X4 = 0</td><td>0.08</td></tr>
<tr><td>8</td><td>(X6,X4)|{Cov,X1,X2,X5}</td><td>X6 ~ Cov+ X1+I(X1^2)+X2+I(X2^2)+X5+X4</td><td>lmer</td><td>||X4 = 0</td><td>0.40</td></tr>
<tr><td>9</td><td>(X7,X4)|{Cov,X1,X2,X3}</td><td>X7 ~ Cov+ X1+I(X1^2)+X2+I(X2^2)+X3+X4</td><td>lmer</td><td>||X4 = 0</td><td>0.62</td></tr>
<tr><td>10</td><td>(X7,X5)|{Cov,X1,X2,X3}</td><td>X7 ~ Cov+ X1+I(X1^2)+X2+I(X2^2)+X3+X5</td><td>lmer</td><td>||X5 = 0</td><td>0.74</td></tr>
<tr><td>11</td><td>(X7,X6|{Cov,X1,X2,X3}</td><td>X7 ~ Cov+ X1+I(X1^2)+X2+I(X2^2)+X3+X6</td><td>lmer</td><td>||X6 = 0</td><td>0.09</td></tr>
</table>

Table S8. Conditional independence claims applied in the different hypotheses of the d-sep model implied by the hypothesized path models for soil fertility. Value of C statistic (*P* value) = 23.30 (0.50), df = 24. Remainder of legend as in table S4.

Link	D-sep independence claims	Formula	Model	H0	*P value*
1	(X3,X2)|{Cov}	X3 ~ Cov + X2	lmer	||X2 = 0	0.06
2	(X4,X1)|{Cov}	X4 ~ Cov + X1	lmer	||X1 = 0	0.41
3	(X4,X2)|{Cov}	X4 ~ Cov + X3	lmer	||X3 = 0	0.79
4	(X4,X3)|{Cov}	X4 ~ Cov + X3	lmer	||X3 = 0	0.93
5	(X5,X3)|{Cov,X1,X2}	X5 ~ Cov+ X1+I(X1^2)+X2+I(X2^2)+X3	lmer	||X3 = 0	0.65
6	(X6,X3)|{Cov,X1,X2,X5}	X6 ~ Cov+ X1+I(X1^2)+X2+I(X2^2)+X5+X3	lmer	||X3 = 0	0.82
7	(X5,X4)|{Cov,X1,X2}	X5 ~Cov+ X1+I(X1^2)+X2+I(X2^2)+X4	lmer	||X4 = 0	0.08
8	(X6,X4)|{Cov,X1,X2,X5}	X6 ~ Cov+ X1+I(X1^2)+X2+I(X2^2)+X5+X4	lmer	||X4 = 0	0.40
9	(X7,X4)|{Cov,X1,X2,X3}	X7 ~ Cov+ X1+I(X1^2)+X2+I(X2^2)+X3+X4	lmer	||X4 = 0	0.62
10	(X7,X5)|{Cov,X1,X2,X3}	X7 ~ Cov+ X1+I(X1^2)+X2+I(X2^2)+X3+X5	lmer	||X5 = 0	0.74
11	(X7,X6|{Cov,X1,X2,X3}	X7 ~ Cov+ X1+I(X1^2)+X2+I(X2^2)+X3+X6	lmer	||X6 = 0	0.09
12	(Y,X7|{Cov,X1,X2,X3,X4, X5,X6}	Y ~ Cov+ X1+I(X1^2)+X2+I(X2^2)+X3+X5+I(X5^2)+X6+X4+X4:X5+ X4:X6+X7	lmer	||X7 = 0	0.57

Table S9. Conditional independence claims applied in the different hypotheses of the d-sep model implied by the hypothesized path models for aboveground plant biomass and its temporal stability. Value of C statistic (*P* value) = 30.30 (0.44), df = 30. Remainder of legend as in table S4.

<table>
<tr><th>Link</th><th>D-sep independence claims</th><th>Formula</th><th>Model</th><th>H0</th><th>P value</th></tr>
<tr><td>1</td><td>(X3,X2)|{Cov}</td><td>X3 ~ Cov + X2</td><td>lmer</td><td>||X2 = 0</td><td>0.16</td></tr>
<tr><td>2</td><td>(X4,X1)|{Cov}</td><td>X4 ~ Cov + X1</td><td>lmer</td><td>||X1 = 0</td><td>0.20</td></tr>
<tr><td>3</td><td>(X4,X2)|{Cov}</td><td>X4 ~ Cov + X3</td><td>lmer</td><td>||X3 = 0</td><td>0.68</td></tr>
<tr><td>4</td><td>(X4,X3)|{Cov}</td><td>X4 ~ Cov + X3</td><td>lmer</td><td>||X3 = 0</td><td>0.79</td></tr>
<tr><td>5</td><td>(X5,X3)|{Cov,X1,X2}</td><td>X5 ~ Cov+ X1+I(X1^2)+X2+I(X2^2)+X3</td><td>lmer</td><td>||X3 = 0</td><td>0.89</td></tr>
<tr><td>6</td><td>(X6,X3)|{Cov,X1,X2,X5}</td><td>X6 ~ Cov+ X1+I(X1^2)+X2+I(X2^2)+X5+X3</td><td>lmer</td><td>||X3 = 0</td><td>0.98</td></tr>
<tr><td>7</td><td>(X5,X4)|{Cov,X1,X2}</td><td>X5 ~Cov+ X1+I(X1^2)+X2+I(X2^2)+X4</td><td>lmer</td><td>||X4 = 0</td><td>0.28</td></tr>
<tr><td>8</td><td>(X6,X4)|{Cov,X1,X2,X5}</td><td>X6 ~ Cov+ X1+I(X1^2)+X2+I(X2^2)+X5+X4</td><td>lmer</td><td>||X4 = 0</td><td>0.96</td></tr>
<tr><td>9</td><td>(X7,X4)|{Cov,X1,X2,X3}</td><td>X7 ~ Cov+ X1+I(X1^2)+X2+I(X2^2)+X3+X4</td><td>lmer</td><td>||X4 = 0</td><td>0.56</td></tr>
<tr><td>10</td><td>(X7,X5)|{Cov,X1,X2,X3}</td><td>X7 ~ Cov+ X1+I(X1^2)+X2+I(X2^2)+X3+X5</td><td>lmer</td><td>||X5 = 0</td><td>0.68</td></tr>
<tr><td>11</td><td>(X7,X6|{Cov,X1,X2,X3}</td><td>X7 ~ Cov+ X1+I(X1^2)+X2+I(X2^2)+X3+X6</td><td>lmer</td><td>||X6 = 0</td><td>0.11</td></tr>
<tr><td>12</td><td>(X8,X2)|{Cov,X1,X6}</td><td>X8 ~ Cov+ X1+X6+X2</td><td>glmer (poisson)</td><td>||X2 = 0</td><td>0.26</td></tr>
<tr><td>13</td><td>(X8,X3)|{Cov,X1,X6}</td><td>X8 ~ Cov+ X1+X6+X3</td><td>glmer (poisson)</td><td>||X3 = 0</td><td>0.59</td></tr>
<tr><td>14</td><td>(X8,X4)|{Cov,X1,X6}</td><td>X8 ~ Cov+ X1+X6+X4</td><td>glmer (poisson)</td><td>||X4 = 0</td><td>0.02</td></tr>
<tr><td>15</td><td>(X8,X5)|{Cov,X1,X6}</td><td>X8 ~ Cov+ X1+X6+X5</td><td>glmer (poisson)</td><td>||X5 = 0</td><td>0.43</td></tr>
</table>

Table S10. Conditional independence claims applied in the different hypotheses of the d-sep model implied by the hypothesized path models for wood quantity. Value of C statistic (*P* value) = 24.48 (0.43), df = 24. Remainder of legend as in table S4.

Link	D-sep independence claims	Formula	Model	H0	*P value*
1	(X3,X2)|{Cov}	X3 ~ Cov + X2	lmer	||X2 = 0	0.06
2	(X4,X1)|{Cov}	X4 ~ Cov + X1	lmer	||X1 = 0	0.43
3	(X4,X2)|{Cov}	X4 ~ Cov + X3	lmer	||X3 = 0	0.79
4	(X4,X3)|{Cov}	X4 ~ Cov + X3	lmer	||X3 = 0	0.93
5	(X5,X3)|{Cov,X1,X2}	X5 ~ Cov+ X1+I(X1^2)+X2+I(X2^2)+X3	lmer	||X3 = 0	0.65
6	(X6,X3)|{Cov,X1,X2,X5}	X6 ~ Cov+ X1+I(X1^2)+X2+I(X2^2)+X5+X3	lmer	||X3 = 0	0.82
7	(X5,X4)|{Cov,X1,X2}	X5 ~Cov+ X1+I(X1^2)+X2+I(X2^2)+X4	lmer	||X4 = 0	0.08
8	(X6,X4)|{Cov,X1,X2,X5}	X6 ~ Cov+ X1+I(X1^2)+X2+I(X2^2)+X5+X4	lmer	||X4 = 0	0.40
9	(X7,X4)|{Cov,X1,X2,X3}	X7 ~ Cov+ X1+I(X1^2)+X2+I(X2^2)+X3+X4	lmer	||X4 = 0	0.62
10	(X7,X5)|{Cov,X1,X2,X3}	X7 ~ Cov+ X1+I(X1^2)+X2+I(X2^2)+X3+X5	lmer	||X5 = 0	0.75
11	(X7,X6|{Cov,X1,X2,X3}	X7 ~ Cov+ X1+I(X1^2)+X2+I(X2^2)+X3+X6	lmer	||X6 = 0	0.09
12	(Y,X6)|{Cov,X1,X2,X3,X4,X5,X7}	Y ~Cov+X1+I(X1^2)+X2+I(X2^2)+X3 +X5+X7+X4+X4:X5+X4:X7+X6+I(X6^2)	lmer	||X6 = 0	0.31

Table S11. Conditional independence claims applied in the different hypotheses of the d-sep model implied by the hypothesized path models for forage quantity. Value of C statistic (*P* value) = 29.46 (0.49), df = 30. Remainder of legend as in table S4.

Link	D-sep independence claims	Formula	Model	H0	*P value*
1	(X3,X2)|{Cov}	X3 ~ Cov + X2	lmer	||X2 = 0	0.06
2	(X4,X1)|{Cov}	X4 ~ Cov + X1	lmer	||X1 = 0	0.41
3	(X4,X2)|{Cov}	X4 ~ Cov + X3	lmer	||X3 = 0	0.78
4	(X4,X3)|{Cov}	X4 ~ Cov + X3	lmer	||X3 = 0	0.93
5	(X5,X3)|{Cov,X1,X2}	X5 ~ Cov+ X1+I(X1^2)+X2+I(X2^2)+X3	lmer	||X3 = 0	0.65
6	(X6,X3)|{Cov,X1,X2,X5}	X6 ~ Cov+ X1+I(X1^2)+X2+I(X2^2)+X5+X3	lmer	||X3 = 0	0.82
7	(X5,X4)|{Cov,X1,X2}	X5 ~Cov+ X1+I(X1^2)+X2+I(X2^2)+X4	lmer	||X4 = 0	0.08
8	(X6,X4)|{Cov,X1,X2,X5}	X6 ~ Cov+ X1+I(X1^2)+X2+I(X2^2)+X5+X4	lmer	||X4 = 0	0.40
9	(X7,X4)|{Cov,X1,X2,X3}	X7 ~ Cov+ X1+I(X1^2)+X2+I(X2^2)+X3+X4	lmer	||X4 = 0	0.62
10	(X7,X5)|{Cov,X1,X2,X3}	X7 ~ Cov+ X1+I(X1^2)+X2+I(X2^2)+X3+X5	lmer	||X5 = 0	0.74
11	(X7,X6)|{Cov,X1,X2,X3}	X7 ~ Cov+ X1+I(X1^2)+X2+I(X2^2)+X3+X6	lmer	||X6 = 0	0.09
12	(Y,X1)|{Cov,X4,X5,X7}	Y ~ Cov+ X4+X5+X7+X1	lmer	||X1 = 0	0.50
13	(Y,X1)|{Cov,X4,X5,X7}	Y ~ Cov+ X4+X5+X7+X2	lmer	||X2 = 0	0.21
14	(Y,X1)|{Cov,X4,X5,X7}	Y ~ Cov+ X4+X5+X7+X3	lmer	||X3 = 0	0.40
15	(Y,X1)|{Cov,X4,X5,X7}	Y ~ Cov+ X4+X5+X7+X6	lmer	||X6 = 0	0.60

Table S12. Conditional independence claims applied in the different hypotheses of the d-sep model implied by the hypothesized path models for forage quality. Value of C statistic (*P* value) = 32.45 (0.54), df = 34. Remainder of legend as in table S4.

<table>
<tr><th>Link</th><th>D-sep independence claims</th><th>Formula</th><th>Model</th><th>H0</th><th>P value</th></tr>
<tr><td>1</td><td>(X3,X2)|{Cov}</td><td>X3 ~ Cov + X2</td><td>lmer</td><td>||X2 = 0</td><td>0.16</td></tr>
<tr><td>2</td><td>(X4,X1)|{Cov}</td><td>X4 ~ Cov + X1</td><td>lmer</td><td>||X1 = 0</td><td>0.20</td></tr>
<tr><td>3</td><td>(X4,X2)|{Cov}</td><td>X4 ~ Cov + X3</td><td>lmer</td><td>||X3 = 0</td><td>0.68</td></tr>
<tr><td>4</td><td>(X4,X3)|{Cov}</td><td>X4 ~ Cov + X3</td><td>lmer</td><td>||X3 = 0</td><td>0.79</td></tr>
<tr><td>5</td><td>(X5,X3)|{Cov,X1,X2}</td><td>X5 ~ Cov+ X1+I(X1^2)+X2+I(X2^2)+X3</td><td>lmer</td><td>||X3 = 0</td><td>0.89</td></tr>
<tr><td>6</td><td>(X6,X3)|{Cov,X1,X2,X5}</td><td>X6 ~ Cov+ X1+I(X1^2)+X2+I(X2^2)+X5+X3</td><td>lmer</td><td>||X3 = 0</td><td>0.98</td></tr>
<tr><td>7</td><td>(X5,X4)|{Cov,X1,X2}</td><td>X5 ~Cov+ X1+I(X1^2)+X2+I(X2^2)+X4</td><td>lmer</td><td>||X4 = 0</td><td>0.28</td></tr>
<tr><td>8</td><td>(X6,X4)|{Cov,X1,X2,X5}</td><td>X6 ~ Cov+ X1+I(X1^2)+X2+I(X2^2)+X5+X4</td><td>lmer</td><td>||X4 = 0</td><td>0.96</td></tr>
<tr><td>9</td><td>(X7,X4)|{Cov,X1,X2,X3}</td><td>X7 ~ Cov+ X1+I(X1^2)+X2+I(X2^2)+X3+X4</td><td>lmer</td><td>||X4 = 0</td><td>0.56</td></tr>
<tr><td>10</td><td>(X7,X5)|{Cov,X1,X2,X3}</td><td>X7 ~ Cov+ X1+I(X1^2)+X2+I(X2^2)+X3+X5</td><td>lmer</td><td>||X5 = 0</td><td>0.68</td></tr>
<tr><td>11</td><td>(X7,X6|{Cov,X1,X2,X3}</td><td>X7 ~ Cov+ X1+I(X1^2)+X2+I(X2^2)+X3+X6</td><td>lmer</td><td>||X6 = 0</td><td>0.11</td></tr>
<tr><td>12</td><td>(X8,X2)|{Cov,X1,X6}</td><td>X8 ~ Cov+ X1+X6+X2</td><td>glmer (poisson)</td><td>||X2 = 0</td><td>0.26</td></tr>
<tr><td>13</td><td>(X8,X3)|{Cov,X1,X6}</td><td>X8 ~ Cov+ X1+X6+X3</td><td>glmer (poisson)</td><td>||X3 = 0</td><td>0.59</td></tr>
<tr><td>14</td><td>(X8,X4)|{Cov,X1,X6}</td><td>X8 ~ Cov+ X1+X6+X4</td><td>glmer (poisson)</td><td>||X4 = 0</td><td>0.02</td></tr>
<tr><td>15</td><td>(X8,X5)|{Cov,X1,X6}</td><td>X8 ~ Cov+ X1+X6+X5</td><td>glmer (poisson)</td><td>||X5 = 0</td><td>0.43</td></tr>
<tr><td>16</td><td>(Y,X3)|{Cov,X1,X2,X4,X5,X7,X8}</td><td>Y ~ Cov+ X1+X2+X5+X7+X8+X4+X4:X5+X4:X8+X3</td><td>lmer</td><td>||X3 = 0</td><td>0.66</td></tr>
<tr><td>17</td><td>(Y,X6)|{Cov,X1,X2,X4,X5,X7,X8}</td><td>Y ~ Cov+ X1+X2+X5+X7+X8+X4+X4:X5+X4:X8+X3</td><td>lmer</td><td>||X6 = 0</td><td>0.52</td></tr>
</table>

Table S13. Results of the model selection procedure for regulating ecosystem services using site as a random effect (random intercept, 1|site). The best models for each ecosystem service and biodiversity proxy are shown. We indicate marginal and conditional *R*², the number of observations (n), predictor estimates, standard errors and *P* values, the number of times each predictor was selected in the set of best models (*n*), predictor importance based on sum of weights (Imp.), variance inflation factors (VIF), and the results of Moran tests for spatial autocorrelation. These tests were performed with the residuals of the models at different spatial scales (using the 10, 20, and 50 closest plots); their results show no evidence for spatial autocorrelation. The VIF values obtained were below 10 in all cases, hence multicollinearity was not problematic (*267*). pH = soil pH, and Sand = soil sand content. Results of the model selection procedure for regulating ecosystem services using grazing nested within site as a random effect (random intercept, Grazing|site) are available in table S16. Results of model preselection based on AIC are available on table S25.

	Soil carbon storage						
	R²m = 0.77				R²c = 0.94		
	n = 300						
	Moran test: n = 10, p = 0.99; n = 20, p = 0.98; n = 50, p = 0.87						
	Est.		Std Er.	*P value*	n	Imp.	VIF
Latitude	0.136	±	0.046	0.003			1.42
Longitude (cos)	0.026	±	0.042	0.547			1.20
Longitude (sin)	-0.018	±	0.046	0.699			1.33
Elevation	-0.349	±	0.048	<0.001			1.55
Slope	0.045	±	0.030	0.130			1.18
Mean annual precipitation (MAP)	0.398	±	0.055	<0.001	6	1.00	2.01
MAP²	-0.067	±	0.029	0.023	6	1.00	1.32
Mean annual temperature (MAT)	-0.448	±	0.064	<0.001	6	1.00	2.86
MAT²	-0.252	±	0.044	<0.001	6	1.00	2.49
Rainfall seasonality (RASE)	0.214	±	0.052	<0.001	6	1.00	1.96
pH	-0.099	±	0.046	0.032	6	1.00	1.95
pH²	-0.038	±	0.024	0.111	4	0.62	1.29
Sand content	-0.337	±	0.037	<0.001	6	1.00	1.35
Plant richness	0.177	±	0.037	<0.001	6	1.00	1.36
Herbivore richness	0.065	±	0.025	0.011	6	1.00	1.16
Belowground diversity							
Grazing presure (Graz)	0.011	±	0.015	0.474	6	1.00	1.11
Graz × MAP							
Graz × MAT	-0.034	±	0.015	0.024	6	1.00	1.25
Graz × RASE	-0.027	±	0.014	0.059	4	0.62	1.09
Graz × pH	-0.010	±	0.016	0.560	1	0.10	1.22
Graz × Sand content	-0.010	±	0.015	0.492	1	0.10	1.12
Graz × Plant richness							
Graz × Herbivore richness							
Graz × Belowground diversity							

	Organic matter decomposition						
	R²m = 0.75				R²c = 0.89		
	n = 242						
	Moran test: n = 10, p = 0.98; n = 20, p = 0.91; n = 50, p = 0.79						
	Est.		Std Er.	*P value*	n	Imp.	VIF
Latitude	0.082	±	0.031	0.008			1.41
Longitude (cos)	-0.008	±	0.029	0.772			1.30
Longitude (sin)	0.053	±	0.031	0.083			1.44
Elevation	-0.187	±	0.033	<0.001			1.79
Slope	0.012	±	0.022	0.584			1.24
Mean annual precipitation (MAP)	0.164	±	0.040	<0.001	4	1.00	2.97
MAP²	-0.029	±	0.022	0.181	1	0.28	1.75
Mean annual temperature (MAT)	-0.317	±	0.046	<0.001	4	1.00	3.17
MAT²	-0.160	±	0.033	<0.001	4	1.00	2.98
Rainfall seasonality (RASE)	0.132	±	0.040	<0.001	4	1.00	2.42
pH	-0.099	±	0.037	0.008	4	1.00	2.72
pH²	-0.061	±	0.023	0.008	4	1.00	1.62
Sand content	-0.179	±	0.026	<0.001	4	1.00	1.41
Plant richness	0.085	±	0.027	0.002	4	1.00	1.64
Herbivore richness							
Belowground diversity	0.062	±	0.020	0.002	4	1.00	1.28
Grazing presure (Graz)	0.031	±	0.012	0.010	4	1.00	1.05
Graz × MAP	0.010	±	0.013	0.405	1	0.16	1.12
Graz × MAT	-0.026	±	0.013	0.048	3	0.82	1.09
Graz × RASE							
Graz × pH							
Graz × Sand content							
Graz × Plant richness							
Graz × Herbivore richness							
Graz × Belowground diversity							

	Erosion control						
	R²m = 0.53				R²c = 0.91		
	n = 242						
	Moran test: n = 10, p = 0.99; n = 20, p = 0.99; n = 50, p = 0.91						
	Est.		Std Er.	*P value*	n	Imp.	VIF
Latitude	0.014	±	0.013	0.261			1.32
Longitude (cos)	0.007	±	0.012	0.547			1.22
Longitude (sin)	0.028	±	0.012	0.025			1.37
Elevation	-0.008	±	0.013	0.555			1.55
Slope	0.009	±	0.007	0.186			1.16
Mean annual precipitation (MAP)	0.055	±	0.017	<0.001	6	1.00	2.33
MAP²	-0.017	±	0.008	0.038	5	0.89	1.68
Mean annual temperature (MAT)	-0.046	±	0.018	0.013	6	1.00	2.85
MAT²	-0.039	±	0.013	0.002	6	1.00	2.64
Rainfall seasonality (RASE)	0.041	±	0.016	0.013	6	1.00	2.33
pH	-0.023	±	0.012	0.051	5	0.89	1.90
pH²	-0.011	±	0.007	0.093	3	0.53	1.31
Sand content	-0.046	±	0.009	<0.001	6	1.00	1.24
Plant richness	0.023	±	0.008	0.004	6	1.00	1.33
Herbivore richness							
Belowground diversity							
Grazing presure (Graz)	-0.009	±	0.003	0.003	6	1.00	1.07
Graz × MAP							
Graz × MAT	-0.007	±	0.003	0.040	6	1.00	1.04
Graz × RASE							
Graz × pH							
Graz × Sand content	-0.004	±	0.003	0.237	2	0.29	1.07
Graz × Plant richness							
Graz × Herbivore richness							
Graz × Belowground diversity							

	Water regulation						
	R²m = 0.63				R²c = 0.92		
	n = 317						
	Moran test: n = 10, p = 0.99; n = 20, p = 0.99; n = 50, p = 0.93						
	Est.		Std Er.	*P value*	n	Imp.	VIF
Latitude	-0.009	±	0.013	0.476			1.42
Longitude (cos)	-0.010	±	0.011	0.354			1.15
Longitude (sin)	0.013	±	0.012	0.287			1.30
Elevation	-0.038	±	0.012	0.002			1.55
Slope	0.004	±	0.007	0.542			1.13
Mean annual precipitation (MAP)	0.048	±	0.013	<0.001	15	1.00	2.00
MAP²	-0.012	±	0.008	0.118	8	0.54	1.40
Mean annual temperature (MAT)	-0.064	±	0.014	<0.001	15	1.00	2.80
MAT²	0.010	±	0.009	0.286	3	0.18	2.34
Rainfall seasonality (RASE)	0.012	±	0.012	0.327	3	0.17	2.00
pH	0.000	±	0.011	0.992	4	0.22	1.75
pH²	-0.010	±	0.005	0.074	4	0.22	1.19
Sand content	-0.114	±	0.009	<0.001	15	1.00	1.28
Plant richness	0.005	±	0.008	0.544	15	1.00	1.29
Herbivore richness							
Belowground diversity							
Grazing presure (Graz)	-0.005	±	0.003	0.141	15	1.00	1.05
Graz × MAP							
Graz × MAT	0.004	±	0.003	0.232	4	0.25	1.08
Graz × RASE							
Graz × pH							
Graz × Sand content	0.002	±	0.003	0.518	2	0.10	1.07
Graz × Plant richness	-0.011	±	0.004	0.003	15	1.00	1.02
Graz × Herbivore richness							
Graz × Belowground diversity							

Table S14. Results of the model selection procedure for supporting ecosystem services using site as a random effect (random intercept, 1|site). The best models for each ecosystem service and biodiversity proxy are shown. See table S17 for model results using grazing pressure nested within site (random slope and intercept, grazing|site). Plant biomass & stability = aboveground plant biomass and its temporal stability. Remainder of legend as in table S13.

	Plant biomass & stability							**Soil fertility**						
	$R^2m = 0.56$				$R^2c = 0.92$			$R^2m = 0.62$				$R^2c = 0.95$		
	n = 296							n = 320						
	Moran test: n = 10, p = 0.99; n = 20, p = 0.99; n = 50, p = 0.87							Moran test: n = 10, p = 0.99; n = 20, p = 0.99; n = 50, p = 0.93						
	Est.		Std Er.	*P value*	n	Imp.	VIF	Est.		Std Er.	*P value*	n	Imp.	VIF
Latitude	0.045	±	0.013	0.001			1.37	-0.014	±	0.026	0.589			1.35
Longitude (cos)	-0.014	±	0.012	0.259			1.17	0.010	±	0.024	0.672			1.12
Longitude (sin)	-0.006	±	0.014	0.642			1.32	0.008	±	0.025	0.763			1.29
Elevation	0.004	±	0.014	0.766			1.44	-0.099	±	0.026	<0.001			1.48
Slope	-0.009	±	0.007	0.216			1.18	0.003	±	0.013	0.819			1.14
Mean annual precipitation (MAP)	0.033	±	0.014	0.018	21	1.00	1.81	0.132	±	0.029	<0.001	6	1.00	1.84
MAP²							1.35	-0.033	±	0.015	0.030	6	1.00	1.47
Mean annual temperature (MAT)	0.028	±	0.019	0.133	21	1.00	2.67	-0.171	±	0.036	<0.001	6	1.00	2.69
MAT²	-0.065	±	0.013	<0.001	21	1.00	2.31	-0.071	±	0.024	0.003	6	1.00	2.25
Rainfall seasonality (RASE)	0.025	±	0.015	0.104	16	0.78	1.92	0.083	±	0.030	0.006	6	1.00	1.91
pH	-0.068	±	0.011	<0.001	21	1.00	1.70	0.043	±	0.020	0.028	6	1.00	1.57
pH²	0.014	±	0.005	0.009	21	1.00	1.22	-0.023	±	0.010	0.015	6	1.00	1.17
Sand content		±						-0.206	±	0.017	<0.001	6	1.00	1.24
Plant richness	0.020	±	0.009	0.026	21	1.00	1.25	0.015	±	0.015	0.305	6	0.15	1.23
Herbivore richness	0.013	±	0.006	0.027	20	0.97	1.21							
Belowground diversity														
Grazing presure (Graz)	-0.001	±	0.003	0.843	19	0.92	1.20	0.016	±	0.005	0.003	6	1.00	1.05
Graz × MAP	0.003		0.003	0.357	1	0.03	1.55	0.008	±	0.006	0.137	1	0.16	1.67
Graz × MAT	-0.005	±	0.003	0.120	9	0.44	1.29	-0.006	±	0.006	0.356	1	0.14	1.24
Graz × RASE	0.006	±	0.003	0.074	10	0.51	1.16	-0.004	±	0.005	0.503	1	0.11	1.11
Graz × pH	0.004	±	0.003	0.281	2	0.07	1.73	-0.011	±	0.006	0.064	4	0.68	1.82
Graz × Sand content								-0.014	±	0.006	0.014	6	1.00	1.28
Graz × Plant richness	0.006	±	0.004	0.110	11	0.53	1.20							
Graz × Herbivore richness	0.006	±	0.003	0.059	15	0.73	1.17							
Graz × Belowground diversity														

Table S15. Results of the model selection procedure for provisioning ecosystem services using site as a random effect (random intercept, 1|site). The best models for each ecosystem service and biodiversity proxy are shown. See table S18 for model results using grazing pressure nested within site (random slope and intercept, grazing|site). Remainder of legend as in table S13.

Forage quantity

$R^2m = 0.27$ $R^2c = 0.77$

n = 326

Moran test: n = 10, p = 0.99; n = 20, p = 0.99; n = 50, p = 0.91

	Est.		Std Er.	*P value*	n	Imp.	VIF
Latitude	0.033	±	0.111	0.767			1.40
Longitude (cos)	0.154	±	0.106	0.147			1.16
Longitude (sin)	0.026	±	0.107	0.811			1.30
Elevation	0.036	±	0.111	0.746			1.55
Slope	0.111	±	0.074	0.136			1.12
Mean annual precipitation (MAP)	-0.055	±	0.100	0.585	1	0.07	1.61
MAP²							
Mean annual temperature (MAT)	-0.139	±	0.130	0.285	2	0.19	2.67
MAT²	-0.130	±	0.083	0.119	1	0.10	2.27
Rainfall seasonality (RASE)	-0.086	±	0.102	0.402	1	0.09	1.92
pH	-0.047	±	0.091	0.609	1	0.07	1.82
pH²							
Sand content	0.162	±	0.088	0.067	8	0.81	1.26
Plant richness	0.486	±	0.083	<0.001	10	1.00	1.33
Herbivore richness							
Belowground diversity							
Grazing presure (Graz)	-0.254	±	0.035	<0.001	10	1.00	1.02
Graz × MAP							
Graz × MAT							
Graz × RASE							
Graz × pH							
Graz × Sand content	-0.016	±	0.036	0.662	1	0.07	1.02
Graz × Plant richness	-0.041	±	0.038	0.275	2	0.19	1.01
Graz × Herbivore richness							
Graz × Belowground diversity							

Forage quality

$R^2m = 0.23$ $R^2c = 0.89$

n = 277

Moran test: n = 10, p = 0.99; n = 20, p = 0.99; n = 50, p = 0.89

	Est.		Std Er.	*P value*	n	Imp.	VIF
Latitude	0.096	±	0.064	0.135			1.33
Longitude (cos)	-0.005	±	0.056	0.930			1.11
Longitude (sin)	0.032	±	0.063	0.612			1.32
Elevation	0.059	±	0.060	0.329			1.30
Slope	0.000	±	0.030	0.992			1.15
Mean annual precipitation (MAP)	-0.189	±	0.061	0.002	9	1.00	1.35
MAP²	0.057	±	0.035	0.107	5	0.58	1.41
Mean annual temperature (MAT)	-0.123	±	0.065	0.061	7	0.79	1.85
MAT²	-0.037	±	0.044	0.404	2	0.17	1.36
Rainfall seasonality (RASE)							
pH							
pH²							
Sand content	0.064	±	0.040	0.116	9	1.00	1.21
Plant richness	0.146	±	0.037	<0.001	9	1.00	1.20
Herbivore richness	0.012	±	0.026	0.650	9	1.00	1.17
Belowground diversity							
Grazing presure (Graz)	-0.044	±	0.014	0.002	9	1.00	1.14
Graz × MAP	-0.009	±	0.015	0.559	1	0.08	1.12
Graz × MAT							
Graz × RASE							
Graz × pH							
Graz × Sand content	-0.031	±	0.014	0.025	9	1.00	1.15
Graz × Plant richness	-0.012	±	0.015	0.423	2	0.17	1.11
Graz × Herbivore richness	-0.035	±	0.014	0.010	9	1.00	1.14
Graz × Belowground diversity							

Wood quantity

$R^2m = 0.28$ $R^2c = 0.86$

n = 326

Moran test: n = 10, p = 0.99; n = 20, p = 0.99; n = 50, p = 0.87

	Est.		Std Er.	*P value*	n	Imp.	VIF
Latitude	0.331	±	0.224	0.141			1.38
Longitude (cos)	-0.009	±	0.203	0.966			1.13
Longitude (sin)	-0.140	±	0.216	0.520			1.29
Elevation	-0.182	±	0.229	0.428			1.50
Slope	0.099	±	0.122	0.417			1.13
Mean annual precipitation (MAP)	0.797	±	0.238	0.001	12	1.00	1.86
MAP²	-0.359	±	0.135	0.008	12	1.00	1.40
Mean annual temperature (MAT)	0.240	±	0.308	0.439	12	1.00	2.63
MAT²	-0.553	±	0.211	0.009	12	1.00	2.21
Rainfall seasonality (RASE)	0.497	±	0.256	0.054	11	0.93	1.92
pH	-0.218	±	0.182	0.233	5	0.34	1.64
pH²							
Sand content	0.112	±	0.153	0.466	9	0.76	1.25
Plant richness	0.275	±	0.141	0.052	12	1.00	1.26
Herbivore richness							
Belowground diversity							
Grazing presure (Graz)	-0.106	±	0.053	0.045	12	1.00	1.02
Graz × MAP	0.067	±	0.059	0.259	4	0.26	1.17
Graz × MAT							
Graz × RASE	0.084	±	0.056	0.134	6	0.49	1.09
Graz × pH							
Graz × Sand content	0.124	±	0.054	0.023	9	0.76	1.07
Graz × Plant richness	0.196	±	0.059	<0.001	12	1.00	1.16
Graz × Herbivore richness							
Graz × Belowground diversity							

Table S16. Results of the model selection procedure for regulating ecosystem services using grazing pressure nested within site (random slope and intercept, grazing|site). The best models for each ecosystem service and biodiversity proxy are shown. Results of model preselection based on AIC are available on table S26. Remainder of legend as in table S13.

	Soil carbon storage						
	R^2m = 0.77			R^2c = 0.94			
	n = 300						
	Moran test: n = 10, p = 0.99; n = 20, p = 0.98; n = 50, p = 0.87						
	Est.		Std Er.	*P value*	n	Imp.	VIF
Latitude	0.134	±	0.046	0.004			1.42
Longitude (cos)	0.024	±	0.042	0.572			1.20
Longitude (sin)	-0.027	±	0.046	0.556			1.33
Elevation	-0.348	±	0.048	<0.001			1.54
Slope	0.045	±	0.030	0.133			1.17
Mean annual precipitation (MAP)	0.396	±	0.055	<0.001	9	1.00	2.06
MAP²	-0.071	±	0.029	0.015	9	1.00	1.35
Mean annual temperature (MAT)	-0.448	±	0.063	<0.001	9	1.00	2.90
MAT²	-0.251	±	0.044	<0.001	9	1.00	2.50
Rainfall seasonality (RASE)	0.216	±	0.052	<0.001	9	1.00	1.98
pH	-0.100	±	0.046	0.029	9	1.00	1.95
pH²	-0.039	±	0.024	0.101	6	0.64	1.30
Sand content	-0.337	±	0.038	<0.001	9	1.00	1.35
Plant richness	0.176	±	0.037	<0.001	9	1.00	1.37
Herbivore richness	0.059	±	0.026	0.022	9	1.00	1.14
Belowground diversity							
Grazing presure (Graz)	0.011	±	0.016	0.479	9	1.00	1.10
Graz × MAP							
Graz × MAT	-0.033	±	0.016	0.043	7	0.84	1.26
Graz × RASE	-0.029	±	0.016	0.068	7	0.77	1.10
Graz × pH	-0.014	±	0.017	0.434	1	0.08	1.19
Graz × Sand content	-0.017	±	0.017	0.313	3	0.23	1.14
Graz × Plant richness							
Graz × Herbivore richness							
Graz × Belowground diversity							

	Organic matter decomposition						
	R^2m = 0.75			R^2c = 0.89			
	n = 242						
	Moran test: n = 10, p = 0.97; n = 20, p = 0.90; n = 50, p = 0.82						
	Est.		Std Er.	*P value*	n	Imp.	VIF
Latitude	0.083	±	0.030	0.007			1.40
Longitude (cos)	-0.010	±	0.029	0.737			1.30
Longitude (sin)	0.054	±	0.030	0.079			1.45
Elevation	0.015	±	0.021	0.473			1.83
Slope	-0.183	±	0.033	<0.001			1.25
Mean annual precipitation (MAP)	0.167	±	0.042	<0.001	4	1.00	2.95
MAP²	-0.031	±	0.021	0.150	2	0.45	1.72
Mean annual temperature (MAT)	-0.311	±	0.046	<0.001	4	1.00	3.15
MAT²	-0.155	±	0.033	<0.001	4	1.00	2.97
Rainfall seasonality (RASE)	0.126	±	0.040	0.002	4	1.00	2.40
pH	-0.098	±	0.037	0.009	4	1.00	2.70
pH²	-0.056	±	0.023	0.015	4	1.00	1.56
Sand content	-0.183	±	0.026	<0.001	4	1.00	1.42
Plant richness	0.086	±	0.027	0.001	4	1.00	1.66
Herbivore richness							
Belowground diversity	0.058	±	0.020	0.003	4	1.00	1.25
Grazing presure (Graz)	0.032	±	0.012	0.008	4	1.00	1.04
Graz × MAP							
Graz × MAT	-0.027	±	0.013	0.048	2	0.68	1.04
Graz × RASE							
Graz × pH							
Graz × Sand content							
Graz × Plant richness							
Graz × Herbivore richness							
Graz × Belowground diversity							

	Erosion control						
	R^2m = 0.53			R^2c = 0.91			
	n = 242						
	Moran test: n = 10, p = 0.99; n = 20, p = 0.99; n = 50, p = 0.91						
	Est.		Std Er.	*P value*	n	Imp.	VIF
Latitude	0.016	±	0.012	0.202			1.35
Longitude (cos)	0.009	±	0.011	0.440			1.22
Longitude (sin)	0.032	±	0.012	0.008			1.37
Elevation	0.010	±	0.007	0.141			1.55
Slope	-0.009	±	0.012	0.474			1.15
Mean annual precipitation (MAP)	0.054	±	0.016	0.001	14	1.00	2.33
MAP²	-0.015	±	0.008	0.055	14	1.00	1.70
Mean annual temperature (MAT)	-0.049	±	0.018	0.007	14	1.00	2.94
MAT²	-0.040	±	0.012	0.001	14	1.00	2.67
Rainfall seasonality (RASE)	0.041	±	0.016	0.011	14	1.00	2.35
pH	-0.022	±	0.011	0.051	14	1.00	1.91
pH²	-0.011	±	0.007	0.087	7	0.54	1.34
Sand content	-0.044	±	0.009	<0.001	14	1.00	1.28
Plant richness	0.024	±	0.008	0.003	14	1.00	1.34
Herbivore richness							
Belowground diversity							
Grazing presure (Graz)	-0.009	±	0.003	0.005	14	1.00	1.06
Graz × MAP							
Graz × MAT	-0.006	±	0.004	0.080	8	0.62	1.12
Graz × RASE							
Graz × pH							
Graz × Sand content	-0.005	±	0.003	0.128	8	0.53	1.08
Graz × Plant richness							
Graz × Herbivore richness							
Graz × Belowground diversity							

	Water regulation						
	R^2m = 0.63			R^2c = 0.92			
	n = 317						
	Moran test: n = 10, p = 0.99; n = 20, p = 0.99; n = 50, p = 0.91						
	Est.		Std Er.	*P value*	n	Imp.	VIF
Latitude	-0.008	±	0.012	0.538			1.45
Longitude (cos)	-0.011	±	0.011	0.327			1.17
Longitude (sin)	0.012	±	0.012	0.311			1.31
Elevation	0.003	±	0.007	0.697			1.64
Slope	-0.038	±	0.012	0.002			1.15
Mean annual precipitation (MAP)	0.049	±	0.013	<0.001	15	1.00	2.08
MAP²	-0.013	±	0.007	0.093	9	0.62	1.35
Mean annual temperature (MAT)	-0.062	±	0.014	<0.001	5	0.29	2.89
MAT²	0.012	±	0.010	0.205	15	1.00	2.41
Rainfall seasonality (RASE)	0.013	±	0.012	0.277	3	0.17	1.97
pH	0.002	±	0.011	0.888	6	0.34	1.90
pH²	-0.011	±	0.006	0.050	6	0.34	1.20
Sand content	-0.113	±	0.009	<0.001	15	1.00	1.35
Plant richness	0.006	±	0.008	0.477	15	1.00	1.36
Herbivore richness							
Belowground diversity							
Grazing presure (Graz)	-0.004	±	0.003	0.178	15	1.00	1.04
Graz × MAP							
Graz × MAT	0.004	±	0.003	0.263	3	0.18	1.11
Graz × RASE							
Graz × pH							
Graz × Sand content	0.002	±	0.003	0.606	1	0.04	1.13
Graz × Plant richness	-0.011	±	0.004	0.003	15	1.00	1.05
Graz × Herbivore richness							
Graz × Belowground diversity							

Table S17. Results of the model selection procedure for supporting ecosystem services using grazing pressure nested within site (random slope and intercept, grazing|site). The best models for each ecosystem service and biodiversity proxy are shown. Results of model preselection based on AIC are available on table S26. Plant biomass & stability = aboveground plant biomass and its temporal stability. Remainder of legend as in table S13.

	Plant biomass & stability							**Soil fertility**						
	$R^2m = 0.55$			$R^2c = 0.94$				$R^2m = 0.62$			$R^2c = 0.95$			
	n = 296							n = 320						
	Moran test: n = 10, p = 0.99; n = 20, p = 0.99; n = 50, p = 0.88							Moran test: n = 10, p = 0.99; n = 20, p = 0.99; n = 50, p = 0.92						
	Est.		Std Er.	*P value*	n	Imp.	VIF	Est.		Std Er.	*P value*	n	Imp.	VIF
Latitude	0.042	±	0.014	0.002			1.36	-0.018	±	0.026	0.499			1.39
Longitude (cos)	-0.015	±	0.013	0.238			1.17	0.015	±	0.023	0.506			1.09
Longitude (sin)	-0.006	±	0.014	0.668			1.32	-0.002	±	0.025	0.942			1.29
Elevation	0.006	±	0.014	0.691			1.45	-0.106	±	0.025	<0.001			1.43
Slope	-0.009	±	0.007	0.219			1.19	0.003	±	0.013	0.834			1.14
Mean annual precipitation (MAP)	0.035	±	0.014	0.012	13	1.00	1.86	0.133	±	0.028	<0.001	3	1.00	1.92
MAP^2	-0.006	±	0.008	0.433	1	0.06	1.42	-0.036	±	0.015	0.016	3	1.00	1.42
Mean annual temperature (MAT)	0.029	±	0.019	0.133	13	1.00	2.67	-0.179	±	0.036	<0.001	3	1.00	2.86
MAT^2	-0.063	±	0.013	<0.001	13	1.00	2.29	-0.075	±	0.024	0.002	3	1.00	2.33
Rainfall seasonality (RASE)	0.027	±	0.015	0.079	9	0.71	1.92	0.087	±	0.030	0.004	3	1.00	1.96
pH	-0.065	±	0.011	<0.001	13	1.00	1.66	0.043	±	0.020	0.030	3	1.00	1.72
pH^2	0.012	±	0.005	0.022	13	1.00	1.23	-0.023	±	0.010	0.020	3	1.00	1.19
Sand content								-0.195	±	0.017	<0.001	3	1.00	1.29
Plant richness	0.019	±	0.009	0.030	13	1.00	1.24							
Herbivore richness	0.012	±	0.006	0.028	11	0.87	1.16							
Belowground diversity														
Grazing presure (Graz)	-0.001	±	0.004	0.859	11	0.82	1.15	0.018	±	0.006	0.004	3	1.00	1.03
Graz × MAP														
Graz × MAT	-0.005	±	0.004	0.160	3	0.24	1.27	-0.007	±	0.007	0.339	1	0.23	1.27
Graz × RASE	0.004	±	0.004	0.260	3	0.18	1.16	-0.007	±	0.006	0.236	1	0.30	1.12
Graz × pH	0.003	±	0.004	0.356	1	0.06	1.72	-0.016	±	0.007	0.015	3	1.00	1.21
Graz × Sand content								-0.020	±	0.006	0.001	3	1.00	1.12
Graz × Plant richness	0.004	±	0.004	0.253	3	0.18	1.20							
Graz × Herbivore richness	0.007	±	0.003	0.030	11	0.82	1.12							
Graz × Belowground diversity														

Table S18. Results of the model selection procedure for provisioning ecosystem services using grazing pressure nested within site (random slope and intercept, grazing|site). The best models for each ecosystem service and biodiversity proxy are shown. Results of model preselection based on AIC are available on table S26. Remainder of legend as in table S13.

Forage quantity — R²m = 0.27; R²c = 0.83; n = 326; Moran test: n = 10, p = 0.99; n = 20, p = 0.99; n = 50, p = 0.90

	Est.		Std Er.	*P value*	n	Imp.	VIF
Latitude	0.035	±	0.112	0.756			1.40
Longitude (cos)	0.177	±	0.105	0.093			1.16
Longitude (sin)	0.064	±	0.113	0.574			1.30
Elevation	-0.007	±	0.115	0.951			1.53
Slope	0.160	±	0.074	0.031			1.12
Mean annual precipitation (MAP)	-0.060	±	0.099	0.545	1	0.07	1.62
MAP²							
Mean annual temperature (MAT)	-0.197	±	0.132	0.139	5	0.45	2.74
MAT²	-0.149	±	0.083	0.073	4	0.35	2.27
Rainfall seasonality (RASE)	-0.098	±	0.102	0.340	1	0.09	1.95
pH	-0.084	±	0.096	0.380	2	0.16	1.81
pH²							
Sand content	0.192	±	0.091	0.035	10	0.92	1.26
Plant richness	0.468	±	0.083	<0.001	11	1.00	1.36
Herbivore richness							
Belowground diversity							
Grazing presure (Graz)	-0.262	±	0.042	<0.001	11	1.00	1.01
Graz × MAP							
Graz × MAT	0.038	±	0.044	0.386	1	0.07	1.09
Graz × RASE							
Graz × pH							
Graz × Sand content							
Graz × Plant richness	-0.036	±	0.043	0.407	2	0.14	1.07
Graz × Herbivore richness							
Graz × Belowground diversity							

Forage quality — R²m = 0.23; R²c = 0.91; n = 277; Moran test: n = 10, p = 0.99; n = 20, p = 0.99; n = 50, p = 0.91

	Est.		Std Er.	*P value*	n	Imp.	VIF
Latitude	0.096	±	0.064	0.135			1.33
Longitude (cos)	0.000	±	0.057	0.996			1.11
Longitude (sin)	0.023	±	0.063	0.718			1.31
Elevation	0.067	±	0.060	0.265			1.34
Slope	0.000	±	0.031	0.993			1.14
Mean annual precipitation (MAP)	-0.198	±	0.062	0.002	15	1.00	1.39
MAP²	0.060	±	0.035	0.087	11	0.72	1.46
Mean annual temperature (MAT)	-0.121	±	0.065	0.063	11	0.77	1.88
MAT²	-0.041	±	0.044	0.352	1	0.06	1.36
Rainfall seasonality (RASE)							
pH							
pH²							
Sand content	0.069	±	0.042	0.101	13	0.86	1.23
Plant richness	0.143	±	0.038	<0.001	15	1.00	1.21
Herbivore richness	0.017	±	0.027	0.522	12	0.83	1.14
Belowground diversity							
Grazing presure (Graz)	-0.040	±	0.016	0.015	15	1.00	1.11
Graz × MAP							
Graz × MAT	0.010	±	0.016	0.553	1	0.04	1.19
Graz × RASE							
Graz × pH							
Graz × Sand content	-0.030	±	0.016	0.063	10	0.67	1.14
Graz × Plant richness	-0.018	±	0.017	0.317	2	0.10	1.15
Graz × Herbivore richness	-0.036	±	0.015	0.018	12	0.83	1.11
Graz × Belowground diversity							

Wood quantity — R²m = 0.28; R²c = 0.86; n = 326; Moran test: n = 10, p = 0.99; n = 20, p = 0.99; n = 50, p = 0.88

	Est.		Std Er.	*P value*	n	Imp.	VIF
Latitude	0.343	±	0.224	0.128			1.38
Longitude (cos)	-0.010	±	0.203	0.961			1.13
Longitude (sin)	-0.138	±	0.216	0.526			1.29
Elevation	-0.193	±	0.229	0.402			1.50
Slope	0.097	±	0.121	0.425			1.13
Mean annual precipitation (MAP)	0.796	±	0.235	0.001	11	1.00	1.86
MAP²	-0.359	±	0.135	0.008	11	1.00	1.40
Mean annual temperature (MAT)	0.253	±	0.310	0.416	11	1.00	2.64
MAT²	-0.547	±	0.211	0.010	11	1.00	2.21
Rainfall seasonality (RASE)	0.493	±	0.257	0.056	11	1.00	1.92
pH	-0.213	±	0.182	0.243	4	0.29	1.64
pH²							
Sand content	0.118	±	0.153	0.443	8	0.75	1.26
Plant richness	0.283	±	0.141	0.046	11	1.00	1.26
Herbivore richness							
Belowground diversity							
Grazing presure (Graz)	-0.105	±	0.053	0.046	11	1.00	1.02
Graz × MAP	0.066	±	0.059	0.260	3	0.22	1.17
Graz × MAT							
Graz × RASE	0.085	±	0.056	0.129	5	0.46	1.09
Graz × pH							
Graz × Sand content	0.124	±	0.054	0.022	8	0.75	1.07
Graz × Plant richness	0.197	±	0.059	0.001	11	1.00	1.16
Graz × Herbivore richness							
Graz × Belowground diversity							

Table S19. Results of the model selection procedure for regulating ecosystem services using dung mass as a proxy of grazing pressure. Results of model preselection based on AIC are available on table S27. Remainder of legend as in table S13.

	Soil carbon storage							**Organic matter decomposition**						
	$R^2m = 0.79$			$R^2c = 0.94$				$R^2m = 0.79$			$R^2c = 0.92$			
	n = 265							n = 183						
	Moran test: n = 10, p = 0.99; n = 20, p = 0.97; n = 50, p = 0.78							Moran test: n = 10, p = 0.97; n = 20, p = 0.93; n = 50, p = 0.72						
	Est.		Std Er.	*P value*	n	Imp.	VIF	Est.		Std Er.	*P value*	n	Imp.	VIF
Latitude	0.148	±	0.048	0.002			1.59	0.095	±	0.036	0.008			1.47
Longitude (cos)	0.024	±	0.042	0.568			1.24	0.015	±	0.034	0.668			1.47
Longitude (sin)	-0.035	±	0.045	0.439			1.26	0.007	±	0.036	0.854			1.40
Elevation	-0.331	±	0.047	<0.001			1.53	-0.158	±	0.037	<0.001			1.77
Slope	0.022	±	0.031	0.472			1.19	-0.009	±	0.024	0.703			1.25
Mean annual precipitation (MAP)	0.393	±	0.055	<0.001	11	1.00	2.09	0.175	±	0.044	<0.001	9	1.00	3.07
MAP^2	-0.059	±	0.029	0.041	10	0.93	1.37	-0.028	±	0.024	0.238	2	0.18	1.78
Mean annual temperature (MAT)	-0.392	±	0.070	<0.001	11	1.00	3.56	-0.283	±	0.063	<0.001	9	1.00	4.21
MAT^2	-0.222	±	0.049	<0.001	11	1.00	3.08	-0.142	±	0.046	0.002	9	1.00	4.10
Rainfall seasonality (RASE)	0.228	±	0.050	<0.001	11	1.00	1.83	0.119	±	0.046	0.010	9	1.00	2.45
pH	-0.106	±	0.044	0.017	11	1.00	1.86	-0.080	±	0.040	0.046	9	1.00	2.36
pH^2	-0.020	±	0.025	0.410	3	0.19	1.18	-0.048	±	0.025	0.053	7	0.83	1.25
Sand content	-0.371	±	0.038	<0.001	11	1.00	1.37	-0.203	±	0.029	<0.001	9	1.00	1.36
Plant richness	0.187	±	0.038	<0.001	11	1.00	1.48	0.061	±	0.032	0.059	7	0.81	1.78
Herbivore richness	0.060	±	0.025	0.015	11	1.00	1.10							
Belowground diversity								0.079	±	0.024	0.001	9	1.00	1.34
Grazing presure (Graz)	-0.003	±	0.015	0.861	9	0.82	1.07	0.010	±	0.012	0.415	4	0.44	1.05
Graz × MAP	0.025	±	0.016	0.119	5	0.45	1.97							
Graz × MAT	-0.032	±	0.015	0.033	9	0.82	1.25	-0.025	±	0.013	0.052	3	0.35	1.03
Graz × RASE	-0.015	±	0.015	0.326	2	0.16	1.13							
Graz × pH	0.017	±	0.019	0.376	1	0.07	1.18							
Graz × Sand content	-0.013	±	0.016	0.420	1	0.07	1.24							
Graz × Plant richness	-0.037	±	0.016	0.020	9	0.82	1.24	-0.020	±	0.012	0.105	2	0.21	1.07
Graz × Herbivore richness														
Graz × Belowground diversity														

	Erosion control							**Water regulation**						
	$R^2m = 0.54$			$R^2c = 0.91$				$R^2m = 0.70$			$R^2c = 0.92$			
	n = 265							n = 253						
	Moran test: n = 10, p = 0.99; n = 20, p = 0.99; n = 50, p = 0.91							Moran test: n = 10, p = 0.99; n = 20, p = 0.98; n = 50, p = 0.87						
	Est.		Std Er.	*P value*	n	Imp.	VIF	Est.		Std Er.	*P value*	n	Imp.	VIF
Latitude	0.010	±	0.013	0.422			1.55	-0.010	±	0.013	0.451			1.60
Longitude (cos)	0.007	±	0.011	0.534			1.21	-0.020	±	0.011	0.063			1.16
Longitude (sin)	0.025	±	0.012	0.037			1.25	0.000	±	0.012	0.969			1.20
Elevation	-0.009	±	0.012	0.465			1.45	-0.039	±	0.012	0.001			1.37
Slope	0.007	±	0.007	0.313			1.19	0.007	±	0.008	0.378			1.16
Mean annual precipitation (MAP)	0.051	±	0.013	<0.001	12	1.00	1.87	0.039	±	0.012	0.002	13	1.00	2.05
MAP^2	-0.017	±	0.007	0.018	12	1.00	1.45	-0.006	±	0.007	0.379	1	0.07	1.36
Mean annual temperature (MAT)	-0.042	±	0.020	0.041	11	0.91	3.44	-0.064	±	0.013	<0.001	13	1.00	1.79
MAT^2	-0.025	±	0.012	0.040	8	0.71	2.89							
Rainfall seasonality (RASE)	0.024	±	0.013	0.065	9	0.77	1.79	0.008	±	0.011	0.456	3	0.19	1.28
pH	-0.020	±	0.009	0.036	12	1.00	1.57	-0.014	±	0.011	0.219	3	0.25	1.73
pH^2								-0.007	±	0.006	0.221	1	0.08	1.14
Sand content	-0.049	±	0.008	<0.001	12	1.00	1.30	-0.118	±	0.010	<0.001	13	1.00	1.38
Plant richness	0.022	±	0.008	0.006	12	1.00	1.36	0.010	±	0.009	0.301	13	1.00	1.34
Herbivore richness														
Belowground diversity														
Grazing presure (Graz)	-0.007	±	0.003	0.021	12	1.00	1.07	0.000	±	0.004	0.970	13	1.00	1.09
Graz × MAP	0.003	±	0.003	0.385	2	0.13	1.97	-0.005	±	0.004	0.214	3	0.21	1.25
Graz × MAT	0.004	±	0.003	0.229	3	0.24	1.37	-0.007	±	0.004	0.065	9	0.72	1.34
Graz × RASE	-0.004	±	0.003	0.121	5	0.41	1.17	0.006	±	0.004	0.085	2	0.12	1.18
Graz × pH	-0.002	±	0.003	0.543	1	0.05	1.98							
Graz × Sand content	-0.008	±	0.003	0.013	12	1.00	1.49	0.007	±	0.004	0.064	8	0.67	1.35
Graz × Plant richness	-0.002	±	0.003	0.486	1	0.05	1.21	-0.011	±	0.004	0.006	13	1.00	1.19
Graz × Herbivore richness														
Graz × Belowground diversity														

Table S20. Results of the model selection procedure for supporting ecosystem services using dung mass as a proxy of grazing pressure. Results of model preselection based on AIC are available on table S27. Remainder of legend as in table S13.

	Aboveground plant biomass and its temporal stability							**Soil fertility**						
	R^2m = 0.56			R^2c = 0.93				R^2m = 0.65			R^2c = 0.96			
	n = 260							n = 257						
	Moran test: n = 10, p = 0.99; n = 20, p = 0.99; n = 50, p = 0.88							Moran test: n = 10, p = 0.99; n = 20, p = 0.99; n = 50, p = 0.99						
	Est.		Std Er.	*P value*	n	Imp.	VIF	Est.		Std Er.	*P value*	n	Imp.	VIF
Latitude	0.037	±	0.016	0.024			1.52	-0.016	±	0.030	0.591			1.53
Longitude (cos)	-0.019	±	0.014	0.168			1.17	0.010	±	0.026	0.701			1.19
Longitude (sin)	-0.017	±	0.015	0.256			1.23	-0.009	±	0.028	0.761			1.24
Elevation	0.019	±	0.014	0.188			1.35	-0.104	±	0.028	<0.001			1.42
Slope	-0.006	±	0.008	0.419			1.16	0.024	±	0.014	0.093			1.17
Mean annual precipitation (MAP)	0.046	±	0.016	0.005	7	1.00	1.84	0.086	±	0.027	0.001	7	1.00	1.81
MAP^2	-0.012	±	0.009	0.149	3	0.43	1.48	-0.014	±	0.016	0.365	2	0.21	1.59
Mean annual temperature (MAT)	0.054	±	0.022	0.015	7	1.00	3.42	-0.189	±	0.044	<0.001	7	1.00	3.38
MAT^2	-0.038	±	0.015	0.009	7	1.00	2.74	-0.090	±	0.029	0.002	7	1.00	2.78
Rainfall seasonality (RASE)	0.020	±	0.016	0.230	2	0.30	1.71	0.091	±	0.031	0.003	7	1.00	1.74
pH	-0.059	±	0.012	<0.001	7	1.00	1.59	0.019	±	0.020	0.347	2	0.22	1.41
pH^2	0.013	±	0.005	0.014	7	1.00	1.11							
Sand content	0.006	±	0.010	0.526	2	0.18	1.22	-0.232	±	0.018	<0.001	7	1.00	1.25
Plant richness								0.036	±	0.017	0.033	7	1.00	1.22
Herbivore richness														
Belowground diversity														
Grazing presure (Graz)	-0.002	±	0.003	0.605	1	0.09	1.04	0.013	±	0.006	0.026	7	1.00	1.07
Graz × MAP								0.018	±	0.006	0.002	7	1.00	1.22
Graz × MAT								0.005	±	0.006	0.401	1	0.11	1.32
Graz × RASE														
Graz × pH														
Graz × Sand content								-0.010	±	0.006	0.088	4	0.61	1.29
Graz × Plant richness								-0.019	±	0.006	0.001	7	1.00	1.14
Graz × Herbivore richness														
Graz × Belowground diversity														

Table S21. Results of the model selection procedure for provisioning ecosystem services using dung mass as a proxy of grazing pressure. Results of model preselection based on AIC are available on table S27. Remainder of legend as in table S13.

	Forage quantity							Forage quality							Wood quantity						
	R^2m = 0.26				R^2c = 0.76			R^2m = 0.20				R^2c = 0.88			R^2m = 0.32				R^2c = 0.86		
	n = 258							n = 245							n = 265						
	Moran test: n = 10, p = 0.99; n = 20, p = 0.99; n = 50, p = 0.90							Moran test: n = 10, p = 0.99; n = 20, p = 0.99; n = 50, p = 0.86							Moran test: n = 10, p = 0.99; n = 20, p = 0.98; n = 50, p = 0.83						
	Est.		Std Er.	*P value*	n	Imp.	VIF	Est.		Std Er.	*P value*	n	Imp.	VIF	Est.		Std Er.	*P value*	n	Imp.	VIF
Latitude	0.049	±	0.119	0.683			1.17	0.135	±	0.064	0.037			1.51	0.084	±	0.267	0.753			1.55
Longitude (cos)	0.144	±	0.116	0.216			1.18	-0.028	±	0.061	0.652			1.08	0.036	±	0.231	0.878			1.21
Longitude (sin)	0.164	±	0.121	0.175			1.10	0.009	±	0.064	0.890			1.21	-0.162	±	0.250	0.520			1.25
Elevation	-0.044	±	0.122	0.718			1.30	0.082	±	0.063	0.195			1.24	-0.069	±	0.250	0.782			1.44
Slope	0.143	±	0.088	0.104			1.14	0.009	±	0.036	0.806			1.14	0.048	±	0.141	0.735			1.13
Mean annual precipitation (MAP)	-0.107	±	0.140	0.447	11	0.92	1.85	-0.204	±	0.065	0.002	14	1.00	1.39	0.870	±	0.279	0.002	7	1.00	1.87
MAP^2	-0.114	±	0.079	0.152	4	0.28	1.29	0.066	±	0.038	0.084	9	0.67	1.44	-0.274	±	0.147	0.064	5	0.76	1.43
Mean annual temperature (MAT)								-0.061	±	0.074	0.414	2	0.11	1.69	-0.074	±	0.389	0.850	7	1.00	3.43
MAT^2									±						-0.778	±	0.267	0.004	7	1.00	2.87
Rainfall seasonality (RASE)								0.037	±	0.060	0.546	1	0.05	1.24	0.656	±	0.275	0.018	7	1.00	1.77
pH	-0.194	±	0.123	0.116	2	0.81	1.80								-0.272	±	0.200	0.176	3	0.40	1.55
pH^2	0.117	±	0.067	0.081	1	0.33	1.13														
Sand content	0.176	±	0.102	0.087	11	0.02	1.31	0.049	±	0.047	0.299	4	0.22	1.26	0.117	±	0.175	0.507	1	0.10	1.27
Plant richness	0.518	±	0.100	<0.001	16	1.00	1.29	0.169	±	0.042	<0.001	14	1.00	1.20	0.460	±	0.171	0.007	7	1.00	1.29
Herbivore richness	-0.163	±	0.071	0.022	16	1.00	1.10	-0.031	±	0.030	0.314	14	1.00	1.14							
Belowground diversity																					
Grazing presure (Graz)	-0.102	±	0.042	0.015	16	1.00	1.07	-0.015	±	0.016	0.346	14	1.00	1.07	-0.063	±	0.060	0.296	2	0.24	1.04
Graz × MAP	0.062	±	0.041	0.134	4	0.44	1.09	0.025	±	0.016	0.118	7	0.51	1.05							
Graz × MAT																					
Graz × RASE																					
Graz × pH		±			11	0.33	1.75														
Graz × Sand content																					
Graz × Plant richness	0.035	±	0.043	0.416	1	0.02	1.12	0.020	±	0.016	0.219	3	0.22	1.13							
Graz × Herbivore richness	-0.070	±	0.043	0.108	10	0.52	1.11	-0.047	±	0.017	0.005	14	1.00	1.16							
Graz × Belowground diversity																					

Table S22. Results of the model selection procedure for regulating ecosystem services using livestock tracks as a proxy of grazing pressure. Results of model preselection based on AIC are available on table S28. Remainder of legend as in table S13.

	Soil carbon storage						
	$R^2m = 0.83$			$R^2c = 0.96$			
	n = 202						
	Moran test: n = 10, p = 0.99; n = 20, p = 0.98; n = 50, p = 0.87						
	Est.		Std Er.	*P value*	n	Imp.	VIF
Latitude	0.165	±	0.053	0.002			1.78
Longitude (cos)	0.005	±	0.042	0.911			1.20
Longitude (sin)	-0.061	±	0.053	0.252			1.55
Elevation	-0.290	±	0.054	<0.001			1.82
Slope	0.040	±	0.029	0.171			1.19
Mean annual precipitation (MAP)	0.414	±	0.060	<0.001	3	1.00	2.17
MAP²	-0.039	±	0.032	0.227	1	0.29	1.38
Mean annual temperature (MAT)	-0.310	±	0.079	<0.001	3	1.00	3.00
MAT²	-0.234	±	0.062	<0.001	3	1.00	2.17
Rainfall seasonality (RASE)	0.096	±	0.056	0.086	3	1.00	1.75
pH	-0.084	±	0.045	0.066	3	1.00	1.81
pH²	-0.043	±	0.022	0.052	2	0.77	1.21
Sand content	-0.364	±	0.039	<0.001	3	1.00	1.41
Plant richness	0.096	±	0.038	0.012	3	1.00	1.46
Herbivore richness	0.076	±	0.023	0.001	3	1.00	1.10
Belowground diversity							
Grazing presure (Graz)	-0.026	±	0.014	0.060	3	1.00	1.11
Graz × MAP							
Graz × MAT							
Graz × RASE	-0.034	±	0.015	0.020	3	1.00	1.16
Graz × pH							
Graz × Sand content							
Graz × Plant richness	-0.034		0.015	0.023	3	1.00	1.14
Graz × Herbivore richness							
Graz × Belowground diversity							

	Organic matter decomposition						
	$R^2m = 0.77$			$R^2c = 0.90$			
	n = 154						
	Moran test: n = 10, p = 0.97; n = 20, p = 0.92; n = 50, p = 0.81						
	Est.		Std Er.	*P value*	n	Imp.	VIF
Latitude	0.108	±	0.046	0.020			1.96
Longitude (cos)	-0.002	±	0.031	0.936			1.35
Longitude (sin)	-0.035	±	0.045	0.431			1.87
Elevation	-0.098	±	0.041	0.016			2.63
Slope	0.004	±	0.025	0.873			1.34
Mean annual precipitation (MAP)	0.120	±	0.050	0.017	7	1.00	4.03
MAP²	-0.029	±	0.025	0.251	2	0.22	2.09
Mean annual temperature (MAT)	-0.168	±	0.070	0.016	5	0.72	4.12
MAT²	-0.150	±	0.054	0.006	5	0.72	3.07
Rainfall seasonality (RASE)	0.118	±	0.054	0.030	6	0.81	2.31
pH	-0.103	±	0.045	0.023	7	1.00	2.75
pH²	-0.063	±	0.031	0.042	5	0.77	1.52
Sand content	-0.221	±	0.029	<0.001	7	1.00	1.40
Plant richness	0.036	±	0.035	0.314	1	0.12	2.40
Herbivore richness							
Belowground diversity	0.074	±	0.025	0.004	7	1.00	1.57
Grazing presure (Graz)							
Graz × MAP							
Graz × MAT							
Graz × RASE							
Graz × pH							
Graz × Sand content							
Graz × Plant richness							
Graz × Herbivore richness							
Graz × Belowground diversity							

	Erosion control						
	$R^2m = 0.42$			$R^2c = 0.92$			
	n = 150						
	Moran test: n = 10, p = 0.99; n = 20, p = 0.96; n = 50, p = 0.86						
	Est.		Std Er.	*P value*	n	Imp.	VIF
Latitude	0.029	±	0.016	0.069			1.23
Longitude (cos)	-0.001	±	0.014	0.948			1.24
Longitude (sin)	-0.005	±	0.018	0.783			1.32
Elevation	0.019	±	0.018	0.284			1.62
Slope	0.011	±	0.008	0.160			1.18
Mean annual precipitation (MAP)	0.035	±	0.018	0.056	16	0.75	2.37
MAP²	-0.010	±	0.011	0.353	2	0.06	1.63
Mean annual temperature (MAT)							
MAT²							
Rainfall seasonality (RASE)							
pH	-0.033	±	0.016	0.040	21	0.96	1.85
pH²	-0.013	±	0.008	0.110	10	0.47	1.14
Sand content	-0.035	±	0.010	0.001	22	1.00	1.18
Plant richness	0.023	±	0.011	0.035	19	0.87	1.50
Herbivore richness							
Belowground diversity	0.004	±	0.007	0.540	8	0.38	
Grazing presure (Graz)	-0.009	±	0.003	0.007	22	1.00	1.12
Graz × MAP	0.004	±	0.004	0.224	3	0.10	2.39
Graz × MAT							
Graz × RASE							
Graz × pH	-0.007	±	0.004	0.031	12	0.58	2.35
Graz × Sand content							
Graz × Plant richness							
Graz × Herbivore richness							
Graz × Belowground diversity	-0.008	±	0.004	0.031	7	0.35	1.22

	Water regulation						
	$R^2m = 0.67$			$R^2c = 0.91$			
	n = 206						
	Moran test: n = 10, p = 0.99; n = 20, p = 0.98; n = 50, p = 0.83						
	Est.		Std Er.	*P value*	n	Imp.	VIF
Latitude	-0.006	±	0.015	0.668			1.69
Longitude (cos)	-0.014	±	0.012	0.232			1.05
Longitude (sin)	-0.029	±	0.014	0.049			1.32
Elevation	-0.024	±	0.013	0.066			1.23
Slope	0.007	±	0.009	0.425			1.14
Mean annual precipitation (MAP)	0.046	±	0.017	0.006	3	1.00	2.08
MAP²	-0.018	±	0.009	0.038	3	1.00	1.33
Mean annual temperature (MAT)	-0.065	±	0.018	<0.001	3	1.00	1.84
MAT²							
Rainfall seasonality (RASE)							
pH	0.000	±	0.013	0.970	3	1.00	1.80
pH²	-0.008	±	0.007	0.260	1	0.26	1.16
Sand content	-0.107	±	0.011	<0.001	3	1.00	1.33
Plant richness							
Herbivore richness							
Belowground diversity							
Grazing presure (Graz)	-0.006	±	0.004	0.171	3	1.00	1.02
Graz × MAP							
Graz × MAT	0.007	±	0.006	0.245	1	0.28	1.47
Graz × RASE							
Graz × pH	0.014	±	0.005	0.003	3	1.00	1.42
Graz × Sand content	0.012	±	0.004	0.006	3	1.00	1.17
Graz × Plant richness							
Graz × Herbivore richness							
Graz × Belowground diversity							

Table S23. Results of the model selection procedure for supporting ecosystem services using livestock tracks as a proxy of grazing pressure. Results of model preselection based on AIC are available on table S28. Remainder of legend as in table S13.

	Aboveground plant biomass and its temporal stability							**Soil fertility**						
	R^2m = 0.62			R^2c = 0.93				R^2m = 0.74			R^2c = 0.95			
	n = 210							n = 318						
	Moran test: n = 10, p = 0.99; n = 20, p = 0.98; n = 50, p = 0.88							Moran test: n = 10, p = 0.99; n = 20, p = 0.98; n = 50, p = 0.88						
	Est.		Std Er.	*P value*	n	Imp.	VIF	Est.		Std Er.	*P value*	n	Imp.	VIF
Latitude	0.037	±	0.013	0.006			1.73	-0.033	±	0.029	0.263			1.67
Longitude (cos)	-0.011	±	0.012	0.385			1.19	-0.016	±	0.023	0.491			1.07
Longitude (sin)	0.001	±	0.013	0.934			1.55	-0.033	±	0.030	0.267			1.45
Elevation	0.004	±	0.013	0.773			1.71	-0.053	±	0.025	0.038			1.26
Slope	-0.006	±	0.007	0.360			1.14	0.024	±	0.016	0.129			1.10
Mean annual precipitation (MAP)	0.038	±	0.013	0.005	4	1.00	2.16	0.133	±	0.030	<0.001	6	1.00	2.02
MAP^2	-0.006	±	0.008	0.400	1	0.19	1.46	-0.028	±	0.018	0.122	3	0.51	1.43
Mean annual temperature (MAT)	0.022	±	0.018	0.234	4	1.00	2.97	-0.195	±	0.041	<0.001	6	1.00	2.42
MAT^2	-0.065	±	0.012	<0.001	4	1.00	2.09	-0.097	±	0.032	0.003	6	1.00	1.69
Rainfall seasonality (RASE)	0.025	±	0.015	0.111	4	1.00	1.68							
pH	-0.059	±	0.010	<0.001	4	1.00	1.75	0.015	±	0.024	0.539	2	0.27	1.71
pH^2	0.013	±	0.005	0.008	4	1.00	1.19	-0.021	±	0.011	0.058	2	0.27	1.17
Sand content							1.28	-0.230	±	0.020	<0.001	6	1.00	1.29
Plant richness	0.013	±	0.008	0.089	4	1.00	1.40							
Herbivore richness														
Belowground diversity														
Grazing presure (Graz)	0.002	±	0.003	0.426	4	1.00	1.02	0.008	±	0.006	0.222	2	0.29	1.06
Graz × MAP														
Graz × MAT	-0.003	±	0.003	0.339	1	0.21	1.38							
Graz × RASE	0.008	±	0.003	0.005	4	1.00	1.18							
Graz × pH	0.003	±	0.003	0.370	1	0.20	1.47							
Graz × Sand content														
Graz × Plant richness	0.008	±	0.003	0.005	4	1.00	1.08							
Graz × Herbivore richness														
Graz × Belowground diversity														

Table S24. Results of the model selection procedure for provisioning ecosystem services using livestock tracks as a proxy of grazing pressure. Results of model preselection based on AIC are available on table S28. Remainder of legend as in table S13.

	Forage quantity							Forage quality							Wood quantity						
	$R^2m = 0.34$			$R^2c = 0.87$				$R^2m = 0.25$			$R^2c = 0.90$				$R^2m = 0.41$			$R^2c = 0.93$			
	n = 207							n = 205							n = 203						
	Moran test: n = 10, p = 0.99; n = 20, p = 0.97; n = 50, p = 0.85							Moran test: n = 10, p = 0.99; n = 20, p = 0.98; n = 50, p = 0.88							Moran test: n = 10, p = 0.98; n = 20, p = 0.99; n = 50, p = 0.86						
	Est.		Std Er.	*P value*	n	Imp.	VIF	Est.		Std Er.	*P value*	n	Imp.	VIF	Est.		Std Er.	*P value*	n	Imp.	VIF
Latitude	0.059	±	0.137	0.666			1.48	0.031	±	0.069	0.659			1.72	0.089	±	0.279	0.751			1.69
Longitude (cos)	0.035	±	0.127	0.786			1.15	-0.037	±	0.062	0.556			1.12	-0.163	±	0.219	0.461			1.14
Longitude (sin)	0.170	±	0.144	0.240			1.23	0.003	±	0.072	0.968			1.32	-0.245	±	0.264	0.357			1.30
Elevation	0.019	±	0.142	0.892			1.51	0.159	±	0.069	0.022			1.42	-0.098	±	0.243	0.688			1.46
Slope	0.277	±	0.080	0.001			1.10	0.024	±	0.035	0.496			1.11	0.149	±	0.118	0.210			1.13
Mean annual precipitation (MAP)								-0.153	±	0.066	0.020	9	1.00	1.75	1.241	±	0.299	<0.001	3	1.00	2.00
MAP²								0.051	±	0.045	0.268	2	0.19	1.37	-0.522	±	0.164	0.002	3	1.00	1.37
Mean annual temperature (MAT)	0.143	±	0.170	0.403	1	0.17	1.66	0.097	±	0.094	0.306	1	0.10	1.95	0.141	±	0.341	0.681	3	1.00	1.97
MAT²									±												
Rainfall seasonality (RASE)	0.075	±	0.148	0.614	1	0.14	1.31	0.080		0.073	0.277	2	0.18	1.33							
pH															-0.336	±	0.192	0.082	3	1.00	1.60
pH²															-0.177	±	0.086	0.042	2	0.77	1.19
Sand content	-0.088	±	0.101	0.389	1	0.17	1.26	0.027	±	0.048	0.577	9	1.00	1.25	0.201	±	0.155	0.196	3	1.00	1.24
Plant richness	0.602	±	0.098	<0.001	5	1.00	1.29	0.186		0.044	<0.001	9	1.00	1.33	0.194	±	0.146	0.187	3	1.00	1.29
Herbivore richness																					
Belowground diversity																					
Grazing presure (Graz)	-0.196	±	0.035	<0.001	5	1.00	1.01	-0.032	±	0.015	0.038	9	1.00	1.03	-0.089	±	0.047	0.061	3	1.00	1.04
Graz × MAP								0.020		0.016	0.200	4	0.37	1.06							
Graz × MAT															-0.179	±	0.061	0.004	3	1.00	1.49
Graz × RASE																					
Graz × pH															-0.066	±	0.056	0.244	1	0.28	1.45
Graz × Sand content								-0.051		0.015	0.001	9	1.00	1.06	0.324	±	0.051	<0.001	3	1.00	1.18
Graz × Plant richness	-0.025	±	0.035	0.487	1	0.15	1.04	-0.018		0.015	0.238	2	0.20	1.07	0.153	±	0.050	0.002	3	1.00	1.10
Graz × Herbivore richness																					
Graz × Belowground diversity																					

Table S25. Model preselection for biodiversity metrics using site as a random effect (random intercept, 1|site). We considered three datasets: (i) a full data set considering all plots (n = 326) with available plant species richness data; (ii) a mammalian herbivore richness data set (n = 300 plots with plant species and mammalian herbivore richness data; (iii) a belowground diversity data set (n = 242 plots with both plant species richness and belowground diversity data). For each dataset we compared models with and without biodiversity metrics and compared their AICs. Bold red numbers show the best model selected for each service and used for the model selection procedure (see "Statistical analyses" section). Plant biomass & stability = aboveground plant biomass and its temporal stability.

Models			Soil carbon storage		Organic matter decomposition		Erosion control		Water regulation		Plant biomass & stability		Soil fertility		Forage quantity		Forage quality		Wood quantity	
			AIC	ΔAIC	AIC	ΔAIC	AIC	ΔAIC	AIC	ΔAIC	AIC	ΔAIC	AIC	ΔAIC	AIC	ΔAIC	AIC	ΔAIC	AIC	ΔAIC
Data set	Full data set with Plant Richness	n = 326																		
Model 1	Full model without plant richness		293.4	0.0	27.1	0.0	-789.7	0.0	-587.6	0.0	-646.6	0.0	-197.7	0.0	885.1	0.0	341.1	0.0	1173.6	0.0
Model 2	Full model + Plant Richness		266.7	-26.7	11.1	-16.0	-800.9	-11.3	**-586.5**	**1.1**	-653.9	-7.3	**-195.9**	**1.9**	**857.2**	**-27.9**	325.8	-15.3	**1165.2**	**-8.4**
Data set	Herbivore richness	n = 300																		
Model 3	Full Model without plant richness		241.8	0.0	-4.5	0.0	-738.1	0.0	-562.2	0.0	-596.4	0.0	-175.4	0.0	813.2	0.0	312.0	0.0	1086.9	0.0
Model 4	Full model + Plant richness		223.0	-18.8	-16.2	-11.7	-745.4	-7.3	-562.1	0.1	-600.7	-4.3	-174.1	1.3	791.8	-21.4	298.2	-13.8	1079.3	-7.6
Model 5	Full model + Herbivore richness		236.7	-5.1	-2.8	1.7	-735.4	2.8	-558.8	3.4	-602.6	-6.2	-172.7	2.7	816.3	3.2	306.5	-5.5	1090.1	3.2
Model 6	Full model + Plant richness + Herbivore richness		**219.3**	**-22.5**	-14.7	-10.2	-742.5	-4.4	-558.4	3.8	**-604.6**	**-8.2**	-172.0	3.4	794.7	-18.5	**294.3**	**-17.7**	1083.0	-3.9
Data set	Belowground diversity	n = 216																		
Model 7	Full Model without plant richness		239.2	0.0	35.3	0.0	-569.4	0.0	-400.7	0.0	-452.0	0.0	-152.6	0.0	635.2	0.0	244.8	0.0	869.7	0.0
Model 8	Full model + Plant richness		223.2	-16.0	26.3	-9.0	-573.5	-4.2	-398.3	2.4	-461.0	-8.9	-150.3	2.3	616.2	-19.0	234.6	-10.2	861.4	-8.3
Model 9	Full model + Belowground diversity (BD)		240.6	1.4	26.6	-8.8	-571.4	-2.0	-399.4	1.3	-449.6	2.5	-149.7	2.9	636.7	1.5	247.4	2.6	869.5	-0.2
Model 10	Full model + Plant richness+ BD.		226.4	-12.8	**22.1**	**-13.2**	**-574.0**	**-4.6**	-396.2	4.5	-459.3	-7.2	-147.7	4.9	620.0	-15.3	237.9	-6.9	864.0	-5.7

Table S26. Model preselection for biodiversity metrics using grazing pressure nested within site (random slope and intercept, grazing|site). Rest of legend as in table S25.

Models			Soil carbon storage		Organic matter decomposition		Erosion control		Water regulation		Plant biomass & stability		Soil fertility		Forage quantity		Forage quality		Wood quantity	
			AIC	ΔAIC	AIC	ΔAIC	AIC	ΔAIC	AIC	ΔAIC	AIC	ΔAIC	AIC	ΔAIC	AIC	ΔAIC	AIC	ΔAIC	AIC	ΔAIC
Data set	Full data set with plant richness	n = 326																		
Model 1	Full model without plant richness		284.6	0.0	25.6	0.0	-790.3	0.0	-589.1	0.0	-654.6	0.0	**-198.2**	**0.0**	876.6	0.0	338.0	0.0	1177.5	0.0
Model 2	Full model + Plant Richness		261.0	-23.6	7.8	-17.8	-802.4	-12.1	**-588.5**	**0.5**	-657.5	-2.9	-195.6	2.6	**852.1**	**-24.6**	326.2	-11.8	**1169.2**	**-8.4**
Data set	Herbivore richness	n = 300																		
Model 3	Full Model without plant richness		242.1	0.0	-0.6	0.0	-735.4	0.0	-558.5	0.0	-600.4	0.0	-176.0	0.0	805.1	0.0	308.2	0.0	1090.8	0.0
Model 4	Full model + Plant richness		223.7	-18.4	-12.7	-12.2	-743.2	-7.8	-558.8	-0.4	-601.9	-1.5	-174.0	1.9	788.5	-16.7	297.6	-10.6	1083.3	-7.5
Model 5	Full model + Herbivore richness		238.2	-3.8	1.1	1.7	-732.5	3.0	-555.0	3.4	-605.3	-4.9	-173.1	2.9	807.2	2.1	305.7	-2.5	1094.1	3.2
Model 6	Full model + Plant richness + Herbivore richness		**221.4**	**-20.7**	-11.2	-10.6	-740.2	-4.8	-555.1	3.4	**-605.5**	**-5.1**	-171.6	4.3	789.7	-15.4	**295.8**	**-12.4**	1087.0	-3.8
Data set	Belowground diversity	n = 216																		
Model 7	Full Model without plant richness		238.5	0.0	36.1	0.0	-570.8	0.0	-404.9	0.0	-455.9	0.0	-154.2	0.0	634.0	0.0	245.5	0.0	873.5	0.0
Model 8	Full model + Plant richness		223.6	-14.9	27.0	-9.1	-575.2	-4.4	-402.9	2.0	-461.2	-5.3	-151.7	2.5	612.7	-21.3	237.6	-7.9	864.9	-8.7
Model 9	Full model + Belowground diversity (BD)		240.2	1.7	27.9	-8.2	-571.6	-0.8	-403.7	1.2	-452.7	3.2	-150.7	3.5	635.1	1.1	248.1	2.6	873.5	0.0
Model 10	Full model + Plant richness+ BD.		227.0	-11.5	**23.4**	**-12.7**	**-574.8**	**-4.0**	-400.8	4.1	-458.5	-2.6	-148.4	5.7	616.4	-17.6	241.2	-4.4	867.6	-5.9

Table S27. Model preselection for biodiversity metrics using dung mass as a proxy of grazing pressure. Rest of legend as in table S25.

Models			Soil carbon storage		Organic matter decomposition		Erosion control		Water regulation		Plant biomass & stability		Soil fertility		Forage quantity		Forage quality		Wood quantity	
			AIC	ΔAIC	AIC	ΔAIC	AIC	ΔAIC	AIC	ΔAIC	AIC	ΔAIC	AIC	ΔAIC	AIC	ΔAIC	AIC	ΔAIC	AIC	ΔAIC
Data set	Full data set with Plant Richness	n = 326																		
Model 1	Full model without plant richness		196.5	0.0	-20.2	0.0	-658.8	0.0	-496.6	0.0	**-525.6**	**0.0**	-144.6	0.0	740.9	0.0	296.3	0.0	968.3	0.0
Model 2	Full model + Plant Richness		174.1	-22.4	-28.2	-7.9	**-661.7**	**-2.8**	**-499.9**	**-3.3**	-522.3	3.4	**-143.3**	**1.4**	723.7	-17.2	285.0	-11.4	**965.9**	**-2.4**
Data set	Herbivore richness	n = 300																		
Model 3	Full Model without plant richness		196.5	0.0	-20.2	0.0	-658.8	0.0	-496.6	0.0	-525.6	0.0	-144.6	0.0	740.9	0.0	296.3	0.0	968.3	0.0
Model 4	Full model + Plant richness		174.1	-22.4	-28.2	-7.9	-661.7	-2.8	-499.9	-3.3	-522.3	3.4	-143.3	1.4	723.7	-17.2	285.0	-11.4	965.9	-2.4
Model 5	Full model + Herbivore richness		194.7	-1.8	-19.9	0.4	-655.4	3.4	-492.7	4.0	-525.8	-0.2	-141.6	3.1	740.6	-0.3	289.6	-6.7	972.3	4.0
Model 6	Full model + Plant richness + Herbivore richness		**172.5**	**-24.0**	-28.1	-7.9	-658.4	0.4	-496.0	0.7	-522.0	3.6	-140.2	4.5	**721.7**	**-19.3**	**279.6**	**-16.7**	969.7	1.4
Data set	Belowground diversity	n = 216																		
Model 7	Full Model without plant richness		150.4	0.0	-4.0	0.0	-439.5	0.0	-311.2	0.0	-329.5	0.0	-98.5	0.0	494.7	0.0	200.1	0.0	670.5	0.0
Model 8	Full model + Plant richness		143.2	-7.3	-7.2	-3.2	-438.5	0.9	-309.0	2.1	-329.9	-0.4	-97.3	1.2	485.3	-9.4	196.4	-3.7	672.2	1.7
Model 9	Full model + Belowground diversity (BD)		149.0	-1.5	-12.1	-8.2	-436.0	3.5	-311.9	-0.8	-325.8	3.7	-98.4	0.1	498.2	3.6	204.0	3.8	673.7	3.2
Model 10	Full model + Plant richness+ BD.		143.3	-7.1	**-14.1**	**-10.1**	-434.6	4.8	-309.6	1.6	-326.4	3.1	-98.2	0.2	489.1	-5.5	199.2	-0.9	675.7	5.3

Table S28. Model preselection for biodiversity metrics using livestock tracks as a proxy of grazing pressure. Rest of legend as in table S25.

Models			Soil carbon storage		Organic matter decomposition		Erosion control		Water regulation		Plant biomass & stability		Soil fertility		Forage quantity		Forage quality		Wood quantity	
				ΔAIC		ΔAIC		ΔAIC		ΔAIC		ΔAIC		ΔAIC		ΔAIC		ΔAIC		ΔAIC
Data set	Full data set with plant richness	n = 326																		
Model 1	Full model without plant richness		121.4	0.0	-28.0	0.0	-509.2	0.0	**-391.7**	**0.0**	-443.1	0.0	**-144.4**	**0.0**	613.9	0.0	203.3	0.0	765.2	0.0
Model 2	Full model + Plant Richness		115.3	-6.1	-34.4	-6.4	-515.1	-5.9	-389.0	2.7	**-444.2**	**-1.1**	-141.7	2.6	**590.3**	**-23.7**	**185.0**	**-18.3**	**765.9**	**0.7**
Data set	Herbivore richness	n = 300																		
Model 3	Full Model without plant richness		120.0	0.0	-26.1	0.0	-493.9	0.0	-385.0	0.0	-413.6	0.0	-132.2	0.0	580.6	0.0	196.2	0.0	726.1	0.0
Model 4	Full model + Plant richness		116.3	-3.6	-31.4	-5.3	-494.3	-0.3	-383.9	1.2	-414.1	-0.5	-129.7	2.6	562.8	-17.9	180.7	-15.5	720.7	-5.4
Model 5	Full model + Herbivore richness		114.4	-5.5	-24.2	1.9	-490.1	3.9	-381.2	3.8	-416.5	-2.9	-129.8	2.4	584.4	3.7	197.8	1.6	730.1	4.0
Model 6	Full model + Plant richness + Herbivore richness		**111.9**	**-8.1**	-30.1	-4.0	-490.5	3.5	-380.7	4.3	-415.4	-1.8	-127.9	4.4	565.6	-15.0	182.7	-13.6	723.0	-3.1
Data set	Belowground diversity	n = 216																		
Model 7	Full Model without plant richness		102.3	0.0	-14.1	0.0	-354.0	0.0	-249.4	0.0	-286.5	0.0	-102.3	0.0	420.5	0.0	139.5	0.0	554.0	0.0
Model 8	Full model + Plant richness		100.7	-1.6	-16.4	-2.3	-353.6	0.4	-248.1	1.4	-287.9	-1.4	-100.2	2.1	408.9	-11.6	129.8	-9.8	553.5	-0.5
Model 9	Full model + Belowground diversity (BD)		104.6	2.3	-17.4	-3.4	-355.0	-1.0	-246.0	3.4	-282.5	4.0	-105.2	-2.9	424.1	3.5	142.7	3.2	558.0	3.9
Model 10	Full model + Plant richness+ BD.		104.0	1.7	**-17.5**	**-3.4**	**-354.7**	**-0.8**	-244.6	4.9	-284.2	2.3	-102.8	-0.5	412.7	-7.9	133.5	-6.0	557.0	2.9

Movie S1. Animated video showing the location of the study sites across the globe, and the location of the plots and watering points within selected sites. The type of vegetation and some herbivores present are also shown for some of these sites.